

MULTICOLOR PHOTOELECTRIC PHOTOMETRY OF THE MOON, VENUS, MARS, AND OTHER PLANETS

by

D. H. MENZEL and W. M. IRVINE

Harvard College Observatory
Cambridge, Massachusetts

GPO PRICE \$ _____

CFSTI PRICE(S) \$ _____

Hard copy (HC) 3.00

Microfiche (MF) .65

ff 653 July 65

FINAL REPORT

Under Grant NsG 89-60

National Aeronautics and Space Administration

15 June 1960 — 31 January 1968

Donald H. Menzel — Principal Investigator



N 68-26604
(ACCESSION NUMBER)
79
(PAGES)
30
(CATEGORY)
FACILITY FORM 602

29 February 1968

MULTICOLOR PHOTOELECTRIC PHOTOMETRY
OF THE MOON, VENUS, MARS, AND OTHER PLANETS

by

D. H. MENZEL and W. M. IRVINE

Harvard College Observatory
Cambridge, Massachusetts

FINAL REPORT

Under Grant Nsg 89-60

National Aeronautics and Space Administration

15 June 1960 - 31 January 1968

Donald H. Menzel - Principal Investigator

29 February 1968

CONTENTS

FINAL REPORT

BIBLIOGRAPHY

APPENDIX I

Multicolor Photoelectric Photometry of the
Brighter Planets. II. Observations from
Le Houga Observatory

APPENDIX II

Multicolor Photoelectric Photometry of the
Brighter Planets. III. Observations from
Boyden Observatory

APPENDIX III

University of Massachusetts Final Report on
Harvard Sub-Contract A 24658 under NASA
NsG 89-60

I. INTRODUCTION

This project was undertaken to provide basic data on the variations of luminosity of the main planets as a function of phase angle and wavelength. The lack of basic empirical data had in the past greatly hindered theoretical studies of planetary atmospheres; in particular, the integral albedo governing the heat balance of the atmosphere remained uncertain and the interpretation of the phase curves through models of the planetary atmospheres was practically impossible. The results obtained under NSG 89-60 have in large measure filled this gap in empirical data. In addition, important new results were obtained concerning instrumentation for photoelectric photometry. Finally, significant advances have been made in the application of radiative transfer theory to planetary atmospheres.

The observational program ran during a three-year period between late 1962 and 1965, at Le Houga Observatory in southern France and the Boyden Observatory in South Africa. Ten narrow-band filters between 3150 Å and 1.06μ and UBV were used for the observations of the planets Mercury, Venus, Mars, Jupiter, Saturn, Uranus and Neptune, and of the moon.

The results of the research appear in the published literature and in Appendices I and II to this report. The following section provides a brief summary of the results and a guide to the Bibliography.

II. RESULTS

The results obtained under this grant can best be described through reference to the Bibliography. Included with each article is the abstract or part of the introduction. Two papers now prepared for publication but for which a journal reference is not yet available are attached as Appendices I and II.

A. Advances in Instrumentation

Important new basic knowledge concerning photomultipliers and their application in astronomical photometry has been obtained through the work undertaken on this grant. Young (1962, 1963) presented the first detailed study of temperature effects in photomultipliers under conditions applicable to astronomical photometry. Irvine, Pikoos, Charon and Lecomte (1964) made what is apparently the first published investigation of the effect of high voltage on spectral sensitivity for photomultipliers in astronomical use. These investigations demonstrated that the effects may be much larger than had previously been realized.

B. Theoretical Studies of Radiative Transfer in Planetary Atmospheres

Under Supplements 1 and 2 to the basic grant and under Harvard Subcontract A24658 to the University of Massachusetts, basic research was undertaken on the theoretical problems that must be solved in order to interpret the observational results. Until quite recently, rigorous radiative transfer theory has been largely confined to problems involving isotropic or Rayleigh scattering. In planetary atmospheres, however, because of the presence of cloud droplets and aerosol particles, the scattering tends to be very anisotropic. Methods for studying the diffuse reflection and transmission in such atmospheres were studied. Irvine (1965b, 1965c) used the Neumann solution to investigate these processes in optically thin layers. A method developed by van de Hulst permitted extension of the results to optically thick and semi-infinite atmospheres (Irvine 1966c, 1968d). Irvine (1966c) investigated the deviations from classical radiative transfer theory that occur when very large particles are present (for example, as may be the case in Saturn's rings). Special problems arise in the

study of absorption line shapes and strengths in multiply-scattering atmospheres. Irvine (1965a, 1966b, 1967a) developed an analytical approach to this problem. Application of the radiative transfer calculations to real atmospheres required a study and review of the optical characteristics of water and ice in the infrared. The results of this study (Irvine, 1967b, and Irvine and Pollack, 1968a) probably provide the best values currently available for the infrared absorption coefficient and index of refraction of water and ice. Because the study of line shapes in the near infrared involves the computation of intensities at a large number of frequency points, it is important to find very rapid means of computing reflection and transmission. Irvine (1966a, 1968c) carried out an evaluation of approximate methods used for such computations. Irvine (1968b) recently published a review of the theoretical results obtained under this grant.

C. The Planetary Observations and Their Interpretation

Menzel (1962a, 1966, 1967a and 1967b) presented an analysis and discussion of previously published observational results for Mars, Venus and the moon. The observational procedures and the goals of the grant research have been discussed by Menzel (1962b) and Young and Irvine (1967). A preliminary discussion of the data obtained at the Le Houga site was presented by Irvine, Simon and Menzel (1968e, 1968f). These observations gave good agreement with previous investigations in areas of overlap. New results include detection of a decline in the albedo of Venus between $\lambda 6250$ and 1.06μ , rather complete data on rotational variations of the Martian albedo, and observations of Jupiter which are compatible with an 11- or 12-year cycle in its albedo. The results of the observations from Le Houga Observatory appear in tabular form in a paper by Irvine, Simon, Menzel, Charon, Lecomte, Griboval and Young (1968g and Appendix I). A similar presentation of the data from the Boyden Observatory has been prepared by Irvine, Simon, Menzel, Pikoos and Young (1968h and Appendix II).

D. Laboratory Experiments

Interpretation of the observational results can be significantly enhanced by certain laboratory experiments. Some initial steps in this direction were taken under the subcontract to the University of Massachusetts and are described in Appendix III. The studies involved investigation of the reflection

spectrum from simulated Venus atmospheres in a long-path absorption cell. Support for the further development of these experiments will be obtained elsewhere.

E. Further Research

The scientific results outlined above do not exhaust the results obtained under NSG 89-60. Further contributions to the scientific literature are in preparation, based on the data obtained under the grant, including:

- a. Observations of Uranus and Neptune with 13 filters. (Because these fainter objects were frequently observed under different conditions of high voltage than the extinction objects, they have been handled separately.)
- b. The observations of the moon. (These observations were made with a separate telescope and are also being reduced separately.)
- c. Further observations of Mercury, Venus, Mars, Jupiter, and Saturn. (Certain observations of these planets under unorthodox conditions are being reduced separately.)
- d. A vast wealth of data on the monochromatic extinction of the atmosphere above the Le Houga and Boyden Observatories as a function of season. These results should be valuable to atmospheric scientists. They may help to decide, for example, the current controversy over whether aerosol particles contain a significant imaginary (absorbing) part to their index of refraction.
- e. Special planetary studies. The tabulated results in Appendices I and II provide a quantity of data for special studies (meteorological conditions on Mars, rotational effects on Mars, Jupiter, and Saturn, possible ultraviolet fluctuations in the albedo of Venus, etc.). These studies are being pursued by Dr. Irvine under NASA Grant NGR 22-010-023.

ACKNOWLEDGMENTS

We regret the death of M. Julien Peridier and express our gratitude for his co-operation in making Le Houga Observatory in France available for part of our observational program. This project could not have succeeded without the active support of our colleagues, whose names appear as co-authors on grant-related papers in the Bibliography. Professor G. de Vaucouleurs has been very generous in his assistance and advice. Mr. E. Barr of Thin Film Products graciously provided his time and facilities for measuring the properties of the filters used in the observations. The reduction of data had the assistance of a large number of people. We would like to particularly acknowledge the very capable assistance of Mrs. Constance Valette, Mrs. Marietta Huguenin, and Mrs. Kathryn Dix. Finally, we gratefully acknowledge the very important assistance rendered the project by the business staff of the Harvard College Observatory, particularly Mrs. Helen S. Federer.

BIBLIOGRAPHY1962

MENZEL, D. H.

(1962a) The Atmosphere of Mars, Mémoires de la Société Royale des Sciences de Liège, Fifth Series, 7, 411, 1962.

A discussion primarily concerned with the H₂O vapour content of the atmosphere. It is inferred that two major layers of particulate matter are present; namely, a thick layer of large ($>1 \mu$) dust particles near the Martian surface that are responsible for the planet's red colour, and a very thin layer of small ($\sim 0.02 \mu$) ice crystals lying probably well above the dust layer. This suggestion is consistent with the observed association between the blue layer and the underlying polar (frost) caps.

-- (1962b) A New Program of Planetary Photography, Mémoires de la Société Royale des Sciences de Liège, Fifth Series, 7, 224, 1962.

This project is designed to make effective use of a new p.e. photometer that enables 13 spectral regions between 3200 Å and $>10,000$ Å to be scanned in rapid succession. Concurrent programmes of multi-colour photometry of the planets Mars and Venus, and of the Moon, with the new 16 inch Cassegrain reflector at Boyden Observatory, S. Africa, and the 12 inch reflector of the Le Houga Observatory, S. France, commenced in the summer of 1962, and will continue until 1965.

YOUNG, A. T.

Temperature Effects in Photomultipliers (Abstract). Astronomical Journal, 67, 286, 1962.

The effect of temperature changes on the spectral response curves of RCA 1P21, EMI 6256 and 9558, and Farnsworth FW-118 photomultipliers has been measured for two tubes of each type. The cathodes are respectively S-4 (Sb-Cs), S-13 (Sb-Cs), S-20 (Sb-Na-K-Cs), and S-1 (Ag-O-Cs). All but the FW-118 have Sb-Cs dynode surfaces.

Cooling from room temperature to dry-ice temperature causes changes in relative spectral response of the order of 10% or less for the Sb-Cs cathodes for $\lambda \leq 5000$ Å, for the S-20 cathode for $\lambda \leq 6250$, and for

the S-1 cathode over at least the range from 6250 to 10,000 Å. At $\lambda=7300$, the S-20 cathode loses about 30% of its normal sensitivity when it is refrigerated. The data are consistent with a temperature coefficient of $-0.04\%/^{\circ}\text{C}$ per stage for the Sb-Cs dynodes.

The Sb-Cs cathodes lose a large fraction of their sensitivity for $\lambda > 5000$ Å when they are refrigerated. This loss is more than enough to account for the discrepancy between observed B-V colors of stars and colors computed from stellar atmosphere theory. The coefficient of the temperature effect between 5000 and 6000 Å is 1.12×10^{-5} mag./ $^{\circ}\text{C}/\text{Å}$. This typically requires a temperature stabilization of one or two degrees if a 1P21 is required to carry a color zero point in this part of the spectrum with an accuracy of 1%.

1963

YOUNG, A. T.

Temperature Effects in Photomultipliers and Astronomical Photometry, Applied Optics, 2, 51, 1963.

Temperature coefficients are reported for photomultiplier tube types used in astronomy. For 1% stability of gain and colour response, temperature regulation of 1°C or better is generally required. This is nearly an order of magnitude better than what is usually achieved at the telescope, but careful use of a well-designed cold box should make 1°C temperature stability possible. For maximum stability and reproducibility, ordinary blue-sensitive tubes should be avoided at wavelengths longer than 5000 Å, and trialkali cathodes should not be used beyond 6500 Å.

1964

IRVINE, W. M.

Effect of High Voltage on Spectral Sensitivity for Two Photomultipliers, with C. Pikoos, J. Charon, and G. Lecomte. Astrophysical Journal, 140, 1629, 1964.

Changes in the spectral sensitivity of the EMI 6256 and Farnsworth FW-118 photomultipliers as a function of the high voltage applied to the tubes were examined by observing intensities of a standard star through various filters. The results showed that there was no appreciable

change in sensitivity with voltage for the 6256 tube, but that there were appreciable effects in the FW-118 tube at larger wavelengths. Reasons for the latter results are discussed, with a possible remedy.

1965

IRVINE, W. M.

- (1965a) The Distribution of Photon Optical Paths in a Scattering Atmosphere (Abstract). *Astronomical Journal*, 70, 679, 1965.

Ordinarily in problems of radiative transfer in media which exhibit both scattering and true absorption it is necessary to solve the equation of transfer separately for each value of the single scattering albedo α . For the study of absorption lines or bands, when α is a rapidly changing function over the frequency range of interest, it would be useful to express the intensity $I(\alpha)$ in terms of the solution $I(1)$ in the conservative case. This is particularly important in the infrared, where the bandwidth of a detector may be such that the transmission function for a sample of the atmosphere cannot be considered exponential. A method of handling such problems for a homogeneous medium is described in terms of the distribution of photon paths in the medium. It is shown that this distribution obeys a generalized equation of transfer and generalized principles of invariance. Solutions in limiting cases are obtained by a transform technique.

- Multiple Scattering by Large Particles, *Astrophysical Journal*, 142, 1563, 1965.

The Neumann solution to the scalar equation of transfer in a homogeneous layer of optical thickness $\tau \leq 1$ is obtained numerically for sample phase functions with large forward and backward peaks. The results are presented graphically and are compared with the intensities and albedos computed by several approximate methods.

- Multiple Scattering by Large Particles (Abstract). *International Union of Geodesy and Geophysics Monograph No. 28*, 11, 1965.

The problem of diffuse reflection and transmission by a homogeneous plane-parallel cloud or dust layer is made difficult by the extreme asymmetry of the phase function (indicatrix) for single scattering. The appropriate

radiative transfer problem has generally been oversimplified, and exact results are needed with which to evaluate the various approximate methods which have been employed. In the present paper the advantages of using the Neumann solution (expansion in successive orders of scattering) are discussed. This series, although slowly convergent, is exact and may be used for machine computation. Results are presented in graphical form for non-emitting layers of optical thickness illuminated unidirectionally from above. Scalar phase functions similar to those given by Deirmendjian (Appl. Optics 3, 187, 1964) for maritime and continental haze were used. The exact results show that the monochromatic albedo may be determined with reasonable accuracy by using methods which take into account the large asymmetry of the phase function, but which use only an approximate description of the multiple scattering process (diffusion-type method of Fritz, two stream theory for normal incidence). Some authors have attempted to obtain a qualitative idea of the effect of multiple, large particle scattering by using exact solutions of the equation of transfer, but a phase function consisting of only two or three terms of a Legendre series (either using the most asymmetric, non-negative such function, or else by equating moments to the exact phase function, which introduces negative scattering at certain angles). These procedures give very erroneous results for the reflection and transmission as a function of angle for the thin layers considered here. A much better procedure is the approximation suggested by Sobolev (Perenos Luchistoi Energii v Atmosferakh Zvesd i Planet, Ch. X). Even the latter method may, however, omit certain subtle but interesting features.

1966

- IRVINE, W. M.
(1966a) Comparison of Exact with Approximate Solutions of the Equation of Transfer for Very Elongated Phase Functions (Abstract). Astronomical Journal, 71, 859, 1966.

The scalar equation of radiative transfer in a homogeneous medium is solved for phase functions characteristic of terrestrial clouds and hazes. Parallel radiation from a distant source is assumed to be incident on a layer which contains no internal sources. The albedo and transmissivity, as calculated from the Neumann solution and the "doubling" method of van de Hulst, are compared with the corresponding results obtained from Eddington's approximation and the two-stream (Schuster-Schwarzschild) approxi-

mation. The two-stream approximation is more accurate for small to medium optical depths, while the Eddington approximation becomes increasingly better for thicker layers. Both approximations fail for large angles of incidence.

A comparison of the reflected and transmitted intensities with corresponding results obtained by Romanova is made.

- (1966b) The Distribution of Photon Optical Paths in a Scattering Atmosphere, *Astrophysical Journal*, 144, 1140, 1966.

The investigation of absorption lines and bands in a scattering and absorbing medium may be elucidated by study of the distribution of photon optical paths $\vartheta(\lambda)$ in a conservative atmosphere with the same scattering properties as the medium of interest. Equations defining $\vartheta(\lambda)$ are derived. Methods of solution are discussed, and the case of reflection from a semi-infinite layer is explicitly described.

- (1966c) Diffuse Reflection and Transmission by Clouds and Haze Layers (Abstract). *Transactions of the American Geophysical Union*, 47, 126, 1966.

Solutions to the scalar equation of radiative transfer in a homogeneous medium are obtained for phase functions characteristic of terrestrial clouds and hazes by means of the Neumann solution and the 'doubling' method of van de Hulst. The influence on the angular structures of the reflected and transmitted light fields of optical thickness of the layer, degree of elongation of the phase function, and single scattering albedo is examined. A comparison of the computed fluxes is made with corresponding results obtained by means of Eddington's approximation. An evaluation of Romanova's method for computing the angular distribution of reflected and transmitted light is made.

- (1966d) The Shadowing Effect in Diffuse Reflection, *Journal of Geophysical Research*, 71, 2931, 1966.

The theory of multiple scattering based on the equation of radiative transfer breaks down for directly backscattered radiation if the scattering particles are large enough and the medium dense enough for the particles to shadow one another. This 'shadowing effect' can be incorporated as a correction into the usual radiative transfer theory. The resultant theory may be applicable to Saturn's rings and the lunar surface.

MENZEL, D. H.

The Surfaces of the Moon, Mars and Venus. In Moon and Planets, edited by A. Dollfus, North-Holland Publishing Company, Amsterdam, 1, 1966.

The nature of the surfaces of the moon and planets must markedly depend on the origin and evolution of these bodies. A magnetohydrodynamic theory of the solar system has many advantages over theories involving capture or contracting nebulae.

Gold's hypothesis of deep layers of dust, the result of meteoric bombardment, is not supported by the photographic evidence from the Ranger series. The surface probably consists of "crunchy", semi-porous rock. The lunar surface may be much older than previously surmised. In an early era of development, a thin solid crust, porous enough to float on a liquid interior, could have formed. Tidal forces could occasionally have cracked open this crust, allowing lava to flow out upon the rock surfaces and form the Maria.

The Mariner "Fly-By" probes were extremely successful, revealing a Martian surface cratered much like that of the moon. Mars also appears to possess a thin ionosphere. The surface of Venus appears to be very hot, about 600°K. Radar observations indicate the presence of mountains and a retrograde rotation period of about 244 days.

1967

IRVINE, W. M.

(1967a) Absorption Bands and Photon Optical Paths in a Non-conservative Scattering Atmosphere, Astrophysical Journal, 147, 1193, 1967.

In previous papers (Irvine 1964, 1966; hereinafter cited as "Paper I" and "Paper II," respectively) it has been shown that the influence of multiple scattering and of finite detector band width on the shape of absorption features formed in a scattering atmosphere can be determined by considering the probability distribution of photon paths in the corresponding conservative atmosphere. Frequently, in cases of interest (e.g., the near-infrared bands of Venus), absorption features may be superimposed upon a background continuum absorption. The present Note shows that the previous method is easily extended to this case. The relevant derivation is given in more detail than heretofore, and certain functions describing the distribution of path lengths are shown to be independent of continuum absorption.

--

- (1967b) Infrared Optical Characteristics of Ice Spheres, Smithsonian Contributions to Astrophysics, 11, 367, 1967.

The scattering and absorption properties of ice particles are important for the study of radiative transfer in the atmospheres of the earth and, possibly, of Venus and Mars, as well as for studies of interplanetary and interstellar dust particles. Published calculations of these parameters for infrared wavelengths are extremely limited (see the review by Feigel'son, 1964); a number of computations have been made by Greenberg (1966), but the cross sections themselves have not been published.

The quantities that are most appropriate for describing the scattering by ice particles will depend on the given physical situation. In the present paper, values of the normalized extinction cross section (efficiency factor) Q_{ext} , the single-scattering albedo α , and the asymmetry factor $\langle \cos \theta \rangle$ are presented for spherical, homogeneous particles of radii 1.0, 4.0, 7.5, 10.0, 12.5, and 15.0 μ for the wavelength interval $1 \mu < \lambda < 150 \mu$. These quantities are of particular interest in the approximate solution of problems of diffuse reflection and transmission by ice clouds, and in the study of the radiative heating of an atmosphere containing such clouds. For other studies (of the zodiacal light, for example) the angular distribution of scattered radiation would be a more relevant quantity.

MENZEL, D. H. (Chairman)

- (1967a) Panel Discussion: The Lunar Surface, in Physics of the Moon, Science and Technology Series, 13, 133, 1967.

At a panel discussion of The Lunar Surface, the chairman, Dr. Menzel, summarized various problems of the lunar surface, such as the origin of craters, the nature of ghost or drowned craters, the origin of cracks and crevasses, and the physical nature of the ray structures. Volcanism, as well as meteoric impact, is responsible for certain formations. Dr. Menzel presented some 3-D slides, made with the Polaroid technique, to display the stereographic structure of lunar craters, obtained from selected Ranger photographs.

--

- (1967b) Draft Report, Commission 17, with B. Bell. International Astronomical Union 13th General Assembly, 341, 1967.

A detailed summary of lunar studies made between the years 1964 and 1967. It lists various official conferences and

important books. A discussion of lunar probes covers the subjects of Hard Landings, Soft Landings, the Moon's Far Side, Lunar Orbiters, Lunar Cartography, Lunar Nomenclature, Lunar Photometry and Polarimetry, Thermal Properties and Infrared Studies, Radio Measures, Lunar Surface Formations, Physical Properties and Chemical Composition of the Surface, Lunar Volcanism, Lunar Luminescence, Lunar Atmosphere and Environment, the Moon's Internal Structure, the Origin and Evolution of the Moon.

- The Nature of the Surface of the Moon: Interpretation of Lunar Probe Data, Publications of the American Astronautical Society, Science and Technology Series, 14, 113, 1967.

An examination of various hypotheses of lunar origin and evolution. The development of a magnetohydrodynamic theory of the origin of the solar system, with reference to the moon as a by-product. The moon appears to have cooled from the outside in, with various lava flows that formed the lunar maria.

YOUNG, A. T.

Multicolor Photoelectric Photometry of the Brighter Planets. I. Program and Procedure, with W. M. Irvine. Astronomical Journal, 72, 945, 1967.

The equipment and procedures of measurement and reduction are described for a 3-1/2 yr program of photoelectric photometry of the brighter planets and the moon. Observations were made in 10 narrow bands between 3150 Å and 1.06μ, and in UBV. A new method of extinction determination is described in some detail.

1968

IRVINE, W. M.

(1968a) Optical Properties of Water and Ice Spheres, with J. Pollack. Icarus, in press.

The literature on the absorption coefficient and reflectivity of water and ice in the infrared is critically reviewed, and best values are chosen for the complex index of refraction for wavelengths $0.7\mu < \lambda < 200\mu$. The Mie theory is then used to compute the single scattering albedo a , asymmetry factor $\langle \cos \theta \rangle$, and normalized extinction cross-section Q_{ext} for spheres of water and ice with radii 0.3, 1.0, 3.0, and 10.0 microns in this wavelength interval.

Significant differences in the absorption spectrum between water and ice and among particles of different radii are illustrated. A useful approximate formula for a is given. The results are important for the study of radiative transfer in planetary cloud layers.

- (1968b) Diffuse Reflection and Transmission by Cloud and Dust Layers, *Journal of Quantitative Spectroscopy and Radiative Transfer*, January, in press.

The problem of radiative transfer in a medium with a strongly anisotropic phase function is considered. Traditional methods of solution of the transfer equation have not proved practicable. Recent calculations using the Neumann solution, Romanova's method, and the "doubling" method of van de Hulst are described. To facilitate the study of absorption features under conditions of multiple scattering, the probability distribution of photon optical paths is introduced. When appropriately normalized, this distribution satisfies a transfer equation.

- (1968c) An Evaluation of Romanova's Method in the Theory of Radiative Transfer. In *Atmospheres of Venus and Mars*, edited by Brandt and McElroy, Gordon and Breach Science Publishers Inc., New York, in press.

The method proposed by Romanova for solution of the radiative transfer equation for very anisotropic phase functions is quite accurate and may effect a very considerable saving in time over more conventional methods. It may in fact reduce computations for very elongated phase functions to times quite comparable with those for isotropic scattering.

- (1968d) Multiple Scattering by Large Particles. II. Optically Thick Layers, *Astrophysical Journal*, June, in press.

Exact solutions to the scalar equation of transfer in a homogeneous layer with optical thickness $2.5 < \tau^* < \infty$ are obtained numerically for phase functions with large forward and backward peaks. The Neumann series solution and the doubling method of van de Hulst are employed. The results are presented graphically and are compared with intensities computed by the small angle method of Romanova and with fluxes computed by Eddington's approximation, the Schuster-Schwarzschild approximation and with a modified two-stream approximation. Romanova's method appears quite accurate, but the latter three approximations must be used with care for single scattering albedos less than unity.

- Multicolor Photoelectric Photometry of the Brighter
(1968e) Planets (Abstract). Astronomical Journal, in press.

Preliminary results are reported from a three year program of photoelectric photometry undertaken to obtain phase curves, monochromatic albedos and radiometric albedos for Mercury, Venus, Mars, Jupiter, Saturn and the Moon. Observations were made in ten narrow bands isolated by interference filters between 3150 Å and 1.06 microns plus UBV. Both a northern hemisphere site (the Le Houga Observatory in France) and a southern hemisphere site (Boyden Observatory in South Africa) were used. For Venus, results from both sites near quadrature indicate that, relative to the sun, Venus is fainter at a wavelength of 1.06 microns than at $\lambda 6250$ by 0.07 ± 0.03 magnitudes. Phase coefficients at these wavelengths appear to be similar, so that this result probably holds also at full phase. For Mars, good agreement is obtained with previous workers for the geometric albedo, but phase coefficients are somewhat higher. As a result values for the monochromatic Bond albedo for Mars are less than those which have been suggested by de Vaucouleurs for $\lambda \gtrsim 6000$ Å. Longitudinal variations are quite prominent for Mars at wavelengths longer than 6000 Å, the amplitude of these increasing to a wavelength of about 8000 Å and then remaining roughly constant to 1.06 microns. For Jupiter, values of the geometric albedo agree quite well with those given by Harris if they are normalized to our value of $V(1,0) = -9.39$.

- Multicolor Photoelectric Photometry of the Brighter
(1968f) Planets, with T. Simon and D. H. Menzel. Transactions of the International Astronomical Union, in press.

Preliminary results are reported from a three year program of photoelectric photometry undertaken to obtain phase curves, monochromatic albedos and radiometric albedos for Mercury, Venus, Mars, Jupiter, Saturn and the Moon. Observations were made in ten narrow bands isolated by interference filters between 3150 Å and 1.06 microns plus UBV. Both a northern hemisphere site (the Le Houga Observatory in France) and a southern hemisphere site (Boyden Observatory in South Africa) were used. For Venus, results from both sites near quadrature indicate that, relative to the sun, Venus is fainter at a wavelength of 1.06 microns than at $\lambda 6250$ by 0.07 ± 0.03 magnitudes. Phase coefficients at these wavelengths appear to be similar, so that this result probably holds also at full phase. For Mars, good agreement is obtained with previous workers for the geometric albedo, but phase coefficients are somewhat higher. As a result values for the monochromatic Bond albedo for Mars are less than those which have been suggested by de

Vaucouleurs for $\lambda \gtrsim 6000 \text{ \AA}$. Longitudinal variations are quite prominent for Mars at wavelengths longer than 6000 \AA , the amplitude of these increasing to a wavelength of about 8000 \AA and then remaining roughly constant to 1.06 microns. For Jupiter, values of the geometric albedo agree quite well with those given by Harris if they are normalized to our value of $V(1,0) = -9.39$.

- (1968g) Multicolor Photoelectric Photometry of the Brighter Planets. II. Observations from Le Houga Observatory, with T. Simon, D. H. Menzel, J. Charon, G. Lecomte, P. Griboval and A. T. Young. Astronomical Journal, in press (Appendix I to this report).

Results of a program of photoelectric photometry of Venus, Mars, Jupiter, and Saturn between 1963 and 1965 are presented. Observations were made in ten narrow bands between 3150 \AA and 1.06 μ and in UBV. Phase curves are presented and monochromatic geometric albedos determined for Mars and Jupiter. The geometric albedos agree well with previous observations, and are compatible with an eleven or twelve year cycle in the albedo of Jupiter. For Venus, observations near quadrature show a decrease in reflectivity between 6250 \AA and 1.06 μ of $0.07 \pm 0.03 \text{ mag}$. Longitudinal variations are not obvious for Jupiter, but are quite prominent for Mars when $\lambda > 6000 \text{ \AA}$.

- (1968h) Multicolor Photoelectric Photometry of the Brighter Planets. III. Observations from the Boyden Observatory, with T. Simon, D. H. Menzel, C. Pikoos, A. Young. To be published (Appendix II to this report).

Results of a program of photoelectric photometry of Mercury, Venus, Mars, Jupiter, and Saturn between 1963 and 1965 are presented. Observations were made in ten narrow bands between 3150 \AA and 1.06 μ and in UBV. Phase curves are presented and monochromatic geometric albedos determined. The results are compared with previous investigations.

APPENDIX I

MULTICOLOR PHOTOELECTRIC PHOTOMETRY
OF THE BRIGHTER PLANETS
II. OBSERVATIONS FROM LE HOUGA OBSERVATORY

WILLIAM M. IRVINE
Department of Physics and Astronomy
University of Massachusetts, Amherst, Massachusetts

THEODORE SIMON and DONALD H. MENZEL
Harvard College Observatory

JACQUES CHARON and G. LECOMTE
Le Houga Observatory, France

PAUL GRIBOVAL
Department of Astronomy, University of Texas

and

ANDREW T. YOUNG
Aerospace Corporation, Los Angeles

ABSTRACT

Results of a program of photoelectric photometry of Venus, Mars, Jupiter, and Saturn between 1963 and 1965 are presented. Observations were made in ten narrow bands between 3150 Å and 1.06μ and UBV. Phase curves are presented and monochromatic geometric albedos determined for Mars and Jupiter. The geometric albedos agree well with previous observations, and are compatible with an eleven- or twelve- year cycle in the albedo of Jupiter. For Venus, observations near quadrature show a decrease in reflectivity between 6250 Å and 1.06μ of 0.07 ± 0.03 mag. Longitudinal variations are not obvious for Jupiter, but are quite prominent for Mars when $\lambda > 6000$ Å.

I. INTRODUCTION

In order to determine the luminosity as a function of phase angle for the brighter planets at wavelengths other than the visual, a three-year program of multicolor photoelectric photometry was conducted between 1962 and 1965 under the direction of the Harvard College Observatory. Observations were made from both Le Houga Observatory in France and the Boyden Observatory in South Africa. This paper presents results for Venus, Mars, Jupiter, and Saturn obtained at Le Houga. Subsequent papers will present the results obtained in South Africa, as well as additional data obtained at Le Houga, particularly the results for the moon and a few observations of Uranus and Neptune.

The motivation for this program and the equipment used were described in an earlier paper (Young and Irvine, 1967, hereinafter referred to as Paper I). Observations were made in ten narrow bands isolated by interference filters between 3150 Å and 1.06μ . These bands will be designated by the letters v-u-s-p-m-l-k-h-g-e (see Table I). In addition, observations were made in UBV (our corresponding natural magnitude system is denoted d-c-b).

II. MAGNITUDE SYSTEM EMPLOYED

Paper I described the reduction of the data. An iterative procedure determined the magnitudes of the standard stars used to measure extinction and to transform to standard conditions. These stars are listed in Table II.

To correct for atmospheric extinction, we divided the observations into approximately monthly periods and then transformed the corrected observations to the standard period (March, 1965); for any band x a linear transformation was used of the form

$$x = x^* + \alpha(x-y)^* + \beta, \quad (1)$$

where the unstarred value refers to the standard period and α and β are constants determined from a least-squares fit to the stellar observations. In this transformation the choice of color $(x-y)$ was the same (except as noted below) as that used in the extinction determination for pass band x . Table VIII gives an estimate of the errors involved in the extinction determination and the transformation to the standard system.

Some non-linearities did occur when the results of the 1963 observations in bands k , p and s were transformed to the standard system. The replacement of the filters which took place in January, 1964, probably accounted for the difficulties. Linear transformations could be obtained by use of the following colors: for p , $(u - p)$; for s , $(s - p)$. These transformations were accordingly employed for the 1963 data in these bands. As reported in Paper I, a red leak existed in the k filter used during 1963. These observations are undergoing further analysis and are not reported here.

After reducing the results to the standard period, we transformed the wide-band $(d-c-b)$ observations to the UBV system of standard values given by Johnson et al. (1966). A least-squares fit gave the following transformations:

$$V = b + 0.014(c - b) - 0.013 \quad (2)$$

$$\epsilon_V = 0.020$$

$$B = c + 0.001(c - b) - 0.006 \quad (3)$$

$$\epsilon_B = 0.017$$

$$U = d + 0.012(d - c) - 0.005 \quad (4)$$

$$\epsilon_U = 0.027$$

where ϵ is the standard error per star for each transformation. Interpolation among the standard stars in $B - V$ (the Boyden observations were included in this determination) then determined the narrow-band color of the sun. A color of $B - V = 0.65$ was chosen for the sun (van den Bergh 1965). To adjust the magnitude scale for any of the narrow bands x , we then set $x - V$ equal to zero for the sun. All narrow band col-

ors are thus color excesses relative to a G2V star. Table III gives an estimate of the internal accuracy obtained in determining the solar color; the estimate is based on the standard error of each zero-point determination and a comparison of the results from Le Houga and Boyden. This error is less than the difference in solar color that would result from a change of ± 0.02 in $(B-V)_{\odot}$.

Table II gives the magnitudes of the extinction stars in the final magnitude system. The quantity \bar{n} is an average (over pass-bands) number of observations of each star; extinction periods during which the star was observed less than three times are excluded. The column labeled n_v gives the number of observations in band v ($\lambda 3147$), which was frequently less than that in the other bands. All stars were observed in at least three extinction periods, with the exception of γ Peg (two periods).

The largest uncertainty in the tabulated magnitudes generally results from the transformation from each such period to the standard period. Table VIII lists the standard errors for these transformations. The magnitudes in Table II are in general reliable to at least ± 0.02 mag. Values in parentheses in Table II are slightly less reliable (perhaps ± 0.03 mag.) and were not used in determination of the standard system, although such observations may have been used in the extinction determination.

III. RESULTS

Tables IV, V, VI, and VII present the results of the planetary photometry. The magnitudes have been reduced to unit distance from the sun and earth. In each table, column 1 assigns a number to each observation of a planet. Column 2 gives the first day of the double date of each observing night; thus FEB 18 65 indicates the night of February 18-19, 1965. (In consequence, the observations tend to be centered around 0 hours UT on the date subsequent to that given in column 2; e.g., February 19.) Column 3 gives the time of observation for filter p, taken half-way through the 13-filter sequence (such a sequence typically lasted 20 minutes, and the order of observation was d-c-b-v-u-s-p-m-l-k-h-g-e). The time reported is local sidereal time for dates from 1963 through February 14-15, 1965; for February 15-16, 1965, through the remainder of 1965 the Universal Time is given. All times

are given in hours and minutes (first and second sub-columns, respectively). Column 4 lists the phase angle i as interpolated from the tables of ephemerides for physical observations in The American Ephemeris and Nautical Almanac, except for phase angles so small that linear interpolation would be inaccurate. In the latter case i was computed from (α, δ) for the planet and the sun. The next 10 columns give the monochromatic magnitudes in the narrow bands in order of increasing wavelength (see Table I), and the following 3 columns give the UBV magnitudes. The last column notes peculiar observing conditions or other problems. The notes include values of air mass M when the planet was observed at an air mass outside the range covered by the extinction stars, or when $M \geq 2.5$. The notes also give approximate values of the residuals r (in magnitudes) determined from the extinction solution for stellar observations either before or after a given planetary observation ($r > 0$ indicated that the extinction was underestimated, and vice-versa). The phrase "end of night" indicates that the planetary observation was not followed by observation of a standard star.

Sky brightness prevented many observations of Venus. The article concerning the South African observations will present further results for this planet and for Mercury. Note that observations of Saturn include the effect of the ring.

To estimate the accuracy of the results, one can examine the rms residual (R) for each band for each monthly extinction solution and the standard error per star (S) for each band obtained in transforming the monthly periods to standard conditions. Table VIII gives these quantities. When we had substantial reason to believe that either error might be a serious underestimate, we included a note in Tables IV-VII, or increased the error to what seemed to be a more realistic estimate; for example, if the color of a planet was outside the range of colors observed for standard stars during this particular period, the transformation to the standard period may be uncertain.

Figures 1 and 2 present sample plots of the resulting phase curves. Note the scatter in the results for Mars, resulting (at least in part) from rotational effects, and the very pronounced effect of Saturn's rings.

Our observations (which included only three points, on

rather poor nights, at phase angles $i < 13^\circ$) did not show the opposition effect for Mars reported by O'Leary (1967) and Bugaenko, Koval', and Morozhenko (1967).

The phase curves for Jupiter show anomalous behavior for bands h and g in 1963 relative to 1964-65. The g magnitudes are systematically fainter in 1963 by about 0.06 mag.; this is probably an artifact of the transformation to the standard system (see Table VIII). The h magnitudes are systematically brighter in 1963 by roughly 0.15 mag.; this appears to be a real effect, indicating a change in color between 1963 and 1964-65 (no systematic changes were seen at ultraviolet or visible wavelengths, or at 1.06μ).

For Venus, for the range of phase angles covered by the observations we have the relation

$$(k_g - e_g) = -0.07 \pm 0.03 \text{ mag}, \quad (5)$$

where the (k-e) color is measured relative to the sun, as noted in section II. Thus, the reflectivity of Venus decreases as we go toward larger wavelengths in this interval. This result appears to hold also at smaller phase angles (preliminary reduction of the South Africa data), and may have important consequences for models of the Venus atmosphere (cf. Pollack 1965).

A linear least-squares fit to the phase curves gives the magnitude at zero phase $m(1,0)$ for each band, listed in Table IX. Table IX also gives preliminary estimates of geometric albedos p for Mars and Jupiter, as computed for each band from the formula (e.g., de Vaucouleurs 1964)

$$\log_{10} p = 0.4 [m_\odot - m(1,0)] - 2 \log_{10} \sin \sigma_1', \quad (6)$$

where σ_1' is related to the apparent equatorial semi-diameter σ_1 of a planet of oblateness f by the expression

$$\sigma_1' = \sigma_1 \sqrt{1-f} \approx \sigma_1 \left(1 - \frac{f}{2}\right). \quad (7)$$

We have taken $\sigma_1 = 4.708''$, $f = 0.0105$ for Mars and $\sigma_1 = 98.32''$, $f = 0.0661$ for Jupiter (de Vaucouleurs 1964, Harris 1961). The solar magnitude was taken as $V = -26.81$ (Harris 1961). The determination of $m(1,0)$ and p included only what appeared to be the best observations (no observations at large M or on poor nights).

Geometric albedos of Venus and Saturn are not given because of the non-linearity of the phase curve and the lack

of data at small phase angles (for Venus) and because of the uncertain extrapolation to "no-ring" (for Saturn). More definitive values for p and estimates of phase coefficients, phase integrals, and Bond albedos for all the planets observed will be presented in a subsequent paper, after the French and South African observations have been compared.

The values of $m(1,0)$ and p obtained for Mars agree quite well (Figures 3 and 4) with values found by Hardie (reported in Harris, 1961) and for $\lambda \gtrsim 7500$ A with the near infrared values found by Tull (1966), Walker (1966), and YOUNKIN (1966). Note that Mars becomes gray (or slightly blue) between $\lambda 3150$ and $\lambda 3570$, in agreement with measurements by Evans (1965), but there is no evidence for the dramatic increase in reflectivity reported by Bogess and Dunkelman (1959) at $\lambda 2740$.

The observations for Jupiter (Table IX) also agree well with those of Hardie (Harris 1961) if we normalize his data to a $V(1,0) = -9.39$. This value agrees with the 1954 determination by Kuiper and Harris (Harris 1961), but is significantly brighter than the mean $V(1,0) = -9.25$ reported by Harris (compare Figures 5 and 6). Thus, our results are compatible with, but of course do not prove, the existence of an eleven- or twelve-year periodicity in the albedo of Jupiter.

Figures 7a through 7c show the variation in the magnitude of Mars as a function of longitude of the central meridian ω (the residual of a given observation relative to the mean phase curve is plotted versus ω). Again, only observations under the best conditions are included. Variations are not obvious for $\lambda \leq 5000$ A. From the amplitude of the variations at longer wavelengths we note that surface contrast on Mars reaches a maximum in the range $\lambda 7300 - \lambda 8600$, remaining at this high value to at least 1.06μ . Similar plots of magnitude versus longitude of the central meridian were made for Jupiter for selected periods, but no correlations were obvious.

ACKNOWLEDGMENTS

We are very grateful to M. Julien Peridier for making the Le Houga Observatory available to us, and to Dr. G. de Vaucouleurs for his assistance and advice. In addition, we would like to acknowledge the assistance during the data reduction of Mesdames O. Kojan, L. Hudson, J. Waldbaum, S. Kothavala, E. Stanley, S. Schofer, M. Bocchino, C. Mohnkern, P. Peck, and T. Wenz, of Mlles. S. Steinberg, G. Flynn and C. Austin, of Mr. R. Berendzen, and particularly of Mrs. Constance Valette, Mrs. Marietta Huguenin and Mrs. Kathryn Dix.

REFERENCES

- Bogess, A. and Dunkelman, L. 1959, Ap. J. 129, 236.
- Bugaenko, L.A., Koval, I.K., and Morozhenko, A.V.
1967, Trans. I.A.U. (Commission 16), Prague.
- de Vaucouleurs, G. 1964, Icarus 3, 187.
- Evans, D.C. 1965, Science 149, 969.
- Harris, D.L. 1961, in Planets and Satellites, ed. G.P.
Kuiper and B.M. Middlehurst (U. Chicago Press) Ch. 8.
- Johnson, H.L., Mitchell, R.I., Iriarte, B., and Wisniewski,
W.Z. 1966, Comm. Lunar Planet. Lab. 4, No. 63.
- O'Leary, B.T. 1967, Ap. J. 149, L147.
- Pollack, J.B. 1965, thesis, Harvard University.
- Tull, R.G. 1966, Icarus 5, 505.
- Young, A.T. and Irvine, W.M. 1967, Astron. J. 72, 945,
(Paper I).
- Younkin, R.L. 1966, Ap. J. 144, 809.
- van den Bergh, S. 1965, J. Roy. Astron. Soc. Canada 59,
253.
- Walker, R.G. 1966, thesis, Harvard University.

Table I

Effective Wavelengths of Pass Bands*

Band	v	u	s	p	m	l	k	h	g	e	d	c	b
λ_{eff}	3147	3590	3926	4155	4573	5012	6264	7297	8595	10,635	U	B	V
half-width	145	120	45	90	85	90	160	200	90	770	580	1020	800

* For details, see Paper I.

TABLE II

MAGNITUDES OF STANDARD STARS AT LE HOUGA

STAR	V	u	s	p	m	l	k	h	g	e	U	B	V	\bar{n}	ny
α AQL	0.255	0.444	-0.293	0.209	0.461	0.612	0.963	1.110	1.257	1.389	1.034	0.968	0.760	123	120
α AQR	4.099	3.829	3.744	3.478	3.187	3.039	2.846	2.784	2.715	2.649	4.642	3.905	2.939	59	17
α ARI	3.832	3.471	3.282	2.927	2.334	2.162	1.823	1.671	1.503	1.328	4.302	3.175	2.030	72	45
α BOO	2.233	1.597	1.408	0.942	0.330	0.141	-0.343	-0.572	-0.757	-0.960	2.427	1.168	-0.059	29	32
α GEN	0.781	1.095	0.153	0.835	1.174	1.396	1.861	2.090	2.331	2.500	1.599	1.622	1.579	19	17
α LEO	-0.128	0.326	-0.309	0.461	0.883	1.134	1.690	1.984	2.239	2.465	0.876	1.242	1.349	33	25
α LYR	-0.872	-0.606	-1.637	-0.865	-0.487	-0.253	0.271	0.524	0.766	0.948(-0.030X-0.034X-0.030)				14	14
α OPH	1.681	1.798	0.923	1.465	1.739	1.919	2.331	2.528	2.662	2.801	2.338	2.236	2.079	12	6
α PEG	1.601	1.926	0.858	1.627	2.026	2.258	2.813	3.067	3.296	3.476	2.369	2.435	2.471	54	48
α SER	4.634	4.237	3.913	3.676	2.933	2.765	2.439	2.291	2.171	1.994	5.053	3.816	2.617	26	5
β ARI	2.072	2.325	1.437	(2.028)(2.311)(2.496)	(2.311)(2.496)	(2.496)(2.924)(3.139)(3.320)(3.461)								42	28
β CNC		5.951	5.758	5.065	4.104	3.83	3.206	2.889	2.634	2.378	6.805	5.014	3.531	19	
β GEM	2.418	2.192	1.980	1.805	1.368	1.261	1.002	0.899	0.810	0.700	3.003	2.141	1.139	38	37
β LEO	1.436	1.764	0.915	1.443	1.727	1.931	2.379	2.603	2.817	2.950	2.273	2.211	2.111	27	27
β OPH		4.370	4.040	3.771	3.068	2.905	2.556	2.432	2.282	2.123	5.171	3.912	2.751	17	
β ORI	-1.527	-1.196	-1.379	-0.625	-0.229	-0.013	0.441	0.686	0.865	1.140	-0.517	0.137	0.182	15	15
β TAU	0.004	0.403	-0.052	0.744	1.185	1.451	2.006	2.284	2.563	2.844	1.037	1.531	1.654	10	7
γ GEM	1.213	1.556	0.487	(1.140)(1.496)(1.715)(2.254)(2.492)(2.694)(2.853)							1.928	1.935	1.919	8	8
γ PEG				1.812	2.289	2.591	3.261	3.590	3.917	4.307	1.772	2.584	2.814	6	
ϵ AQR	2.829	3.364	2.249	2.976	3.352	3.565	4.078	4.331	4.540	4.709	3.760	3.774	3.776	49	16
ϵ CYG	3.817	3.563	3.378	3.135	2.715	2.574	2.336	2.218	2.095	1.983	4.382	3.508	2.493	56	56
η BOO	2.694	2.684	2.478	2.618	2.635	2.664	2.690	2.724	2.760	2.801	3.455	3.251	2.668	24	24
η PEG	3.660	3.614	3.259	3.289	3.073	2.911	2.863	2.807	2.731	2.655	4.359	3.785	2.936	76	68
η SER		4.021	3.891	3.747	3.441	3.310	3.145	3.048	2.955	2.856	4.893	4.198	3.252	10	
κ CET		4.943	4.904	4.891	4.865	4.864	4.815	4.829	4.837	4.858	5.749	5.517	4.839	24	7
δ 5PEG		5.678	5.742	5.768	5.772	5.767	5.722	5.687	5.631	5.598	6.515	6.418	5.748	28	
HR7569		6.158	6.115	6.128	6.137	6.112	6.130	6.149	6.151	6.116	6.961	6.786	6.141	16	12
β LIB	(1.340)	(1.600)	(0.935)	(1.713)	(2.126)	(2.338)	(2.926)	(3.238)	(3.483)	(3.698)				6	
ϵ TAU	(4.854)	(4.641)	(4.385)	(4.273)	(3.783)	(3.653)	(3.431)	(3.348)	(3.264)	(3.184)					

Table III

Color of the Sun in Final Magnitude System for $(B-V)_\odot \equiv 0.65$ $(\epsilon = \text{estimated error})$

	v-V	u-V	s-V	p-V	m-V	l-V	k-V	h-V	g-V	e-V	U-B	B-V
color	0.	0.	0.	0.	0.	0.	0.	0.	0.	0.	0.14*	0.65
ϵ	0.050	0.020	0.030	0.006	0.004	0.005	0.008	0.006	0.009	0.010	---	---

* Harris (1961)

TABLE IV. MONOCHROMATIC MAGNITUDES OF VENUS AT LE HOUCA.

NO	DATE	TIME	PHASE	3147	3590	3926	41:5	4573	5012	6264	7297	8595	10635	U	B	V
1	AUG 24 64	3 22	92.58	-2.67	-2.69	-2.78	-2.87	-2.96	-2.95	-3.10	-3.05	-3.02	-2.97	-1.89	-2.28	-2.99
2	AUG 25 64	3 18	91.92	-2.41	-2.47	-2.59	-2.3	-2.84	-2.86	-3.02	-3.00	-2.97	-2.97	-1.67	-2.15	-2.90
3	AUG 30 64	3 45	88.80	-2.50	-2.58	-2.70	-2.11	-2.89	-2.91	-3.07	-3.07	-3.04	-3.03			*
4	SEP 08 64	4 32	83.48	-2.60	-2.69	-2.79	-2.0	-2.98	-3.00	-3.17	-3.19	-3.16	-3.14			*
5	SEP 09 64	4 19	82.92	-2.56	-2.63	-2.74	-2.18	-2.99	-3.01	-3.17	-3.17	-3.15	-3.13			*
6	SEP 21 64	5 35	76.50	-2.77	-2.86	-2.99	-3.1	-3.19	-3.25	-3.40	-3.37	-3.36	-3.37			*
7	SEP 22 64	5 32	76.00	-2.56	-2.65	-2.78	-2.5	-3.09	-3.14	-3.30	-3.22	-3.30	-3.26			*
8	DEC 07 64	11 57	43.10	-3.35	-3.32	-3.47	-3.2	-3.79	-3.82	-4.03	-4.01	-4.02	-3.97	-2.59	-3.12	-3.93
9	DEC 09 64	14 42	42.40	-3.20	-3.34	-3.43	-3.2	-3.73	-3.80	-3.92	-3.89	-3.85	-3.84	-2.56	-3.00	-3.79
10	JUL 26 65	20 14	41.30		-3.34	-3.51								-2.74	-3.21	-3.85
11	AUG 11 65	19 24	47.80		-3.47	-3.65	-3.6	-3.82	-3.83	-4.16	-4.19	-3.96	-3.96	-2.75	-3.16	-3.78

Notes to Table IV

- (1) Aug 24 64: end of night, $r \approx -0.04$, large extinction
- (2) Aug 25 64: end of night
- (3) Aug 30 64: end of night
- (4) Sep 08 64: end of night, clouds (pml)
- (5) Sep 09 64: end of night, clouds
- (6) Sep 21 64: $r \approx -0.07$
- (7) Sep 22 64: end of night, mist (vus)
- (8) Dec 07 64: $M \approx 3$, mist
- (9) Dec 09 64: daylight obs., extinction poorly determined
- (10) Jul 26 65: $M \approx 7.5$
- (11) Aug 11 65: $4(bcd) \lesssim M \lesssim 6(khge)$

TABLE V. MONOCHROMATIC MAGNITUDES OF MARS AT LE HOUGA.

NU	DATE	TIME	PHASE	3147	3590	3926	4155	4573	5012	6264	7297	8595	10635	U	B	V
1	MAY 03 63	11 40	37.39		0.08	0.05	-0.06	-0.37	-0.59		-1.68	-1.65	-1.67	0.83	0.48	-0.92
2	MAY 16 63	12 04	37.68		0.23	0.15		-0.31	-0.57		-1.76	-1.75	-1.79	1.02	0.55	-0.93
3	MAY 16 63	14 17	37.63		0.18		0.03	-0.29	-0.52		-1.69	-1.66	-1.67	1.04	0.59	-0.77
4	MAY 20 63	12 10	37.65		0.22	0.16	0.03	-0.32	-0.56		-1.84	-1.85	-1.87	0.99	0.52	-1.01
5	MAY 20 63	12 14	37.65		0.31	0.22	0.06	-0.26	-0.51		-1.76	-1.78	-1.79	1.11	0.57	-0.89
6	MAY 24 63	15 19	37.57		0.19	0.12	-0.04	-0.29	-0.57		-1.83	-1.84	-1.88	0.97	0.49	-0.96
7	MAY 24 63	15 04	37.57		0.30	0.24	0.01	-0.36	-0.68		-1.71	-1.63	-1.76	1.13	0.51	-0.87
8	JUN 11 63	15 58	36.71		-0.03	-0.11	-0.22	-0.46	-0.62		-1.60	-1.60	-1.60	0.84	0.39	-0.93
9	JUN 11 63	15 23	36.71		0.12	0.06	-0.01	-0.52	-0.72		-1.66	-1.65	-1.60		0.48	-0.91
10	JUN 17 63	14 18	36.27		0.24	0.20		-0.40	-0.69		-1.50	-1.48	-1.46	0.89	0.43	-0.86
11	JUN 17 63	15 41	36.27		0.11	0.07	-0.11	-0.51	-0.71		-1.86	-1.88	-1.86	0.96	0.47	-0.98
12	JUN 25 63	15 17	35.59		-0.02	-0.10	-0.11	-0.59	-0.82		-1.81	-1.81	-1.83	0.91	0.35	-1.01
13	JUL 11 63	16 10	33.97	-0.10	-0.05	-0.16	-0.21	-0.59	-0.82	-1.75	-1.94	-1.94	-1.95	0.73	0.11	-1.25
14	AUG 24 64	2 54	27.68	0.08	0.09	-0.05	-0.11	-0.51	-0.76	-1.66	-1.86	-1.89	-1.91	0.88	0.24	-1.13
15	AUG 25 64	2 52	27.82	0.05	0.14	0.01	-0.11	-0.46	-0.70	-1.57	-1.77	-1.75	-1.75	0.93	0.36	-0.99
16	AUG 30 64	3 10	28.49	0.16	0.21	0.09	-0.01	-0.38	-0.61	-1.51	-1.71	-1.69	-1.69	1.02	0.45	-0.95
17	SEP 08 64	4 02	29.68	0.10	0.16	0.03	-0.11	-0.42	-0.65	-1.49	-1.70	-1.66	-1.65	0.96	0.42	-0.95
18	SEP 09 64	3 49	29.81	0.05	0.11	-0.02	-0.11	-0.48	-0.75	-1.71	-1.92	-1.94	-1.98	0.90	0.34	-1.09
19	SEP 21 64	4 28	31.33	0.05	0.20	0.06	-0.01	-0.41	-0.68	-1.64	-1.81	-1.90	-1.91	1.02	0.43	-1.02
20	SEP 22 64	4 29	31.45	0.18	0.26	0.22	0.11	-0.27	-0.54	-1.56	-1.81	-1.85	-1.88	1.19	0.55	-0.92
21	DEC 07 64	5 39	36.70	0.36	0.37	0.32	0.03	-0.32	-0.58	-1.57	-1.80	-1.83	-1.84	1.10	0.50	-0.95
22	DEC 07 64	11 23	36.70	0.21	0.27	0.21	0.08	-0.29	-0.57	-1.61	-1.84	-1.91	-1.93	1.13	0.50	-0.96
23	DEC 08 64	8 32	36.63	0.27	0.32	0.19	0.03	-0.29	-0.57	-1.64	-1.82	-1.91	-1.91	1.04	0.42	-0.98
24	JAN 10 65	9 05	32.62	0.13	0.18	0.06	-0.04	-0.39	-0.65	-1.65	-1.89	-1.91	-1.91	1.01	0.42	-0.98
25	JAN 10 65	11 16	32.62	0.01	-0.02	-0.12	-0.17	-0.47	-0.69	-1.64	-1.84	-1.82	-1.78	0.83	0.30	-1.04
26	FEB 02 65	9 20	24.30	0.05	0.10	-0.03	-0.10	-0.42	-0.67	-1.64	-1.85	-1.82	-1.82	0.91	0.35	-1.03
27	FEB 02 65	11 32	24.30	0.07	0.09	0.06	-0.12	-0.44	-0.67	-1.60	-1.80	-1.77	-1.77	0.91	0.34	-1.01
28	FEB 03 65	8 59	23.79	0.07	0.09	0.06	-0.12	-0.44	-0.67	-1.60	-1.80	-1.77	-1.77	0.91	0.34	-1.01
29	FEB 03 65	11 48	23.79	-0.02	0.02	-0.10	-0.16	-0.48	-0.71	-1.66	-1.86	-1.86	-1.84	0.83	0.29	-1.06
30	FEB 04 65	14 08	23.79	-0.04	0.02	-0.10	-0.17	-0.50	-0.74	-1.72	-1.92	-1.92	-1.90	0.86	0.27	-1.10
31	FEB 04 65	9 05	23.28	0.02	-0.00	-0.12	-0.18	-0.48	-0.70	-1.62	-1.83	-1.78	-1.76	0.85	0.32	-1.03
32	FEB 04 65	11 38	23.28	-0.03	-0.01	-0.11	-0.18	-0.48	-0.71	-1.63	-1.82	-1.82	-1.80	0.84	0.29	-1.05
33	FEB 04 65	9 34	20.50	-0.08	-0.06	-0.19	-0.25	-0.48	-0.71	-1.63	-1.82	-1.82	-1.80	0.83	0.21	-1.21
34	FEB 09 65	11 52	20.50	0.02	0.01	-0.14	-0.21	-0.48	-0.71	-1.63	-1.82	-1.82	-1.80	0.88	0.30	-1.08
35	FEB 24 65	22 43	10.40	-0.34	-0.40	-0.52	-0.63	-0.81	-1.01	-1.93	-2.12	-2.12	-2.13	0.50	-0.04	-1.33
36	MAR 09 65	21 42	2.41	-0.43	-0.45	-0.59	-0.7	-0.96	-1.17	-2.01	-2.16	-2.12	-2.08	0.38	-0.18	-1.46
37	MAR 09 65	21 33	2.42	-0.46	-0.43	-0.59	-0.8	-0.99	-1.22	-2.06	-2.22	-2.19	-2.16	0.35	-0.22	-1.50
38	MAR 16 65	21 04	6.61	-0.29	-0.36	-0.47	-0.4	-0.86	-1.08	-1.99	-2.22	-2.22	-2.19			
39	MAR 25 65	20 29	13.45	-0.24	-0.24	-0.36	-0.5	-0.76	-0.99	-1.98	-2.21	-2.22	-2.22	0.57	0.03	-1.33
40	MAR 25 65	23 08	13.45	-0.21	-0.13	-0.27	-0.4	-0.71	-0.94	-2.00	-2.22	-2.22	-2.22	0.66	0.07	-1.32
41	MAR 25 65	1 03	13.45	-0.10	-0.09	-0.23	-0.4	-0.66	-0.91	-1.89	-2.11	-2.12	-2.12	0.71	0.12	-1.26
42	MAR 27 65	19 49	14.91	-0.24	-0.25	-0.36	-0.4	-0.71	-0.91	-1.85	-2.09	-2.08	-2.09	0.55	0.05	-1.27
43	MAR 27 65	22 22	14.91	-0.19	-0.15	-0.28	-0.4	-0.69	-0.92	-1.96	-2.18	-2.19	-2.19	0.63	0.08	-1.32
44	MAR 27 65	1 06	14.91	-0.21	-0.17	-0.30	-0.4	-0.71	-0.94	-1.94	-2.17	-2.17	-2.18	0.66	0.07	-1.31
45	MAR 27 65	2 45	14.91	-0.19	-0.18	-0.31	-0.4	-0.70	-0.92	-1.91	-2.14	-2.11	-2.12	0.67	0.09	-1.29
46	MAR 28 65	20 18	15.63	-0.37	-0.33	-0.45	-0.5	-0.78	-0.97	-1.91	-2.09	-2.11	-2.10	0.47	-0.02	-1.31
47	MAR 28 65	23 01	15.63	-0.22	-0.17	-0.31	-0.4	-0.70	-0.93	-1.97	-2.19	-2.20	-2.21	0.64	0.08	-1.30
48	MAR 28 65	1 06	15.63	-0.16	-0.11	-0.25	-0.34	-0.66	-0.92	-1.93	-2.17	-2.16	-2.19	0.70	0.11	-1.29
49	MAR 28 65	3 00	15.63	-0.08	-0.05	-0.22	-0.34	-0.66	-0.92	-1.93	-2.17	-2.16	-2.19	0.79	0.18	-1.24
50	MAR 29 65	19 30	16.31	-0.21	-0.29	-0.40	-0.45	-0.72	-0.90	-1.82	-2.02	-2.03	-2.00	0.52	0.03	-1.25
51	MAR 29 65	22 05	16.31	-0.25	-0.24	-0.36	-0.43	-0.73	-0.94	-1.91	-2.12	-2.14	-2.13	0.57	0.04	-1.30
52	MAR 29 65	2 42	16.31	-0.25	-0.14	-0.28	-0.36	-0.69	-0.92	-1.93	-2.17	-2.18	-2.18	0.66	0.08	-1.32
53	MAR 29 65	2 30	16.31	-0.07	-0.09	-0.26	-0.33	-0.66	-0.88	-1.89	-2.11	-2.14	-2.15	0.69	0.13	-1.28
54	MAR 30 65	19 45	17.03	-0.32	-0.37	-0.45	-0.52	-0.78	-0.97	-1.90	-2.11	-2.08	-2.06	0.47	-0.02	-1.29
55	MAR 30 65	22 29	17.03	-0.20	-0.19	-0.31	-0.38	-0.67	-0.88	-1.85	-2.09	-2.10	-2.10	0.59	0.08	-1.26

NO	DATE	TIME	PHASE	3147	3590	3926	4155	4573	5012	6264	7297	8595	10635	U	B	V
56	MAR 30 65	1 00	17.03	-0.11	-0.10	-0.21	-0.31	-0.63	-0.86	-1.88	-2.10	-2.12	-2.15	0.69	0.12	-1.27
57	APR 03 65	20 03	17.70			-0.10	-0.25	-0.57	-0.78	-1.74	-1.91	-1.93	-1.91	0.70	0.19	-1.14
58	MAY 08 65	20 29	34.97		0.02	-0.18	-0.12	-0.41	-0.62	-1.48	-1.72	-1.73	-1.72	0.87	0.39	-0.91
59	MAY 08 65	22 13	34.97		-0.07	-0.18	-0.21	-0.50	-0.70	-1.61	-1.85	-1.86	-1.86			*
60	MAY 10 65	20 47	35.45		0.03	-0.09	-0.11	-0.40	-0.61	-1.48	-1.72	-1.71	-1.71	0.90	0.41	-0.90
61	MAY 10 65	23 28	35.45		0.01	-0.12	-0.15	-0.42	-0.66	-1.54	-1.79	-1.79	-1.81	0.83	0.35	-0.97
62	MAY 11 65	20 43	35.68		0.07	-0.05	-0.17	-0.36	-0.59	-1.44	-1.69	-1.68	-1.67	0.92	0.43	-0.90
63	MAY 11 65	5	35.68		-0.04	-0.15	-0.18	-0.46	-0.69	-1.58	-1.82	-1.84	-1.85	0.84	0.36	-0.99
64	MAY 12 65	20 48	35.90		0.10	-0.01	-0.14	-0.34	-0.55	-1.45	-1.68	-1.67	-1.66	0.96	0.46	-0.86
65	MAY 12 65	8	35.90		-0.04	-0.17	-0.9	-0.48	-0.70	-1.44	-1.70	-1.69	-1.68	0.84	0.34	-0.97
66	MAY 13 65	20 47	36.12		0.14	0.01	-0.13	-0.33	-0.57	-1.52	-1.77	-1.74	-1.75	0.97	0.46	-0.90
67	MAY 13 65	23 59	36.12		-0.13	-0.23	-0.6	-0.52	-0.73	-1.52	-1.77	-1.74	-1.75	0.74	0.30	-1.00
68	MAY 19 65	20 55	37.25		0.18	0.04	0.1	-0.30	-0.53					1.01	0.49	-0.87
69	MAY 21 65	21 11	37.57		0.15	0.04	0.10	-0.30	-0.53					1.01	0.50	-0.84
70	MAY 23 65	21 39	37.87		0.07	-0.06	-0.1	-0.36	-0.57	-1.43	-1.65	-1.63	-1.60	0.90	0.43	-0.87
71	MAY 23 65	23 26	37.87		0.24	0.11	0.16	-0.26	-0.50	-1.38	-1.66	-1.64	-1.62	1.06	0.56	-0.83
72	JUN 17 65	21 32	39.80		0.09	-0.03	-0.18	-0.35	-0.54	-1.38	-1.61	-1.63	-1.61	0.92	0.44	-0.84
73	JUN 18 65	21 43	39.83		0.02	-0.09	-0.5	-0.40	-0.60	-1.37	-1.59	-1.60	-1.54	0.86	0.40	-0.88
74	JUN 22 65	22 31	39.88		0.28	0.18	0.11	-0.14	-0.36	-1.36	-1.62	-1.59	-1.54	1.11	0.63	-0.75
75	JUN 24 65	21 31	35.89											1.13	0.59	-0.85
76	JUL 05 65	21 28	39.74		0.27	0.14	0.30	-0.30	-0.50	-1.44	-1.65	-1.65	-1.57	1.08	0.59	-0.85
77	JUL 06 65	21 42	39.71		0.27	0.10	0.39	-0.24	-0.51							*
78	JUL 09 65	21 05	39.61		0.39	0.23	0.15	-0.20	-0.45	-1.46	-1.70	-1.73	-1.72	1.17	0.61	-0.85
79	JUL 10 65	21 10	39.57		0.34	0.24	0.13	-0.21	-0.48	-1.50	-1.74	-1.77	-1.73	1.19	0.60	-0.87
80	JUL 11 65	21 22	39.53		0.14	0.07	-0.32	-0.35	-0.63	-1.55	-1.83	-1.83	-1.83	1.05	0.47	-1.02
81	JUL 16 65	21 09	39.30		0.08	0.06								1.01	0.44	-1.01

Notes to Table V

- (2) May 16 63: clouds
- (7) May 24 63: $M = 3.2$
- (9) Jun 11 63: $M = 3$
- (11) Jun 17 63: $M = 3.4$
- (12) Jun 25 63: $M = 2.5$
- (13) Jul 11 63: $M = 3.5$
- (14) Aug 24 64: end of night, $r \approx -0.04$, large extinction
- (15) Aug 25 64: end of night
- (16) Aug 30 64: end of night
- (17) Sep 08 64: clouds
- (18) Sep 09 64: clouds
- (19) Sep 21 64: $r \approx -0.03$
- (36) Mar 09 65: mist (vus, bcd)
- (37) Mar 09 65: mist (vus)
- (38) Mar 16 65: poor night
- (41) Mar 25 65: clouds, $r \approx 0.04$
- (43) Mar 27 65: clouds (khge)
- (49) Mar 28 65: $M = 2.5$
- (51) Mar 29 65: clouds
- (53) Mar 29 65: clouds
- (54) Mar 30 65: $r \approx -0.05$
- (56) Mar 30 65: clouds
- (59) May 08 65: clouds
- (60) May 10 65: mist (khge)
- (63) May 11 65: $M = 2.8$

- (65) May 12 65: mist (bcd)
- (66) May 13 65: mist
- (67) May 13 65: $M = 2.8$, $r \approx -0.05$ (suv-pml)
- (69) May 21 65: clouds
- (70) May 23 65: clouds (khge)
- (71) May 23 65: $M = 2.7$
- (72) Jun 17 65: clouds
- (73) Jun 18 65: $r \approx -0.03$
- (74) Jun 22 65: $M = 4$, clouds
- (75) Jun 24 65: mist (bcd)
- (76) Jul 05 65: mist, $M = 3$
- (77) Jul 06 65: $M = 3.3$, large extinction
- (78) Jul 09 65: $M = 3$
- (79) Jul 10 65: $M = 3$
- (80) Jul 11 65: $M = 3.3$, $r \approx -0.04$ (vas-pml)
- (81) Jul 16 65: $M = 3.3$, clouds

TABLE VI. MONOCHROMATIC MAGNITUDES OF JUPITER AT LE HUGA.

NO	DATE	TIME	PHASE	3147	3590	3926	415	4573	5012	6264	7297	8595	10635	U	R	V
1	JUL 13 63	21 52	11.83	-8.50	-8.67	-8.89	-8.12	-9.14	-9.23		-9.19		-8.80	-7.95	-8.42	-9.24
2	JUL 13 63	23 19	11.83	-8.44	-8.67	-8.88	-8.14	-9.15	-9.24		-9.17		-8.76	-7.91	-8.39	-9.25
3	JUL 20 63	21 54	11.70	-8.45	-8.69	-8.93	-8.14	-9.17	-9.25		-9.23	-8.70	-8.83	-7.90	-8.41	-9.24
4	JUL 20 63	23 17	11.70	-8.48	-8.72	-8.93	-8.17	-9.18	-9.26		-9.21	-8.67	-8.81	-7.93	-8.42	-9.27
5	JUL 28 63	21 32	11.37								-9.23	-8.67	-8.85			
6	JUL 28 63	23 36	11.37	-8.49	-8.66	-8.86	-8.9	-9.09	-9.18		-9.20	-8.71	-8.82	-7.89	-8.38	-9.21
7	AUG 10 63	22 18	10.40								-9.25	-8.71	-8.84			
8	AUG 10 63	36	10.40								-9.17	-8.64	-8.77			
9	AUG 21 63	22 36	5.14								-9.25	-8.73	-8.86			
10	AUG 22 63	22 30	9.01								-9.25	-8.71	-8.88			
11	AUG 22 63	23 50	5.01								-9.25	-8.72	-8.88			
12	AUG 25 63	22 27	8.98								-9.27	-8.72	-8.87			
13	AUG 25 63	43	8.98								-9.21	-8.67	-8.83			
14	SEP 20 63	22 19	3.88	-8.57	-8.79	-9.01	-9.02	-9.25	-9.32		-9.32	-8.75	-8.88	-8.09	-8.57	-9.36
15	SEP 25 63	22 56	2.80	-8.64	-8.85	-9.05	-9.07	-9.28	-9.35		-9.31	-8.73	-8.83	-8.11	-8.57	-9.37
16	SEP 28 63	22 56	2.15	-8.63	-8.84	-9.03	-9.05	-9.27	-9.34		-9.31	-8.73	-8.84	-8.12	-8.55	-9.36
17	SEP 28 63	1 37	2.15	-8.59	-8.86	-9.05	-9.07	-9.29	-9.35		-9.31	-8.73	-8.84	-8.13	-8.56	-9.38
18	SEP 28 63	3 41	2.15	-8.64	-8.88	-9.08	-9.09	-9.30	-9.36		-9.30	-8.74	-8.85	-8.13	-8.59	-9.39
19	SEP 29 63	22 20	1.93	-8.61	-8.85	-9.04	-9.05	-9.27	-9.34		-9.32	-8.75	-8.86	-8.11	-8.57	-9.37
20	SEP 29 63	26	1.93	-8.57	-8.85	-9.04	-9.07	-9.29	-9.36		-9.32	-8.75	-8.86	-8.13	-8.57	-9.37
21	SEP 29 63	3 33	1.93	-8.54	-8.82	-9.02	-9.04	-9.26	-9.33		-9.30	-8.72	-8.83	-8.07	-8.56	-9.36
22	OCT 08 63	21 49	0.20	-8.58	-8.83	-9.03	-9.06	-9.27	-9.33		-9.34	-8.71	-8.84	-8.05	-8.56	-9.34
23	OCT 08 63	44	0.20	-8.65	-8.86	-9.06	-9.11	-9.29	-9.37		-9.32	-8.71	-8.84	-8.13	-8.56	-9.40
24	OCT 08 63	3 04	0.20	-8.63	-8.91	-9.11	-9.15	-9.35	-9.41		-9.33	-8.73	-8.85	-8.13	-8.51	-9.43
25	OCT 09 63	14	0.48											-8.04	-8.54	-9.35
26	OCT 09 63	24	0.48	-8.51	-8.79	-9.02	-9.03	-9.24	-9.32		-9.30	-8.72	-8.85	-8.08	-8.58	-9.32
27	OCT 10 63	21 45	0.68								-9.27	-8.65	-8.78			
28	OCT 10 63	1	0.68								-9.29	-8.67	-8.79			
29	OCT 15 63	21 35	1.73								-9.33	-8.74	-8.83			
30	OCT 15 63	48	1.73	-8.65	-8.84	-9.03	-5.09	-9.28	-9.35		-9.30	-8.71	-8.81	-8.09	-8.55	-9.37
31	OCT 19 63	21 57	2.61	-8.62	-8.77	-8.99	-5.01	-9.24	-9.30		-9.30	-8.81	-8.90	-8.02	-8.52	-9.33
32	OCT 31 63	22 35	5.11	-8.58	-8.78	-9.00	-5.03	-9.25	-9.33		-9.32	-8.73	-8.84	-8.04	-8.54	-9.35
33	OCT 31 63	2 57	5.11	-8.54	-8.78	-8.98	-5.02	-9.24	-9.31		-9.32	-8.73	-8.84	-8.04	-8.54	-9.35
34	NOV 23 63	2 16	8.94	-8.46	-8.72	-8.87	-1.95	-9.18	-9.27		-9.30	-8.70	-8.81	-6.01	-8.51	-9.34
35	NOV 23 63	4 14	8.94	-8.47	-8.66	-8.82	-1.90	-9.17	-9.23					-7.94	-8.46	-9.29
36	DEC 05 63	2 04	10.26	-8.45	-8.66	-8.88	-1.92	-9.15	-9.23		-9.25	-8.70	-8.80	-7.88	-8.44	-9.28
37	DEC 05 63	4 17	10.26											-7.93	-8.45	-9.28
38	DEC 21 63	1 04	11.25											-8.45	-8.45	-9.29
39	DEC 21 63	1 19	11.25	-8.56	-8.72	-8.88	-1.97	-9.23	-9.28		-9.23	-8.69	-8.75	-7.99	-8.48	-9.29
40	DEC 21 63	4 13	11.25	-8.61	-8.75	-8.93	-1.99	-9.21	-9.31		-9.29	-8.77	-8.79	-7.92	-8.46	-9.30
41	DEC 24 63	2 20	11.35	-8.44	-8.66	-8.82	-1.90	-9.13	-9.20		-9.21	-8.67	-8.75	-7.92	-8.47	-9.31
42	DEC 24 63	4 13	11.35	-8.55	-8.66	-8.81	-1.88	-9.12	-9.20		-9.22	-8.69	-8.75	-7.87	-8.41	-9.25
43	DEC 25 63	2 30	11.37	-8.53	-8.75	-8.93	-1.90	-9.21	-9.29		-9.22	-8.66	-8.78	-7.87	-8.42	-9.26
44	DEC 28 63	1 51	11.42	-8.38	-8.67	-8.84	-1.91	-9.14	-9.24		-9.28	-8.71	-8.82	-7.96	-8.48	-9.33
45	AUG 10 64	23 22	11.67	-8.55	-8.64	-8.84	-1.91	-9.14	-9.24		-9.28	-8.71	-8.82	-7.87	-8.41	-9.27
46	AUG 11 64	23 39	11.69	-8.54	-8.64	-8.86	-1.96	-9.14	-9.25		-9.04	-8.72	-8.83	-7.86	-8.40	-9.27
47	AUG 11 64	1 03	11.69	-8.58	-8.64	-8.85	-1.95	-9.14	-9.23		-9.33	-8.72	-8.83	-7.87	-8.40	-9.27
48	AUG 24 64	23 45	11.63	-8.77	-8.85	-9.04	-1.90	-9.25	-9.33		-9.05	-8.71	-8.82	-7.87	-8.41	-9.28
49	AUG 24 64	2 25	11.63	-8.74	-8.79	-8.98	-1.90	-9.23	-9.30		-9.12	-8.75	-8.84	-8.08	-8.58	-9.40
50	AUG 25 64	23 32	11.60	-8.58	-8.70	-8.90	-1.97	-9.15	-9.25		-9.40	-8.76	-8.83	-8.01	-8.52	-9.37
51	AUG 25 64	2 02	11.60	-8.54	-8.65	-8.86	-1.96	-9.13	-9.23		-9.38	-8.75	-8.85	-7.93	-8.45	-9.34
52	AUG 25 64	3 43	11.60	-8.49	-8.62	-8.84	-1.92	-9.11	-9.19		-9.34	-8.72	-8.82	-7.90	-8.43	-9.30
53	AUG 30 64	23 50	11.42	-8.52	-8.62	-8.82	-1.90	-9.21	-9.24		-9.37	-8.75	-8.81	-7.87	-8.40	-9.28
54	AUG 30 64	1 38	11.42	-8.56	-8.65	-8.87	-1.97	-9.13	-9.21		-9.35	-8.74	-8.79	-7.85	-8.38	-9.24
55	SEP 08 64	50	10.92	-8.58	-8.67	-8.87	-1.97	-9.14	-9.23		-9.36	-8.76	-8.81	-7.90	-8.42	-9.28

NU	DATE	TIME	PHASE	3147	3550	3926	4555	4573	5012	6264	7297	8595	10635	U	B	V
56	SEP 08 64	3 33	10.92	-8.55	-8.65	-8.87	-8.96	-9.14	-9.25	-9.37	-9.09	-8.75	-8.82	-7.88	-8.40	-9.28
57	SEP 09 64	19	10.85	-8.57	-8.66	-8.87	-8.97	-9.14	-9.23	-9.36	-9.08	-8.73	-8.80	-7.91	-8.41	-9.27
58	SEP 09 64	2 46	10.85	-8.57	-8.66	-8.87	-8.96	-9.13	-9.23	-9.38	-9.10	-8.75	-8.81	-7.89	-8.41	-9.27
59	SEP 13 64	29	10.51													
60	SEP 21 64	3 04	9.72	-8.61	-8.72	-8.93	-9.02	-9.18	-9.30	-9.40	-9.10	-8.79	-8.84	-7.96	-8.46	-9.32
61	SEP 22 64	1 30	9.60	-8.58	-8.67	-8.88	-8.97	-9.15	-9.26	-9.37	-9.07	-8.75	-8.81	-7.91	-8.41	-9.28
62	SEP 22 64	3 50	9.60	-8.53	-8.64	-8.85	-8.95	-9.12	-9.24	-9.36	-9.04	-8.75	-8.79	-7.87	-8.39	-9.28
63	SEP 23 64	50	9.47	-8.58	-8.66	-8.88	-8.97	-9.15	-9.24	-9.36	-9.04	-8.75	-8.79	-7.89	-8.41	-9.27
64	NOV 17 64	23 50	1.04	-8.72	-8.81	-8.99	-9.08	-9.24	-9.33	-9.47	-9.18	-8.83	-8.87	-8.04	-8.53	-9.37
65	NOV 17 64	3 15	1.06	-8.69	-8.77	-8.96	-9.06	-9.22	-9.31	-9.43	-9.14	-8.80	-8.84	-8.01	-8.50	-9.35
66	NOV 18 64	23 27	1.29	-8.59	-8.73	-8.86	-9.07	-9.24	-9.32	-9.46	-9.16	-8.84	-8.87	-7.98	-8.51	-9.35
67	NOV 18 64	3 05	1.29	-8.65	-8.77	-8.94	-9.05	-9.22	-9.32	-9.43	-9.17	-8.83	-8.87	-7.99	-8.50	-9.35
68	NOV 24 64	22	2.60	-8.79	-8.82	-9.00	-9.09	-9.25	-9.34	-9.47	-9.16	-8.84	-8.85	-8.01	-8.52	-9.37
69	DEC 07 64	1 15	5.30	-8.67	-8.82	-9.02	-9.09	-9.26	-9.34	-9.47	-9.16	-8.84	-8.85	-8.03	-8.52	-9.38
70	DEC 07 64	2 45	5.30	-8.67	-8.81	-9.00	-9.07	-9.23	-9.32	-9.46	-9.15	-8.84	-8.85	-8.03	-8.52	-9.37
71	DEC 08 64	1 08	5.49	-8.68	-8.82	-9.00	-9.07	-9.23	-9.31	-9.46	-9.14	-8.84	-8.83	-8.03	-8.52	-9.37
72	DEC 08 64	3 12	5.49	-8.62	-8.74	-8.93	-9.00	-9.17	-9.26	-9.41	-9.11	-8.81	-8.81	-7.95	-8.47	-9.31
73	DEC 09 64	43	5.68	-8.60	-8.73	-8.94	-9.02	-9.18	-9.27	-9.41	-9.11	-8.81	-8.82	-7.95	-8.46	-9.32
74	DEC 09 64	3 26	5.68	-8.64	-8.74	-8.94	-9.01	-9.17	-9.26	-9.41	-9.13	-8.81	-8.83	-7.95	-8.46	-9.33
75	JFC 12 64	1 05	6.23	-8.67	-8.78	-8.97	-9.04	-9.20	-9.26	-9.41	-9.10	-8.83	-8.82	-7.97	-8.47	-9.33
76	DEC 12 64	2 43	6.23	-8.63	-8.78	-8.97	-9.04	-9.20	-9.29	-9.42	-9.11	-8.82	-8.82	-7.98	-8.47	-9.32
77	DEC 29 64	2 51	8.90	-8.51	-8.62	-8.84	-9.00	-9.08	-9.18	-9.42	-9.11	-8.82	-8.82	-7.88	-8.38	-9.26
78	DEC 29 64	4 30	8.90											-7.97	-8.47	-9.34
79	DEC 30 64	2 35	9.03	-8.56	-8.71	-8.91	-9.08	-9.16	-9.24	-9.41	-9.10	-8.82	-8.82	-7.93	-8.44	-9.29
80	DEC 30 64	4 07	9.03	-8.51	-8.63	-8.86	-9.03	-9.11	-9.21	-9.37	-9.07	-8.79	-8.79	-7.92	-8.44	-9.30
81	DEC 30 64	7 33	9.03	-8.58	-8.68	-8.90	-9.06	-9.14	-9.22	-9.37	-9.05	-8.77	-8.77	-7.89	-8.43	-9.31
82	JAN 05 65	2 55	9.71	-8.55	-8.66	-8.87	-9.07	-9.15	-9.25	-9.37	-9.05	-8.77	-8.77	-7.93	-8.44	-9.32
83	JAN 05 65	4 20	9.71	-8.59	-8.72	-8.93	-9.01	-9.19	-9.29	-9.37	-9.08	-8.80	-8.80	-7.92	-8.43	-9.28
84	JAN 10 65	5 56	10.19	-8.56	-8.70	-8.93	-9.09	-9.16	-9.27	-9.39	-9.08	-8.80	-8.80	-7.89	-8.43	-9.29
85	JAN 23 65	3 31	11.04	-8.61	-8.69	-8.89	-9.07	-9.13	-9.22	-9.36	-9.03	-8.75	-8.72	-7.89	-8.43	-9.29
86	FEB 02 65	4 39	11.30	-8.56	-8.70	-8.90	-9.06	-9.13	-9.19	-9.36	-9.03	-8.75	-8.72	-7.91	-8.42	-9.27
87	FEB 02 65	7 03	11.30	-8.59	-8.74	-8.96	-9.01	-9.17	-9.25	-9.40	-9.07	-8.78	-8.78	-7.94	-8.45	-9.30
88	FEB 03 65	4 58	11.32	-8.54	-8.68	-8.88	-9.05	-9.11	-9.19	-9.36	-9.03	-8.75	-8.76	-7.90	-8.40	-9.26
89	FEB 03 65	7 24	11.32	-8.57	-8.69	-8.90	-9.06	-9.13	-9.21	-9.33	-9.01	-8.73	-8.75	-7.91	-8.44	-9.29
90	FEB 04 65	4 07	11.33	-8.55	-8.71	-8.92	-9.08	-9.15	-9.23	-9.38	-9.04	-8.76	-8.76	-7.90	-8.42	-9.27
91	FEB 04 65	7 53	11.33	-8.54	-8.75	-8.95	-9.14	-9.21	-9.29	-9.30	-9.00	-8.72	-8.74	-7.90	-8.48	-9.33
92	FEB 05 65	6 18	11.31											-8.00	-8.50	-9.37
93	MAR 09 65	19 29	10.06	-8.54	-8.73	-8.96	-9.02	-9.18	-9.28	-9.37	-9.05	-8.75	-8.75	-7.95	-8.45	-9.30
94	MAR 25 65	19 57	8.63	-8.61	-8.75	-8.97	-9.06	-9.23	-9.30	-9.38	-9.07	-8.76	-8.80	-7.96	-8.48	-9.35
95	MAR 28 65	19 47	8.31	-8.70	-8.78	-9.02	-9.09	-9.23	-9.30	-9.42	-9.10	-8.76	-8.82	-8.01	-8.51	-9.36
96	SEP 14 65	2 44	11.30											-7.95	-8.48	-9.29
97	SEP 19 65	1 50	11.36											-8.04	-8.55	-9.38
98	OCT 02 65	2 56	11.20											-8.03	-8.53	-9.37
99	OCT 11 65	2 55	10.78											-7.99	-8.50	-9.36
100	OCT 12 65	2 25	10.72											-7.98	-8.48	-9.32
101	OCT 27 65	20	9.38											-8.03	-8.53	-9.36
102	NOV 07 65	28	7.94											-8.02	-8.52	-9.33
103	DEC 14 65	21 19	0.78											-8.10	-8.60	-9.42
104	DEC 14 65	23 55	0.75											-8.09	-8.58	-9.40

Notes to Table VI

- (2) Jul 13 63: end of night
- (6) Jul 28 63: $M = 2.0$
- (25) Oct 09 63: poor night, $r \approx \pm 0.06$
- (26) Oct 09 63: poor night, $r \approx \pm 0.06$
- (27) Oct 10 63: poor night, extinction underestimated (?)
- (28) Oct 10 63: poor night, extinction underestimated (?)
- (30) Oct 15 63: extinction poorly determined (vuspmlbcdk)
- (37) Dec 05 63: fog
- (40) Dec 21 63: $M = 2.3$, large extinction (khge)
- (43) Dec 25 63: extinction poorly determined (khge)
- (48)(49) Aug 24 64: $r \approx -0.04$ (bcd-pml), large extinction
- (63) Sep 23 64: clouds (khge)
- (68) Nov 24 64: fog
- (69) Dec 07 64: $r \approx -0.04$ (vus-pml)
- (70) Dec 07 64: $r \approx -0.04$ (vus-pml)
- (77) Dec 29 64: poor night
- (78) Dec 29 64: poor night
- (96) Sep 14 65: fog
- (98) Oct 02 65: $r \approx -0.04$ (suv-pml)
- (101) Oct 27 65: clouds
- (102) Nov 07 65: clouds

TABLE VII. MONOCHROMATIC MAGNITUDES OF SATURN AT LE HOUGA.

NO	DATE	TIME	PHASE	3147	3590	3926	4155	4573	5012	6264	7297	8595	10635	U	B	V
1	MAY 20 63	18 37	5.83		-8.33	-8.42	-8.63	-8.88	-9.03		-9.29	-8.93	-9.10	-7.58	-8.22	-9.10
2	MAY 20 63	19 30	5.83		-8.30	-8.38	-8.59	-8.85	-9.00		-9.30	-8.93	-9.10	-7.52	-8.13	-9.10
3	MAY 24 63	18 24	5.78		-8.37	-8.47	-8.73	-8.97	-9.11					-7.59	-8.27	-9.11
4	MAY 24 63	19 30	5.78		-8.34	-8.43	-8.66	-8.95	-9.06		-9.22	-8.86	-9.05	-7.58	-8.17	-9.15
5	JUN 25 63	18 25	4.44								-9.28	-8.93	-9.15			*
6	JUN 25 63	20 24	4.44	-8.08	-8.29	-8.38	-8.61	-8.88	-9.05		-9.22	-8.89	-9.11	-7.47	-8.10	-9.15
7	JUL 11 63	19 23	3.21	-8.36	-8.45	-8.58	-8.72	-9.04	-9.19		-9.34		-9.25	-7.57	-8.26	-9.26
8	JUL 13 63	18 23	3.04	-8.45	-8.41	-8.60										*
9	JUL 13 63	20 02	3.04								-9.27		-9.18			*
10	JUL 13 63	23 00	3.04								-9.27		-9.17			*
11	JUL 20 63	20 03	2.39				-8.61	-8.95	-9.09		-9.32	-9.05	-9.24	-7.47	-8.14	-9.16
12	JUL 28 63	19 28	1.60	-8.33	-8.28	-8.36	-8.51	-8.90	-9.03		-9.48	-9.04	-9.33	-7.58	-8.20	-9.16
13	JUL 28 63	21 10	1.60	-8.28	-8.34	-8.46	-8.51	-8.87	-9.01		-9.36	-9.03	-9.28	-7.51	-8.13	-9.15
14	AUG 05 63	19 16	0.37								-9.48	-9.20	-9.35			*
15	AUG 10 63	19 29	0.27								-9.48	-9.21	-9.37			*
16	AUG 10 63	21 13	0.27								-9.49	-9.20	-9.37			*
17	AUG 21 63	19 01	0.94								-9.45	-9.14	-9.30			*
18	AUG 21 63	21 06	0.94								-9.41	-9.10	-9.31			*
19	AUG 22 63	18 48	1.04								-9.41	-9.16	-9.36			*
20	AUG 22 63	20 56	1.04								-9.41	-9.08	-9.32			*
21	AUG 25 63	20 33	1.34								-9.42	-9.10	-9.32			*
22	AUG 25 63	23 20	1.34								-9.35	-9.05	-9.27			*
23	SEP 20 63	20 32	3.76	-8.33	-8.44	-8.57	-8.66	-9.00	-9.13		-9.37	-9.04	-9.24	-7.64	-8.27	-9.28
24	SEP 25 63	20 52	4.13	-8.37	-8.43	-8.50	-8.63	-8.96	-9.10					-7.63	-8.25	-9.25
25	SEP 28 63	21 22	4.34	-8.29	-8.40	-8.51	-8.61	-8.93	-9.07		-9.33	-8.99	-9.18	-7.62	-8.21	-9.23
26	SEP 28 63	23 46	4.34	-8.40	-8.40	-8.50	-8.60	-8.93	-9.06		-9.35	-9.01	-9.18	-7.61	-8.22	-9.23
27	SEP 29 63	21 09	4.41	-8.33	-8.44	-8.54	-8.63	-8.96	-9.10		-9.35	-9.00	-9.18	-7.65	-8.24	-9.25
28	SEP 29 63	23 33	4.41	-8.32	-8.42	-8.51	-8.60	-8.93	-9.06		-9.32	-8.98	-9.18	-7.61	-8.23	-9.24
29	OCT 08 63	21 00	4.94	-8.32	-8.42	-8.51	-8.60	-8.93	-9.06		-9.26	-8.88	-9.09	-7.48	-8.11	-9.11
30	OCT 08 63	23 54	4.94	-8.17	-8.29	-8.40	-8.50	-8.88	-9.01		-9.28	-8.87	-9.08	-7.45	-8.16	-9.13
31	OCT 10 63	20 38	5.05	-8.13	-8.27	-8.35					-9.24	-8.87	-9.07			*
32	OCT 10 63	22 56	5.05								-9.21	-8.83	-9.01			*
33	OCT 15 63	20 34	5.27								-9.32	-8.97	-9.15			*
34	OCT 15 63	22 33	5.27								-9.32	-8.96	-9.14			*
35	OCT 19 63	20 11	5.42	-8.45	-8.42	-8.55	-8.65	-9.00	-9.10		-9.47	-9.10	-9.25	-7.66	-8.27	-9.23
36	OCT 19 63	21 33	5.42	-8.35	-8.37	-8.46	-8.56	-8.96	-9.07		-9.42	-9.06	-9.25	-7.56	-8.20	-9.21
37	OCT 31 63	20 35	5.70	-8.33	-8.36	-8.50	-8.60	-8.90	-9.08		-9.30	-8.93	-9.12	-7.60	-8.23	-9.21
38	DEC 24 63	1	4.21	-8.28	-8.26	-8.30	-8.40	-8.82	-8.97		-9.26	-8.92	-9.10	-7.41	-8.05	-9.11
39	DEC 28 63	28	3.95											-7.38	-8.13	-9.18
40	MAY 20 64	19 23	5.90				-8.33	-8.69	-8.88	-9.02	-8.76	-8.62	-8.82	-7.29	-7.92	-8.95
41	JUN 08 64	19 32	5.78	-8.32	-8.09	-8.19	-8.37	-8.66	-8.86		-8.78	-8.54	-8.79	-7.23	-7.85	-8.93
42	JUN 09 64	19 09	5.76	-8.33	-8.01	-8.11	-8.31	-8.60	-8.80	-8.94				-7.25	-7.89	-8.95
43	JUN 09 64	20 24	5.76	-8.22	-8.03	-8.15	-8.33	-8.63	-8.82							*
44	JUN 30 64	20 02	4.91	-8.29	-8.10	-8.21										*
45	JUL 03 64	18 59	4.74				-8.25	-8.59	-8.78					-7.94	-7.94	-9.01
46	JUL 11 64	20 20	4.20	-8.19	-8.00	-8.12	-8.28	-8.56	-8.81	-9.14	-8.91	-8.68	-8.94			*
47	JUL 14 64	19 31	3.97	-8.26	-7.93	-8.06	-8.25	-8.59	-8.80	-8.95	-8.82	-8.54	-8.82	-7.22	-7.91	-8.98
48	JUL 14 64	21 19	3.97	-8.25	-8.01	-8.14	-8.33	-8.65	-8.84	-9.04	-8.87	-8.61	-8.92	-7.23	-7.92	-8.99
49	JUL 15 64	19 21	3.89							-8.94	-8.80	-8.54	-8.90			*
50	JUL 25 64	20 29	3.04	-8.22	-8.08	-8.23	-8.43	-8.73	-8.92	-9.13	-8.91	-8.67	-9.00	-7.22	-7.90	-8.97
51	JUL 30 64	20 40	2.58	-8.14	-8.09	-8.24	-8.43	-8.74	-8.91					-7.35	-8.02	-9.07
52	JUL 30 64	23 11	2.58	-8.24	-8.16	-8.30	-8.47	-8.77	-8.95	-9.14	-8.95	-8.77	-9.02	-7.31	-7.96	-9.00
53	AUG 04 64	19 13	2.09	-8.24	-8.12	-8.26	-8.46	-8.78	-8.89	-9.10	-8.92	-8.70	-8.98	-7.31	-7.97	-9.01
54	AUG 04 64	22 10	2.09	-8.18	-8.10	-8.24	-8.42	-8.73	-8.88	-9.11	-8.90	-8.70	-8.98	-7.31	-7.97	-9.01
55	AUG 10 64	19 56	1.48	-8.30	-8.22	-8.35	-8.54	-8.85	-9.01	-9.15	-8.97	-8.78	-9.05	-7.37	-8.05	-9.10

NO	DATE	TIME	PHASE	3147	3590	3926	4155	4573	5012	6264	7297	8595	10635	U	B	V
113	SEP 14 65	25	0.93		-8.09	-8.19	-8.37	-8.70	-8.88	-9.06	-8.80	-8.56	-8.85	-7.24	-7.93	-8.99
114	SEP 19 65	21 24	1.46		-8.07	-8.14	-8.33	-8.66	-8.84	-9.08	-8.78	-8.55	-8.82	-7.21	-7.89	-8.96
115	SEP 19 65	23 13	1.46		-8.05	-8.14	-8.32	-8.65	-8.83	-9.06	-8.78	-8.54	-8.82	-7.22	-7.88	-8.96
116	SEP 20 65	21 20	1.56		-8.07	-8.11	-8.29	-8.63	-8.79	-9.08	-8.76	-8.52	-8.82	-7.21	-7.84	-8.91
117	SEP 20 65	23 16	1.56		-8.07	-8.13	-8.31	-8.65	-8.83	-9.08	-8.77	-8.54	-8.84	-7.23	-7.88	-8.95
118	OCT 02 65	20 47	2.76		-7.96	-8.06	-8.23	-8.58	-8.77	-9.03	-8.76	-8.50	-8.81	-7.13	-7.81	-8.90
119	OCT 02 65	22 45	2.76		-8.03	-8.11	-8.29	-8.62	-8.80	-9.05	-8.75	-8.49	-8.80	-7.19	-7.85	-8.93
120	OCT 11 65	19 17	3.56		-8.00	-8.04	-8.24	-8.60	-8.78	-9.03	-8.77	-8.48	-8.79	-7.16	-7.82	-8.88
121	OCT 11 65	21 47	3.56		-8.00	-8.09	-8.26	-8.60	-8.79	-9.01	-8.74	-8.47	-8.79	-7.17	-7.82	-8.90
122	OCT 12 65	19 13	3.65		-8.01	-8.07	-8.26	-8.60	-8.77	-9.05	-8.75	-8.49	-8.79	-7.15	-7.83	-8.91
123	OCT 12 65	21 35	3.65		-7.92	-7.98	-8.18	-8.52	-8.72	-8.99	-8.71	-8.46	-8.78	-7.07	-7.75	-8.84
124	OCT 20 65	20 57	4.27		-7.95	-8.02	-8.17	-8.51	-8.70	-8.99	-8.68	-8.42	-8.76	-7.13	-7.79	-8.88
125	OCT 21 65	20 43	4.35		-8.05	-8.09	-8.26	-8.59	-8.77	-8.99	-8.70	-8.43	-8.77	-7.20	-7.85	-8.91
126	OCT 23 65	20 39	4.49		-7.98	-8.04	-8.21	-8.55	-8.75	-9.00	-8.72	-8.46	-8.78	-7.15	-7.80	-8.87
127	OCT 27 65	20 42	4.75		-8.02	-8.06	-8.24	-8.58	-8.76	-8.99	-8.70	-8.46	-8.77	-7.17	-7.81	-8.89
128	DEC 14 65	19 08	5.74		-7.93	-7.99	-8.15	-8.53	-8.70	-8.92	-8.63	-8.37	-8.64	-7.10	-7.74	-8.85

Notes to Table VII

- (1) May 20 63: $M = 3.1$
- (3) May 24 63: $M = 3.3$
- (4) May 24 63: $M = 2.4$
- (5) Jun 25 63: $M = 3.4$
- (7) Jul 11 63: clouds
- (8) Jul 13 63: $M = 3.5$
- (9)(10) Jul 13 63: clouds
- (11) Jul 20 63: $r = \pm .04$ (pmlpcb)
- (12) Jul 28 63: $M = 2.5$
- (14) Aug 09 63: $M = 2.5$
- (15) Aug 10 63: $M = 2.4$
- (17) Aug 21 63: $M = 2.7$
- (19) Aug 22 63: $M = 2.8$, extinction poorly determined (g)
- (20) Aug 22 63: extinction poorly determined (g)
- (23) Sep 20 63: $M = 2.1$
- (24) Sep 25 63: fog
- (26) Sep 28 63: $M = 2.8$
- (30) Oct 08 63: $M = 3.0$
- (31)(32) Oct 10 63: poor night
- (33)(34) Oct 15 63: poor night, $M = 2.2$
- (35)(36) Oct 19 63: $M = 2.2$
- (38) Dec 24 63: $M = 2.7$
- (39) Dec 28 63: $M = 3.4$
- (40) May 20 64: $M = 2.7$
- (41) Jun 08 64: $M = 2.6$

- (42) Jun 09 64: $M = 3.2$
- (44) Jun 30 64: $M = 2.3$
- (45) Jul 03 64: $M = 3.3$, clouds
- (46) Jul 11 64: cirrus, $M = 2.1$
- (47) Jul 14 64: cirrus, $M = 2.6$
- (49) Jul 15 64: $M = 3$, clouds
- (50) Jul 25 64: $M = 2.1$
- (53) Aug 04 64: $M = 2.9$
- (54) Aug 04 64: $r \approx + 0.05$ (vus)
- (55) Aug 10 64: $M = 2.3$
- (57) Aug 11 64: $M = 3.4$
- (59) Aug 24 64: $M = 3.2$, $r \approx + 0.035$ (vuspmlbcd), large extinction
- (60) Aug 24 64: $r \approx -0.04$ (vusbcd), large extinction
- (61) Aug 24 64: $M = 3.1$, $r \approx -0.05$ (vusbcd), large extinction
- (62) Aug 25 64: $M = 3.3$
- (64) Aug 25 64: $M = 2.7$
- (65) Aug 26 64: $M = 3.3$
- (66) Aug 26 64: $r = \pm 0.06$ (vuspmlbcd), large zero point (pmlvus)
- (67) Aug 30 64: $M = 2.6$
- (69) Aug 30 64: $M = 2.4$
- (71) Sep 08 64: light clouds (vus)
- (81) Sep 23 64: clouds (vus)
- (82) Oct 03 64: clouds
- (83) Oct 03 64: clouds
- (84) Oct 05 64: large extinction (bcd)
- (85) Oct 06 64: large extinction (bcdvus)
- (89)(90) Nov 24 64: poor night

- (91) Dec 07 64: $M = 2$, $r < 0$, poor night
- (92) Dec 08 64: $M = 2$, $r < 0$
- (94) Jun 17 65: $M = 2.7$
- (95) Jun 22 65: $M = 2.8$
- (96) Jun 24 65: $r \approx -0.03$ (vuspml)
- (97) Jul 05 65: $r \approx -0.06$ (us)
- (100) Jul 11 65: $r \approx + 0.035$
- (101) Jul 26 65: fog (k)
- (113) Sep 14 65: fog (khge)

TABLE VIII

ESTIMATED ERRORS FOR EACH EXTINCTION PERIOD

Period	*	v	u	s	p	m	l	k	h	g	e	d	c	b
5/3/63-	R		.023	.020	.021	.020	.018	.011	.012	.009	.019	.025	.018	.021
5/24/63	S		.133	.055	.021 ²	.056	.067	.047	.020	.010	.032	.070	.036	.044
6/11/63-	R	.034	.032	.028	.030	.029	.028	.019	.025	.019	.014	.032	.029	.024
6/25/63	S	.097	.024 ¹	.011	.040 ²	.019	.018	.063	.032 ³	.030 ³	.026	.101	.033	.025
7/11/63-	R	.027	.026	.026	.025	.023	.021	.017	.019	.027	.019	.028	.021	.020
7/28/63	S	.039	.053	.054	.016 ²	.024	.024	.017	.030 ³	.031 ³	.020	.040	.041	.031
8/9/63-	R							.014	.016	.012	.017			
8/25/63	S							.012	.031 ³	.015 ³	.009			
9/20/63-	R	.012	.012	.019	.010	.011	.011	.014	.014	.012	.013	.010	.009	.009
9/29/63	S	.039	.036	.027	.011	.012	.016	.019	.026 ³	.019 ³	.015	.032	.008	.013
10/8/63-	R	.020	.021	.021	.021	.018	.016	.014	.013	.011	.010	.017	.016	.017
10/31/63	S	.043	.030	.027	.031	.023	.016	.034	.020 ³	.014 ³	.009	.060	.018	.021
12/5/63-	R	.023	.021	.018	.016	.014	.013	.009	.012	.015	.010	.017	.012	.012
12/28/63	S	.037	.053	.036	.024	.019	.016	.014	.013 ³	.012 ³	.018	.050	.020	.015
5/6/64-	R	.046	.015	.013	.013	.011	.011	.007	.009	.006	.010	.016	.018	.014
5/20/64	S	.002	.019	.003	.014	.011	.011	.030	.020	.015	.022	.025	.027	.016
6/8/64-	R	.027	.022	.019	.016	.016	.015	.013	.011	.010	.008	.014	.015	.012
7/15/64	S	.005	.015	.014	.010	.008	.008	.005	.005	.005	.006	.010	.010	.008
7/2/64-	R	.029	.024	.022	.018	.019	.017	.012	.009	.009	.007	.016	.016	.011
7/15/64	S	.014	.020	.015	.016	.013	.010	.006	.004	.006	.006	.016	.014	.012
7/25/64-	R	.033	.028	.028	.025	.027	.021	.023	.024	.028	.021	.028	.024	.020
8/11/64	S	.020	.034	.035	.025	.027	.022	.028	.023	.026	.016	.029	.031	.030

8/15/64-	R	.033	.026	.022
8/27/64	S	.038 ²	.032 ²	.021
8/24/64-	R	.024	.020	.017
8/25/64	S	.025	.034	.021
8/24/64-	R	.014	.010	.011
8/30/64	S	.010	.010	.010
8/30/64-	R	.014	.014	.011
9/23/64	S	.011	.008	.009
9/8/64-	R	.011	.008	.013
10/6/64	S	.011	.011	.006
11/17/64-	R	.016	.016	.021
11/24/64	S	.010	.010	.030
12/7/64-	R	.014	.012	.011
1/10/65	S	.011	.010	.015
2/2/65-	R	.019	.019	.013
3/30/65	S	.015	.015	.013
2/2/65-	R	.016	.013	.012
2/24/65	S	.010	.006	.009
3/9/65-	R	.018	.015	.013
3/30/65	S	.009	.011	.008
5/8/65-	R	.012	.012	.009
5/23/65	S	.014	.017	.011
6/17/65-	R	.017	.015	.018
7/16/65	S	.014	.008	.020 ⁴
7/26/65-	R	.011	.012	.015
8/11/65	S	.011	.012	.021 ⁴

9713/65	R	.022	.022	.017	.018	.019	.018	.013	.013	.013	.013	.014
10/12/65	S	.013	.011	.015	.014	.015	.007	.007	.009	.020 ⁴	.014	.011
10/2/65	R	.025	.026	.021	.021	.019	.015	.013	.014	.012	.024	.021
10/27/65	S	.010	.012	.013	.011	.010	.008	.012	.010	.007 ⁴	.014	.014
11/7/65	R	.007	.009	.009	.011	.007	.015	.016	.008	.007	.009	.008
12/14/65	S	.040	.035	.013	.010	.010	.007	.010	.010	.010 ⁴	.015	.007

*R = rms residual from extinction solution; S = standard error per star in transformation to standard conditions.

¹transformation extrapolated to color of Venus; for Venus, est. error $\approx \pm 0.09$ 2 transformation extrapolated to color of Mars; for Mars, est. error $\approx \pm 0.10$ ³transformation extrapolated to color of Jupiter; for Jupiter, est. error $\approx \pm 0.06$ ⁴transformation extrapolated to color of Saturn; for Saturn, est. error $\lambda \pm 0.0^{+15}$

TABLE IX
Monochromatic Magnitudes and Geometric Albedos for Mars and Jupiter

Wavelength*	v	u	s	p	m	l	k	h	g	e	U	B	V
Mars													
m(1,0)	-0.40 + .05	-0.38 + .05	-0.52 + .04	-0.63 + .03	-0.93 + .03	-1.14 + .02	-2.15 + .02	-2.33 + .03	-2.32 + .03	-2.31 + .04	0.40 + .04	-0.18 + .03	-1.52 + .02
p	0.053	0.052	0.059	0.065	0.086	0.105	0.265	0.314	0.310	0.308	0.053	0.078	0.149
Jupiter													
m(1,0)	-8.70 + .02	-8.89 + .03	-9.02 + .02	-9.10 + .02	-9.26 + .02	-9.34 + .01	-9.48 + .01	-9.18 + .01	-8.86 + .01	-8.85 + .01	-8.05 + .02	-8.54 + .02	-9.39 + .01
p	0.269	0.320	0.361	0.387	0.450	0.484	0.551	0.418	0.311	0.308	0.305	0.422	0.504

*See Table I.

FIGURE CAPTIONS

Figure 1 (a,b,c,d,e,f): Phase curves for Mars and Jupiter in bands s, l, and g.

Figure 2 (a,b,c): Phase curves for Saturn in bands s, l, and g. Filled circles, MAY - AUG 10, 1963; Open circles, AUG 21 - OCT, 1963; caret, DEC, 1963; Filled triangles, MAY - AUG 24, 1964; Open triangles, AUG 25 - NOV 18, 1964; Squares NOV 24 - DEC, 1964; Crosses, JUN - AUG, 1965; x, SEP - DEC, 1965.

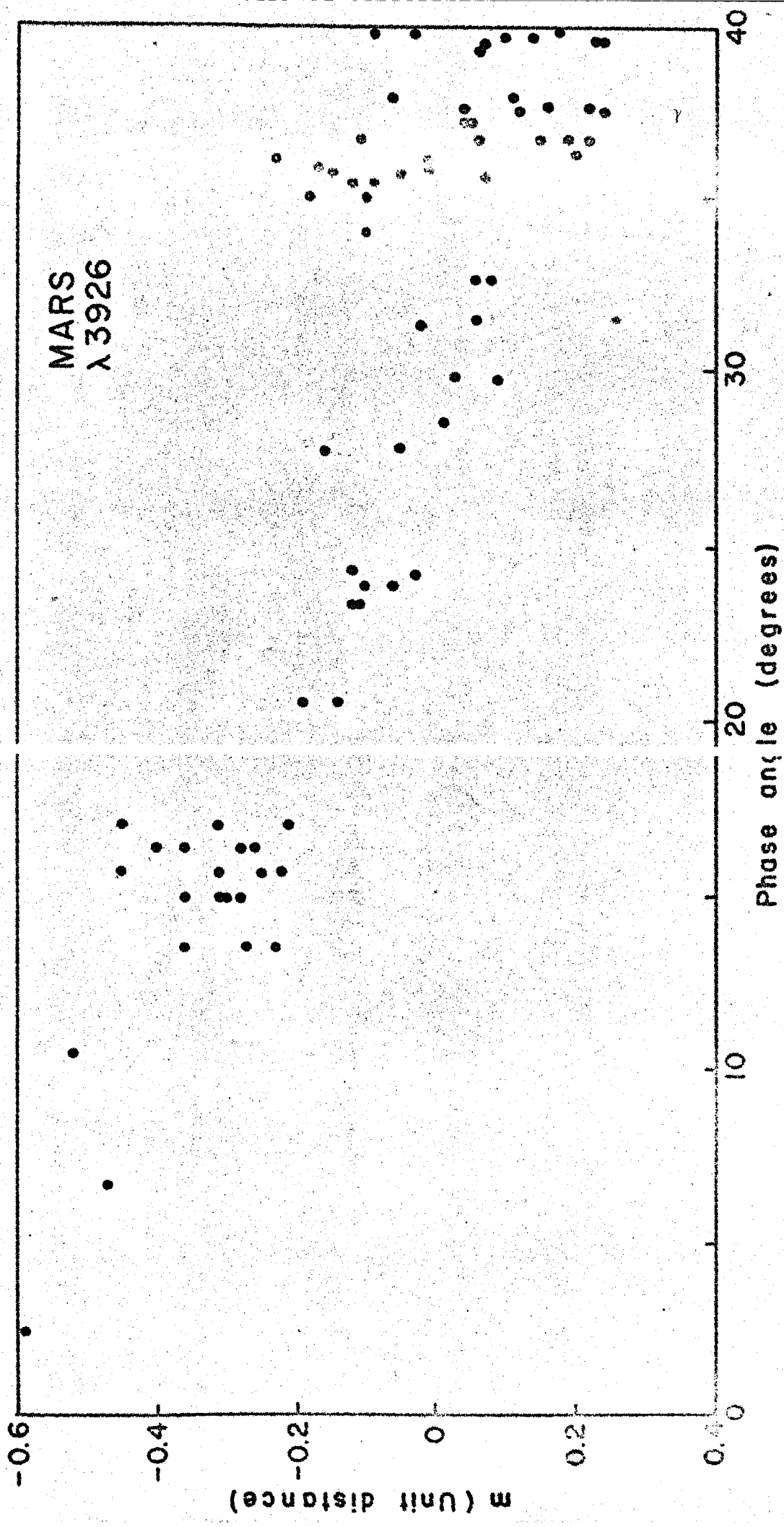
Figure 3: Monochromatic magnitudes at unit distance and full phase for Mars. Other points from Harris (1961).

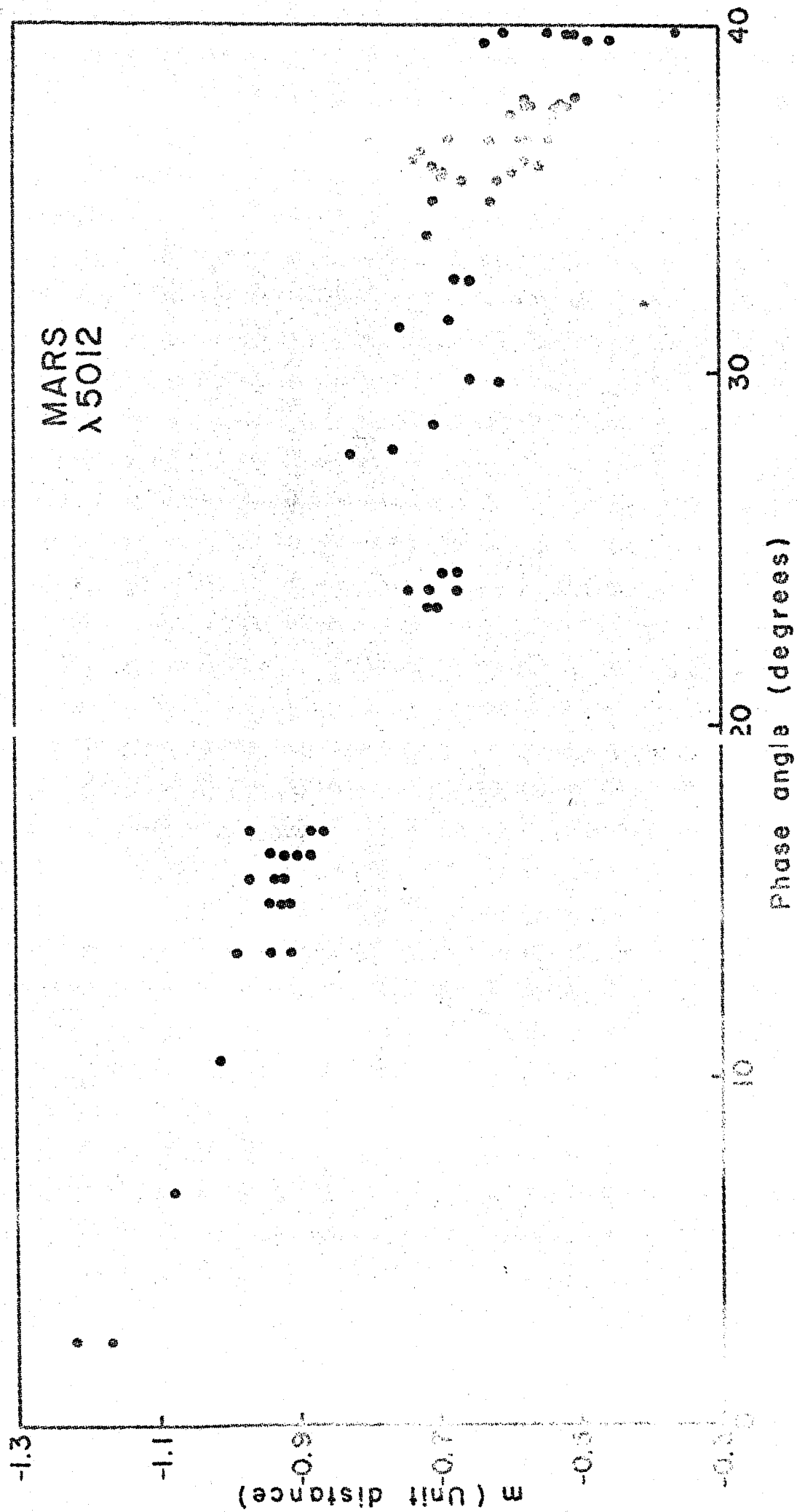
Figure 4: Geometric albedo versus wavelength for Mars. Other points from Harris (1961) and Walker (1966).

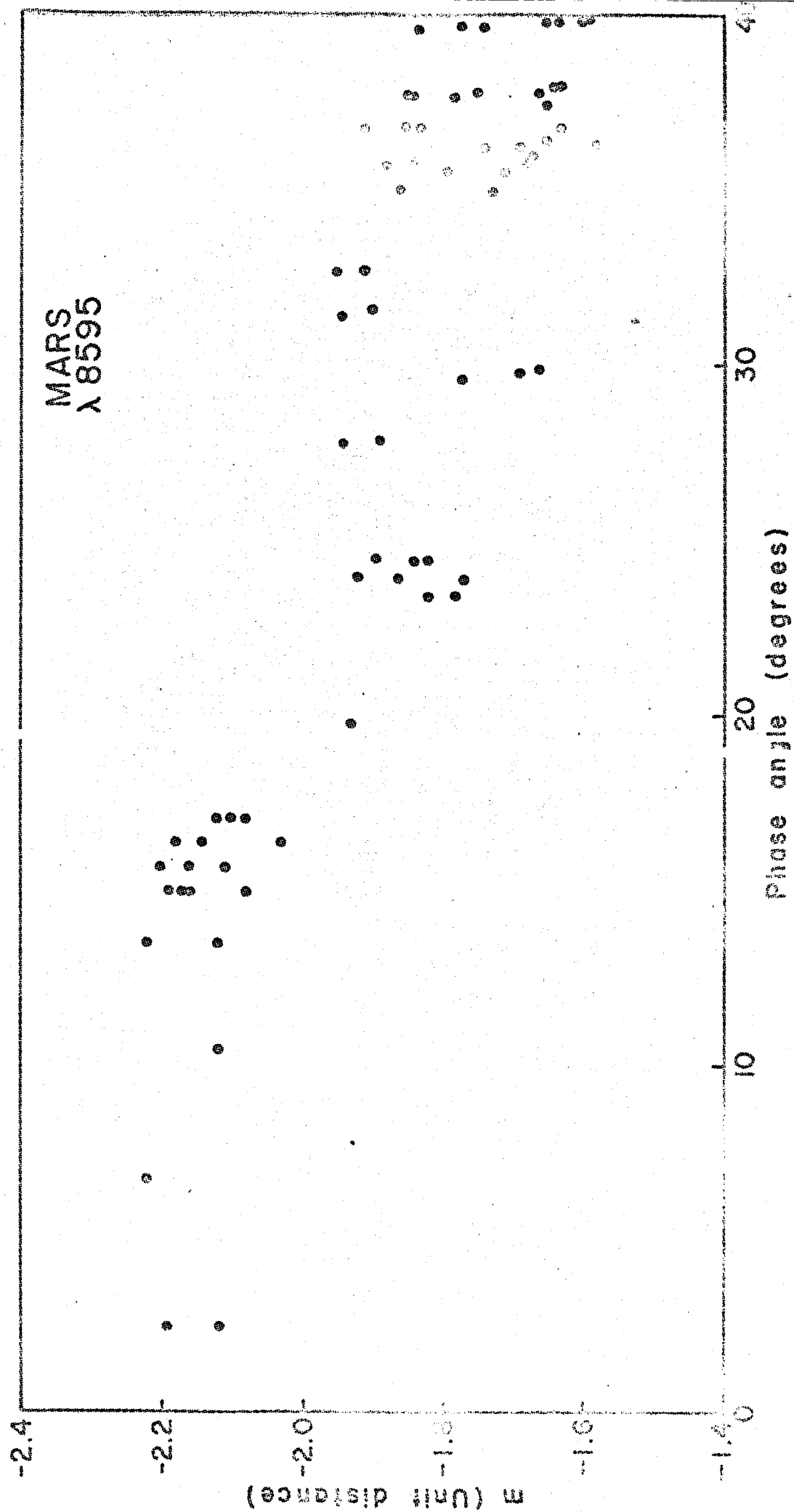
Figure 5: Monochromatic magnitude at unit distance and full phase for Jupiter. Other points from Harris (1961) normalized to $V(1,0) = -9.39$.

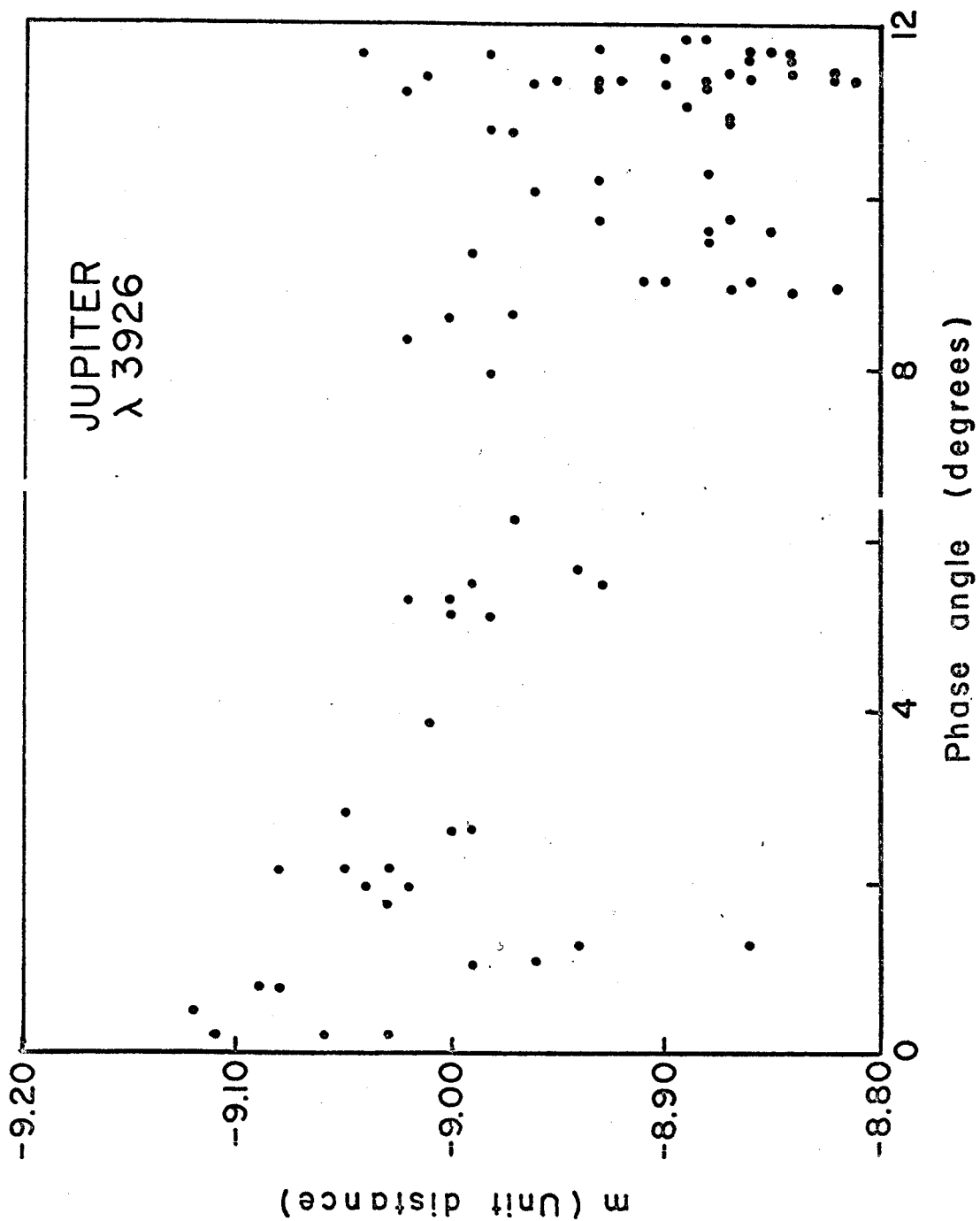
Figure 6: Geometric albedo versus wavelength for Jupiter. Points from Harris (1961) based on $V(1,0) = -9.25$.

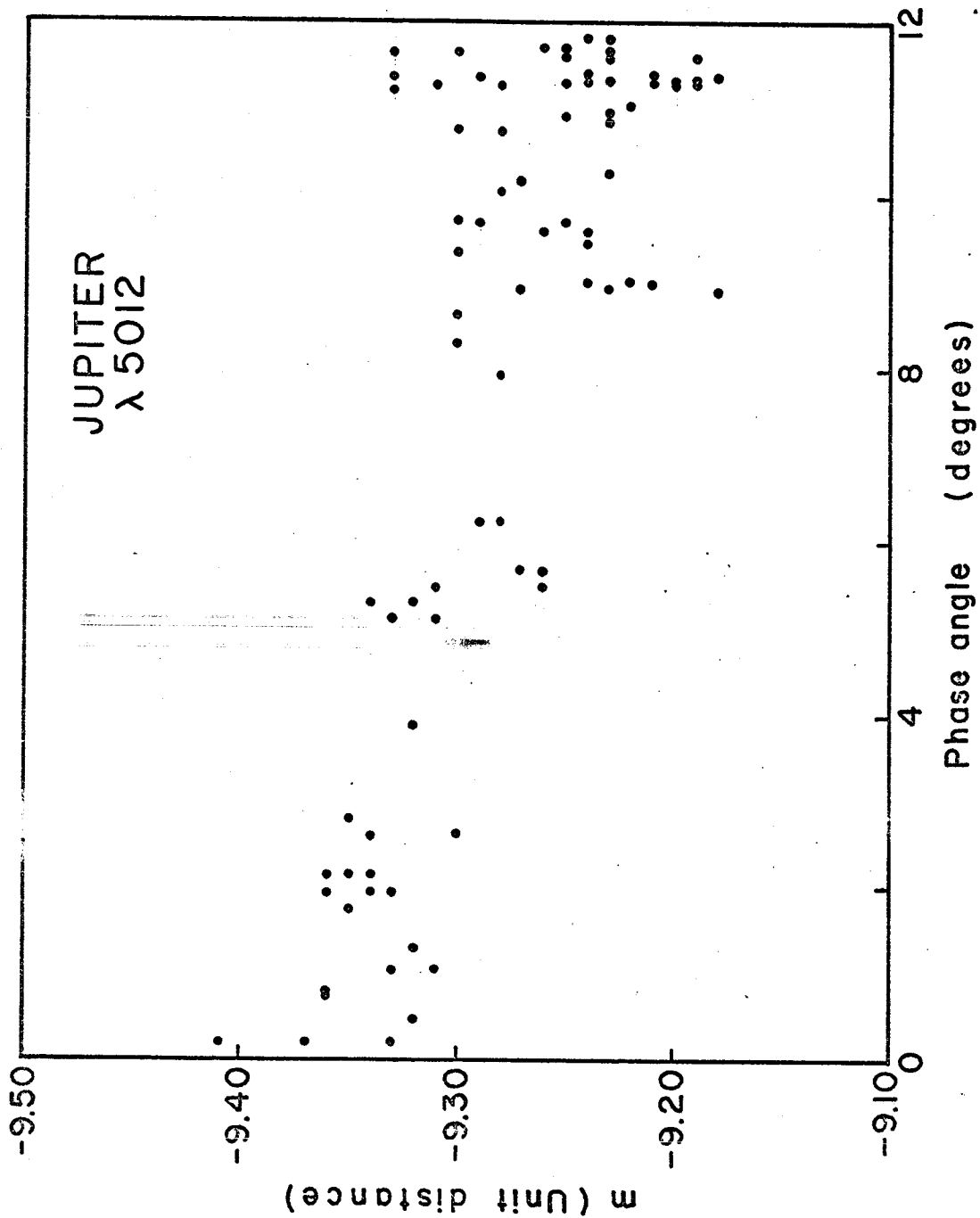
Figure 7 (a,b,c): Residuals relative to the mean phase curve for Mars plotted versus longitude of the central meridian ω .

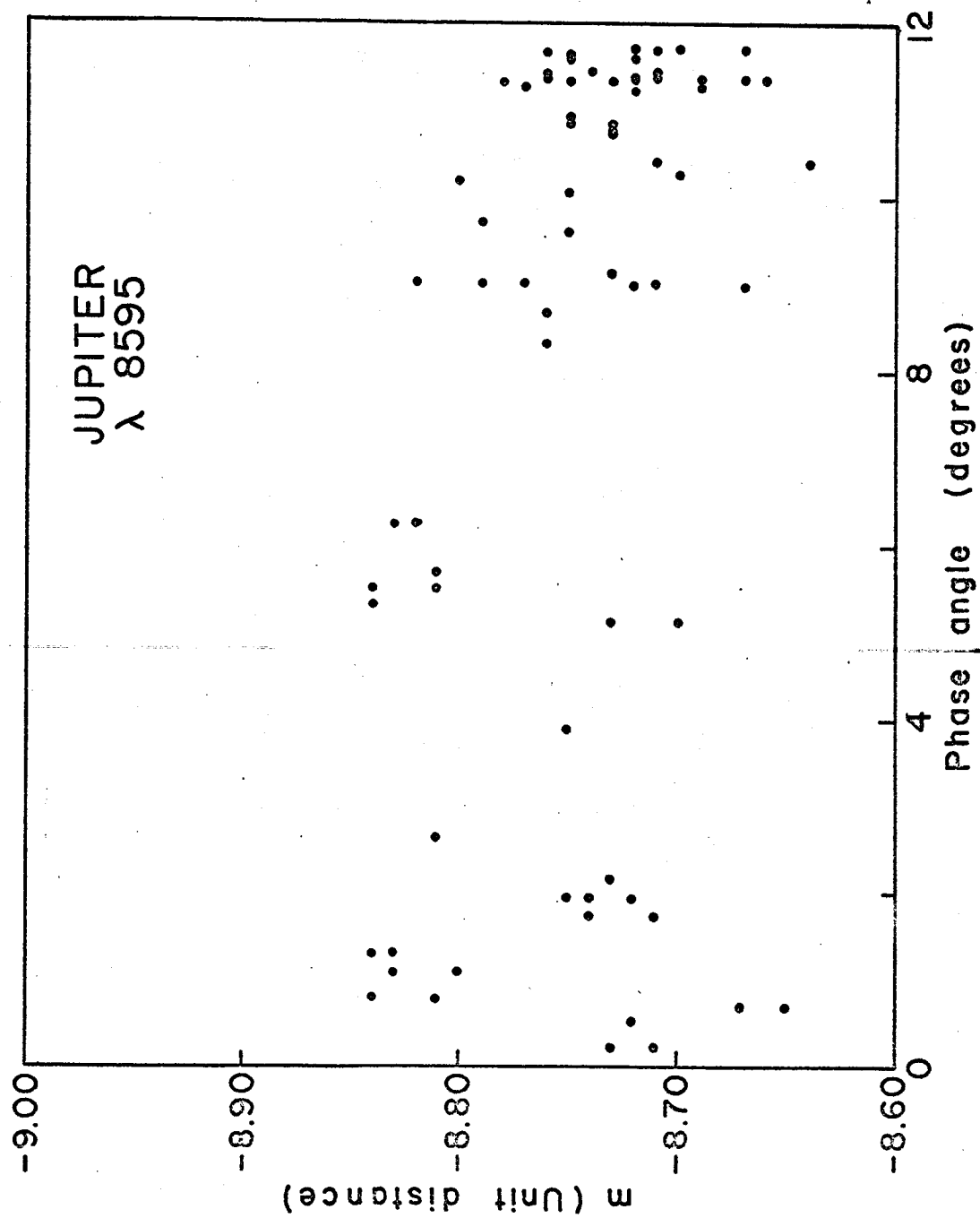










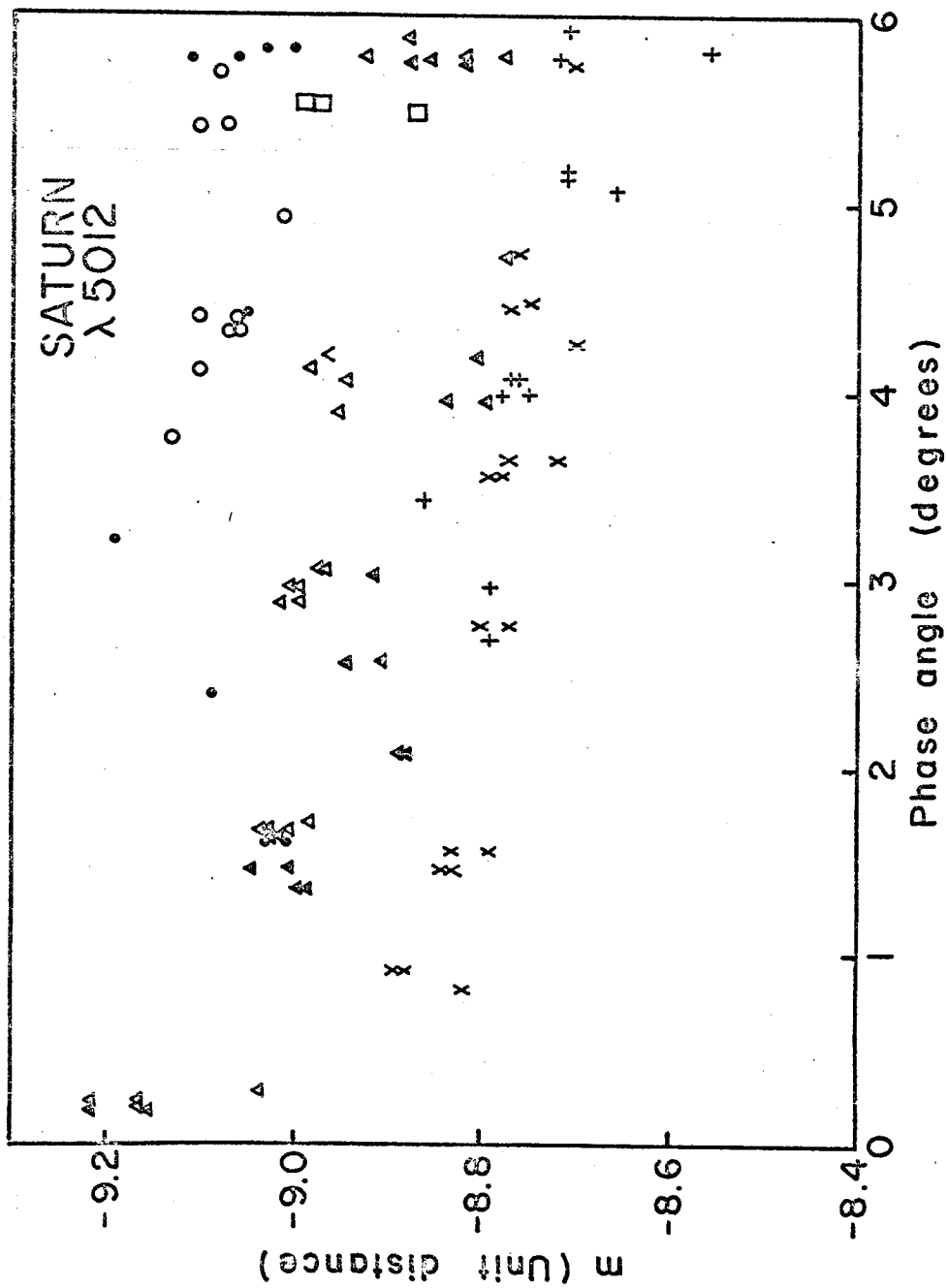


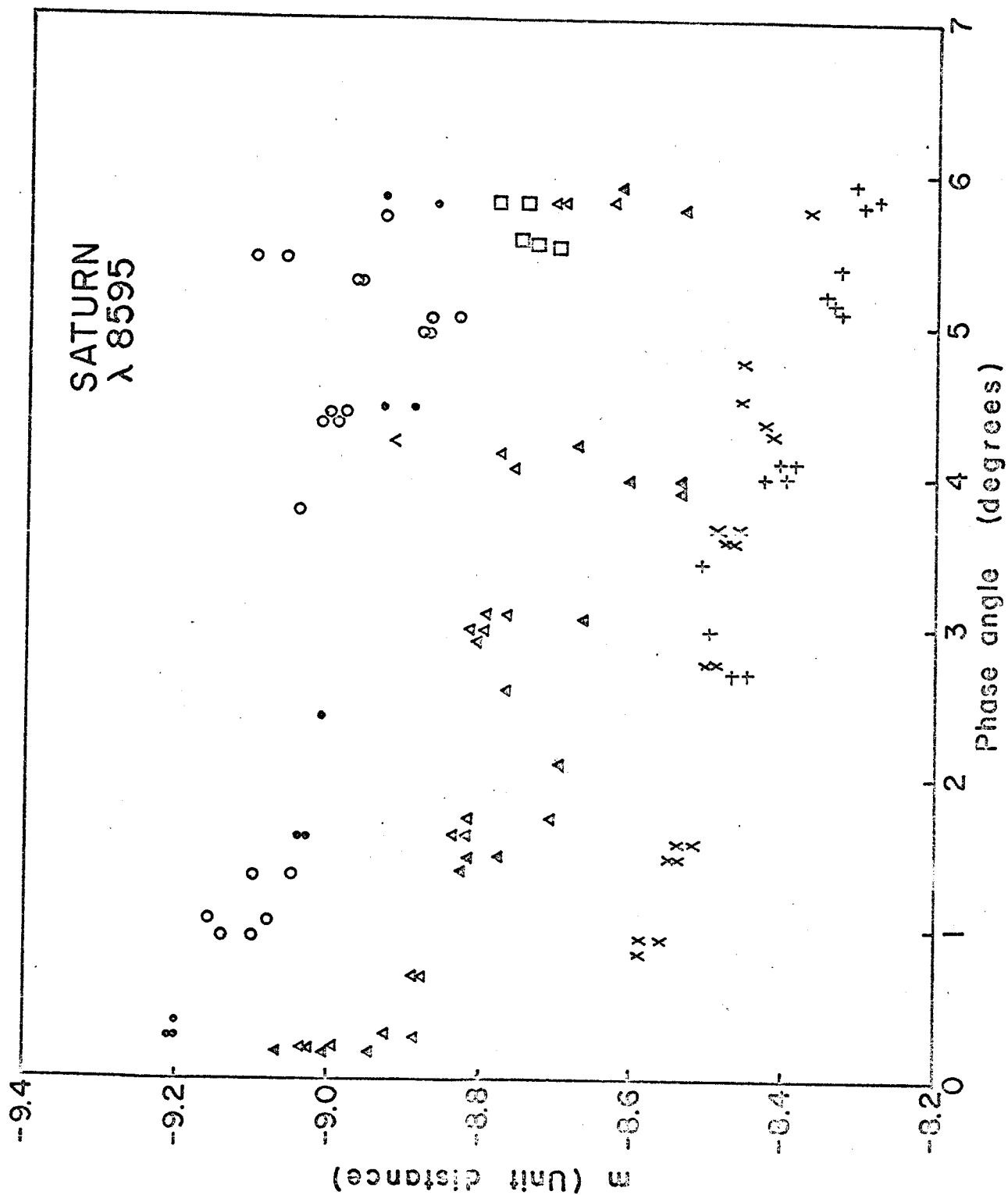
**SATURN
λ 3926**

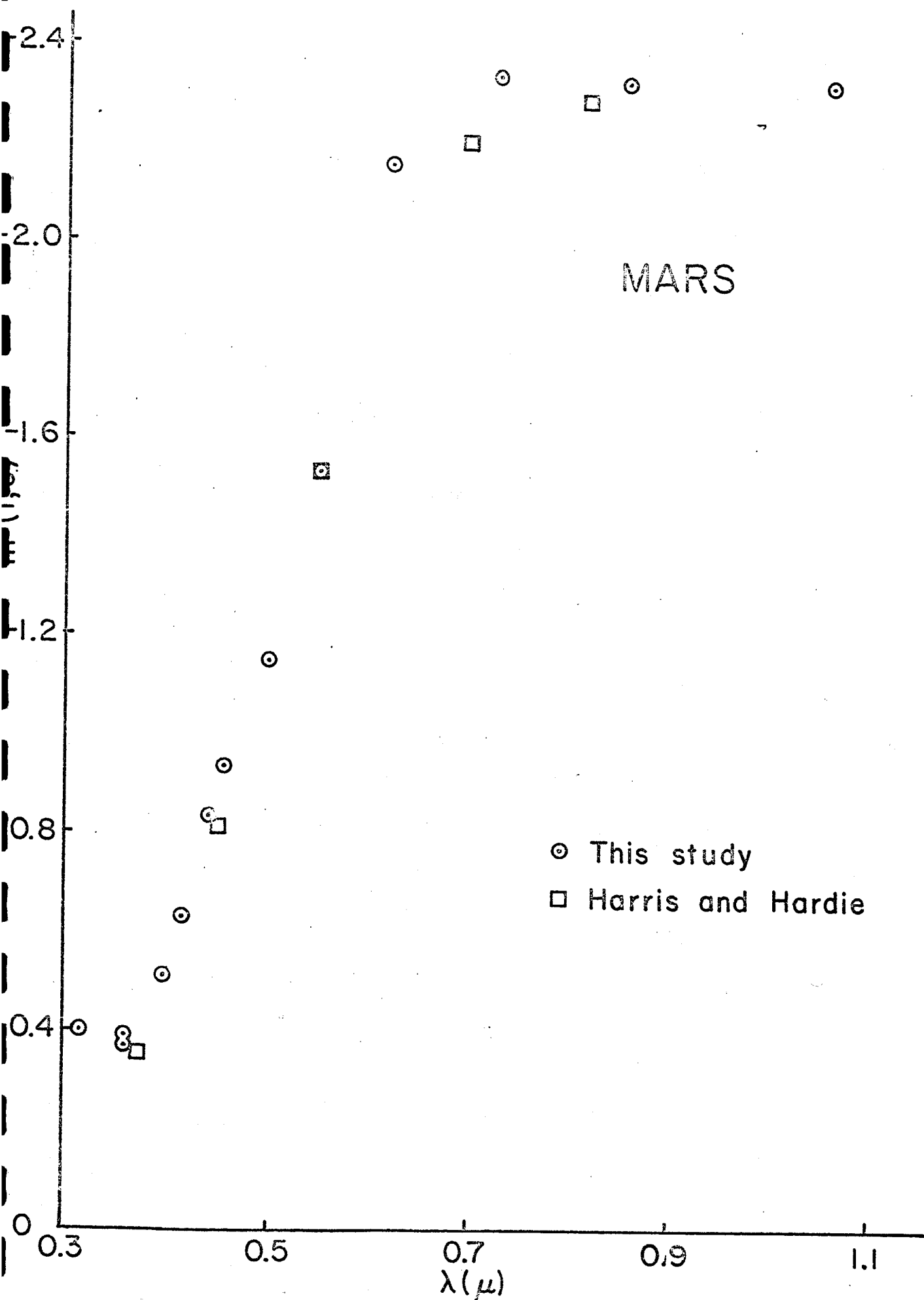
m (Unit distance)

Phase angle (degrees)

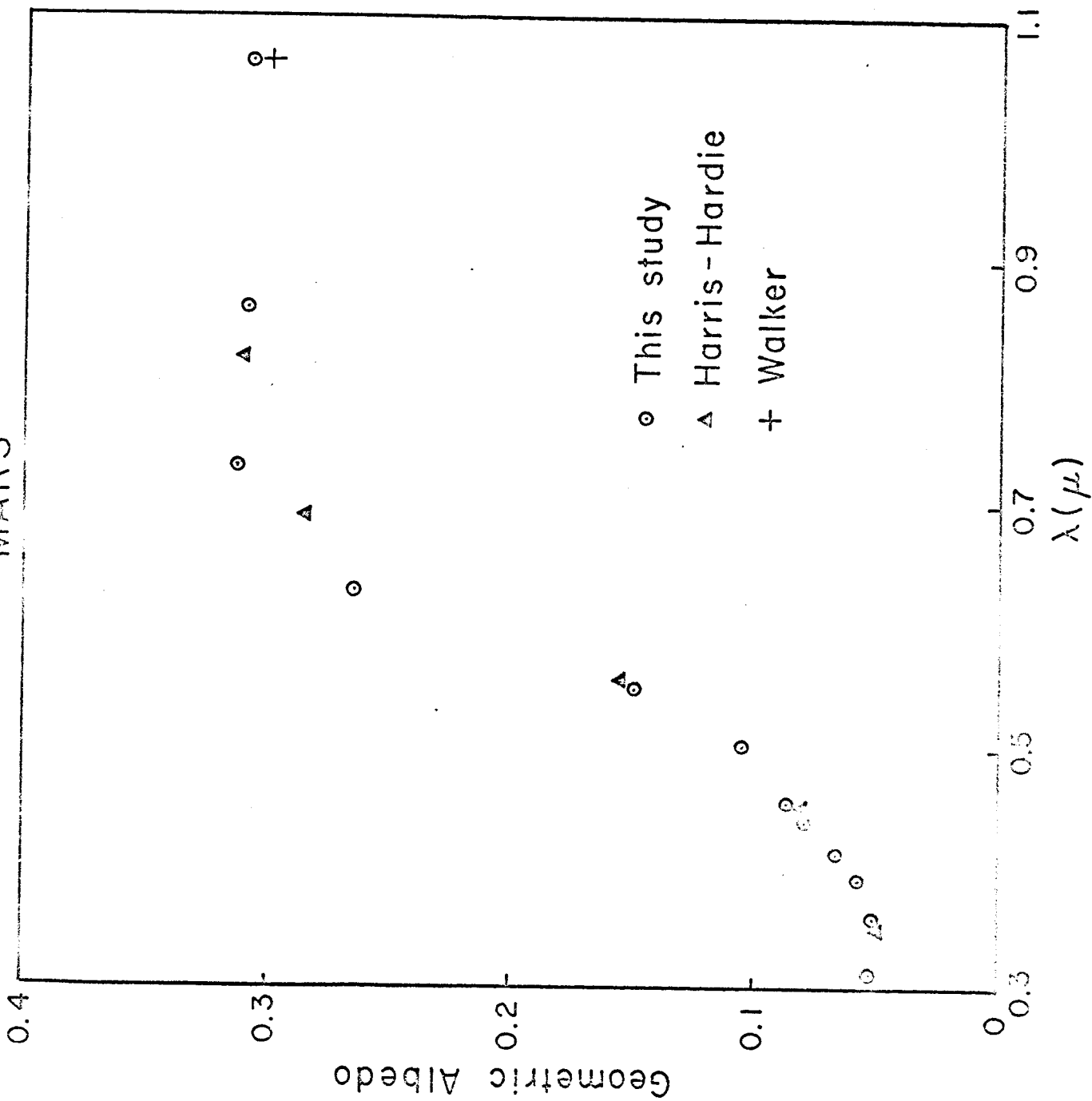
Phase angle (degrees)

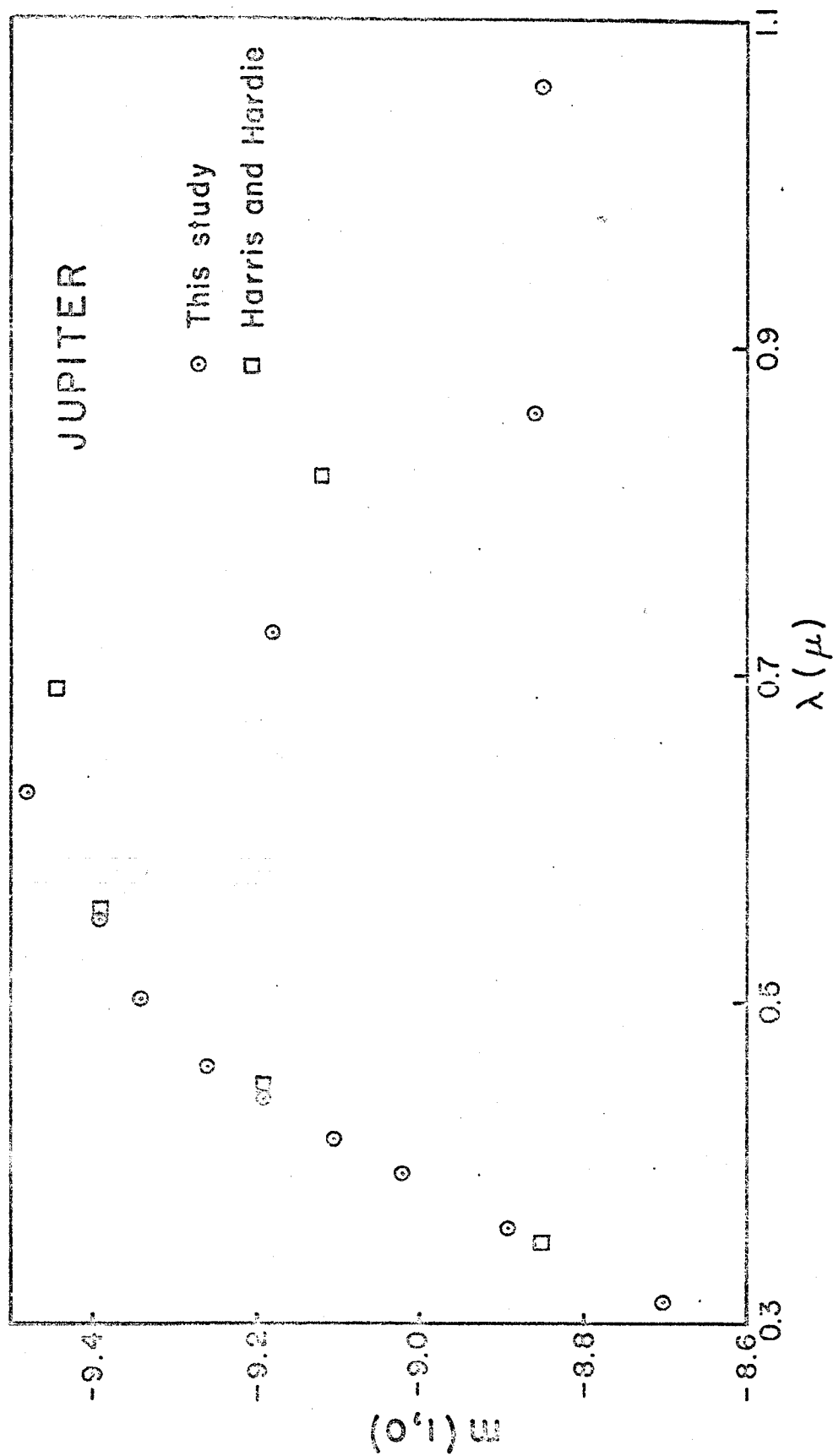




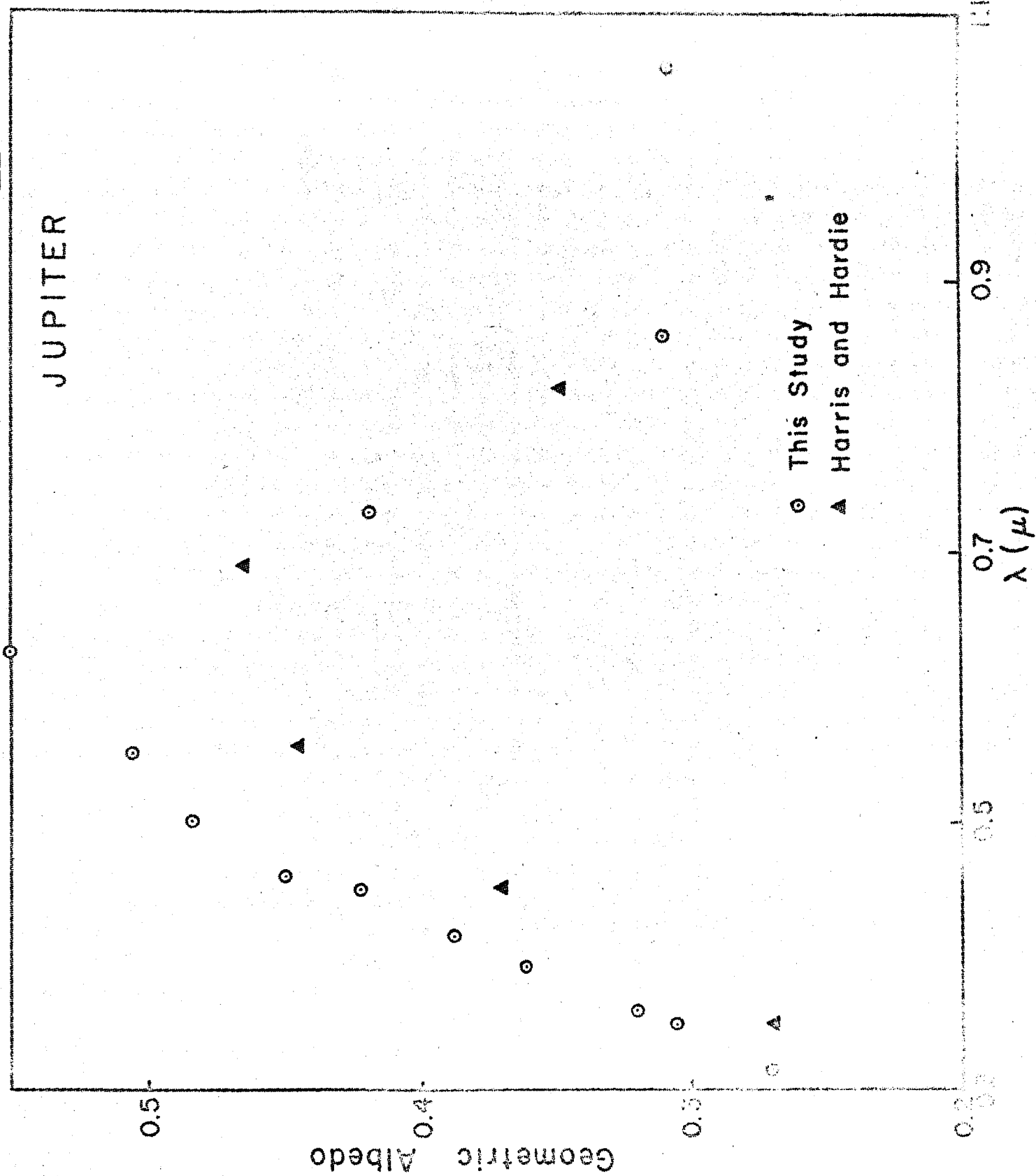


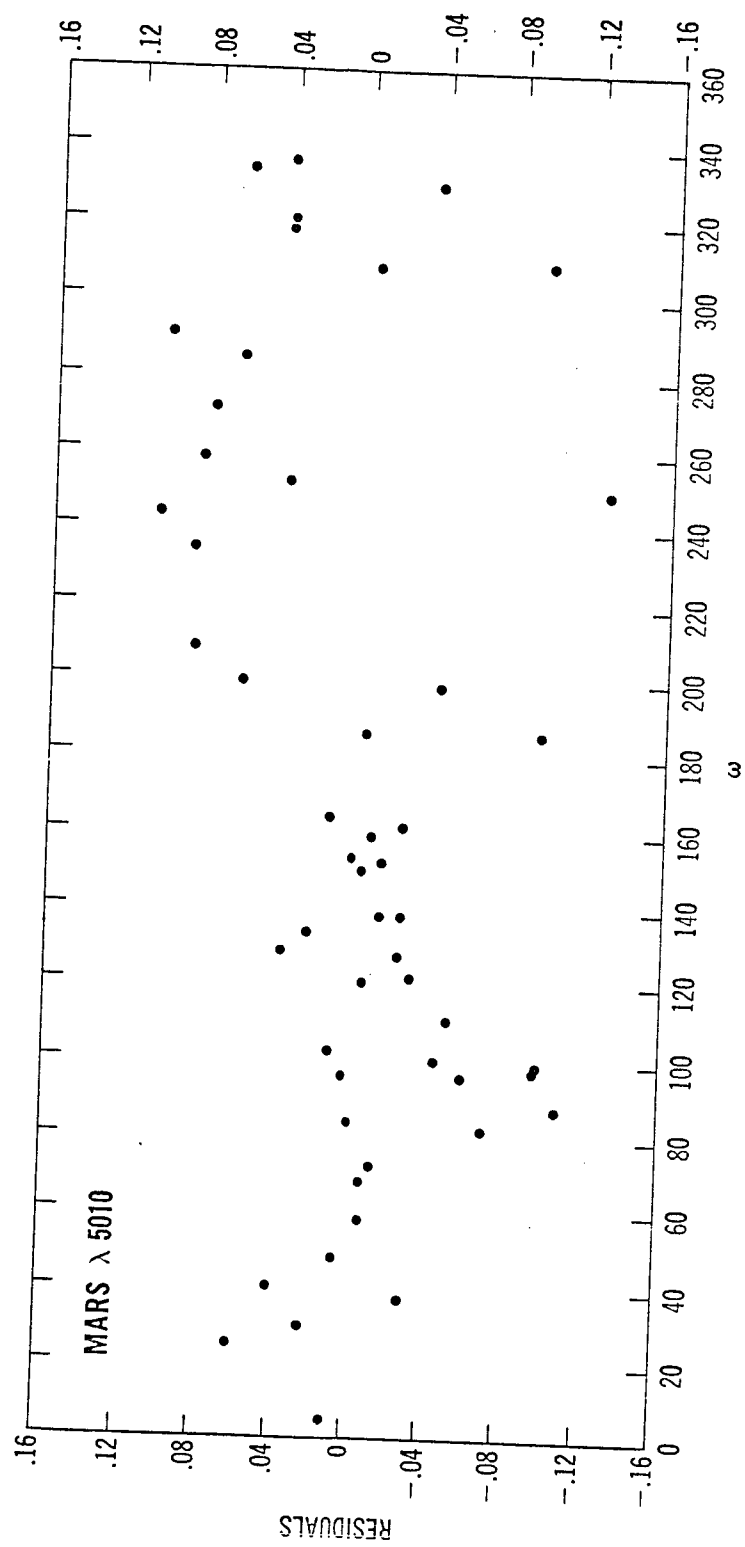
MARS

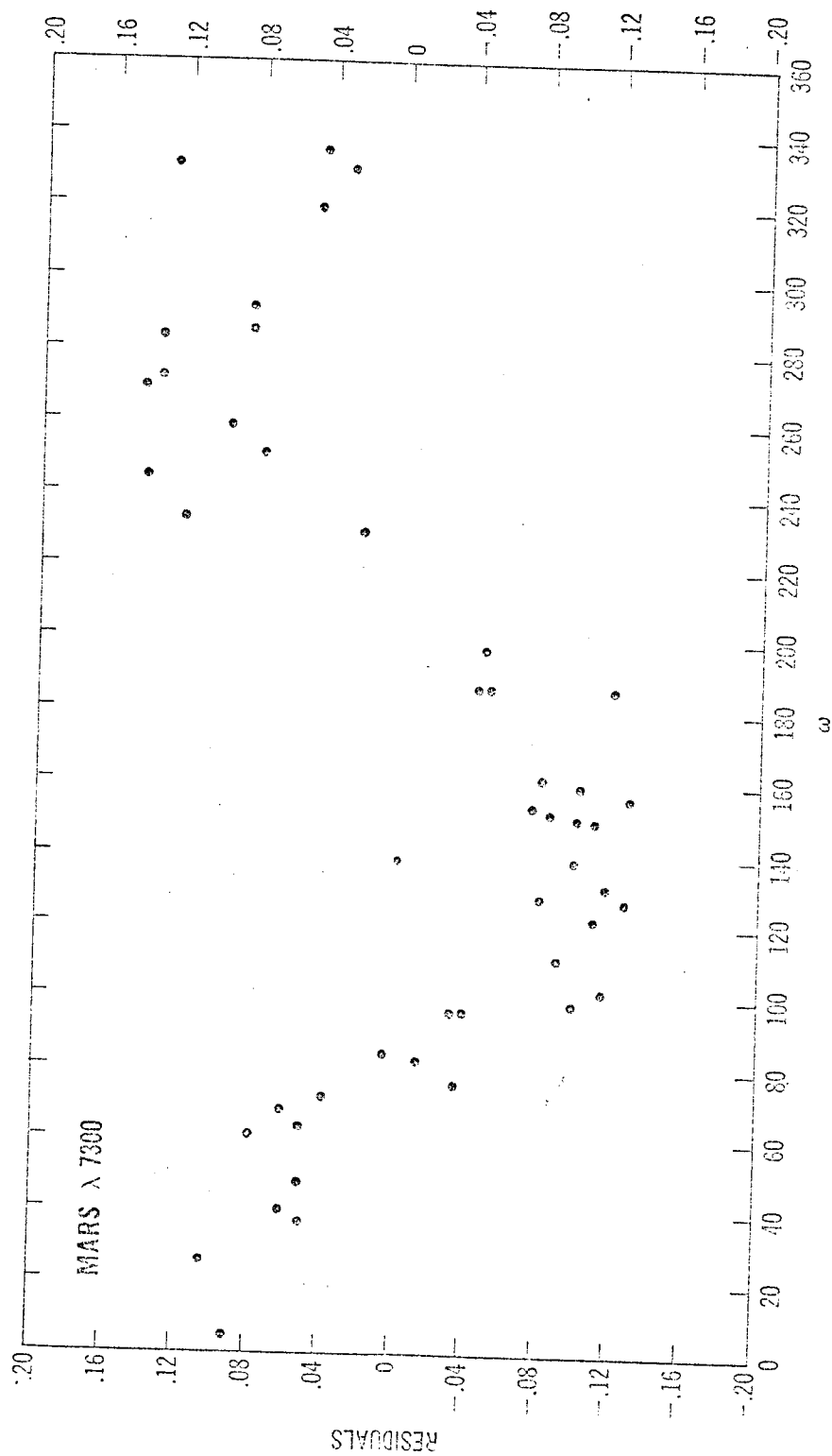




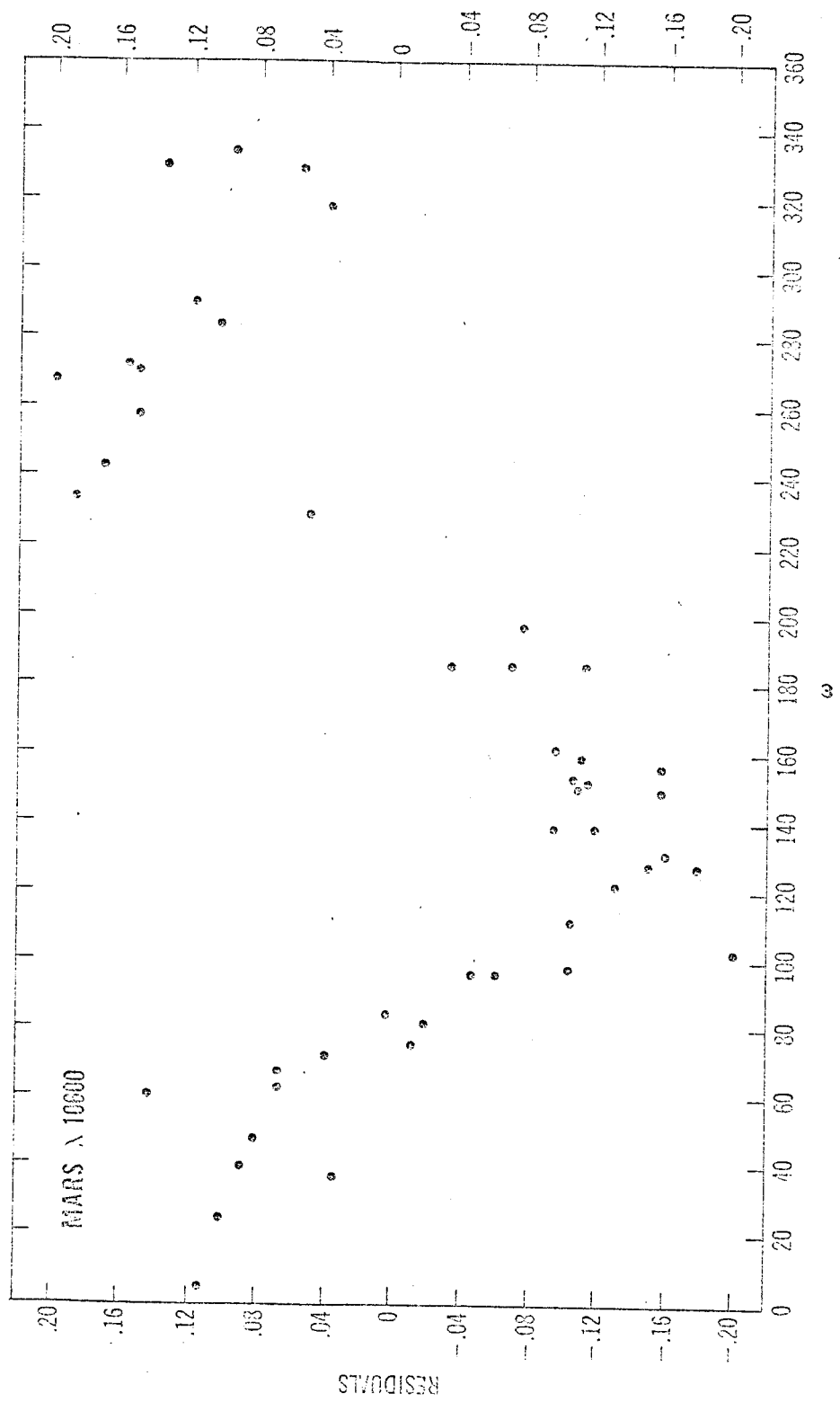
JUPITER







1.4 best obs



APPENDIX II

MULTICOLOR PHOTOELECTRIC PHOTOMETRY
OF THE BRIGHTER PLANETS
III. OBSERVATIONS FROM BOYDEN OBSERVATORY

WILLIAM M. IRVINE
Department of Physics and Astronomy
University of Massachusetts, Amherst, Massachusetts

THEODORE SIMON and DONALD H. MENZEL
Harvard College Observatory

C. PIKOOS
Boyden Observatory

and

ANDREW T. YOUNG
Aerospace Corporation, Los Angeles

ABSTRACT

Results of a program of photoelectric photometry of Mercury, Venus, Mars, Jupiter, and Saturn between 1963 and 1965 are presented. Observations were made in ten narrow bands between 3150 Å and 1.06μ and in UBV. Phase curves are presented and monochromatic geometric albedos determined. The results are compared with previous investigations.

I. INTRODUCTION

This is the third paper in a series describing a three-year program of multicolor photoelectric photometry of the brighter planets conducted between 1962 and 1965 under the direction of the Harvard College Observatory. Young and Irvine (1967, hereinafter referred to as Paper I) described the motivation for the program, and the equipment and reduction procedures employed. Irvine, Simon, Menzel, Charon, Lecomte, Griboval and Young (1968, hereinafter referred to as Paper II) discussed the observational results obtained at Le Houga Observatory in France. The present paper describes the observations obtained during the same period at the Boyden Observatory in South Africa. Subsequent papers in the series will present further results obtained under special conditions (particularly observations of the moon, Uranus, and Neptune), a tabulation of the extinction coefficients which may be of interest to atmospheric scientists, and further intercomparison and evaluation of all the observational data.

Observations were made in ten narrow bands isolated by interference filters between 3150 Å and 1.06μ. These bands were designated by the letters v-u-s-p-m-l-k-h-g-e (see Table I). Observations were also made in UBV, with our corresponding natural magnitude system noted by d-c-b.

II. REDUCTION TO A STANDARD MAGNITUDE SYSTEM

Papers I and II described the data reduction procedure. A set of standard stars was used for extinction determination and transformation to standard conditions. The magnitude of these stars, determined iteratively, is listed in Table II. To correct for atmospheric extinction, we grouped the observations into approximately monthly periods, and then transformed the corrected observations to a standard Boyden period (May, 1965), using for any band x a linear transformation of the form

$$x = x^* + \alpha(x-y)^* + \beta. \quad (1)$$

The starred values in equation (1) refer to the period of observation and the unstarred magnitudes to the standard period. The constants α and β were determined from a least-squares fit to the observations of standard stars. The same color ($x-y$) was used in this transformation as was used in the extinction determination for pass band x , except for the 1963 observations in band s (see below). An estimate of the errors introduced by the extinction determination and the transformation to the standard system appears following the discussion of the planetary observations (see Table IX).

The filters used during 1963 were replaced in January, 1964. The replacement apparently introduced non-linearities in the transformation of the 1963 observations in band s to the standard system when the ($u-s$) color was employed in this transformation (this was the color used for the extinction solution and the 1964-65 transformations to standard conditions). We found that a linear transformation could be obtained using the ($s-p$) color for this data. As reported in Paper I, the v filter showed serious deterioration during 1963 and in late 1965. It has not proved possible to obtain a simple transformation of the 1963 v results to the standard period, and they are consequently omitted here.

After reducing the results to the standard period, we transformed them to the final Le Houga magnitude system (Paper II), again using a linear transformation of the form equation (1). Table III lists coefficients for the transformation and corresponding standard errors. The zero points in this final magnitude system for the narrow bands were chosen so that all colors are color excesses relative to the sun (that is, $x-V = 0$ for the sun, where x is any of the narrow bands). The color of the sun was determined by interpolating among the standard stars in $B-V$, assuming $(B-V)_{\odot} = 0.65$ (see Paper I). The internal errors of the determination are probably less than the uncertainty in $(B-V)_{\odot}$.

The wide band ($d-c-b$) observations were transformed directly from the standard Boyden magnitude system to UBV , using the standard values given by Johnson et al. (1966). Transformation coefficients and standard errors are given in Table III.

The magnitudes of the standard stars observed at Boyden are given in Table II in the final magnitude system. Those stars observed in common with Le Houga, and used for the transformation between observatories, are labeled with an asterisk. All stars in the Table were observed in at least three separate monthly periods with at least three observations in each period. The results are believed to be accurate to ± 0.02 mag. except for the values enclosed in parentheses, which are slightly less

accurate (perhaps ± 0.03 mag.); the latter values were not used in transformations to the standard system.

III. RESULTS

Tables IV, V, VI, VII, and VIII present the results of the planetary photometry. The magnitudes have been reduced to unit distance from the sun and earth. In each table, column 1 assigns a number to each observation of a planet. Column 2 gives the first day of the double date of each observing night; thus FEB 18 65 indicates the night of February 18-19, 1965. (In consequence, the observations tend to be centered around 0 hours UT on the date subsequent to that given in column 2; e.g., February 19.) Column 3 gives the time of observation for filter d (= U). If there was no d observation, the time for another filter (generally v) is given. During 1965, observations with d were taken half-way through the 13-filter sequence. Such a sequence typically lasted 35 minutes, and the order of observation was e-g-h-k-b-c-d-l-m-p-s-u-v. When the red-sensitive photocell was not in use (no k-h-g-e observations), the sequence lasted about 20 minutes. During 1963-64 the order of observation was e-g-h-k-l-m-p-s-u-v-b-c-d, so that the d-time records the end of the 13-filter sequence for this period. The time reported is local sidereal time for 1963 and 1964; for 1965 the Universal Time is given. All times are given in hours and minutes (first and second sub-columns, respectively). Column 4 lists the phase angle i as interpolated from the tables of ephemerides for physical observations in The American Ephemeris and Nautical Almanac, except for phase angles so small that linear interpolation would be inaccurate. In the latter case i was computed from (α, δ) for the planet and the sun. The next 10 columns give the monochromatic magnitudes in the narrow bands in order of increasing wavelength (see Table I), and the following 3 columns give the UBV magnitudes. The last column notes peculiar observing conditions or other problems. The notes include values of air mass M when the planet was observed at an air mass outside the range covered by the extinction stars (M is given for all observations of Venus and Mercury for which $M \geq 3.0$, and all observations of the other planets if $M \geq 2.5$). Also listed are approximate values of any unusually large residuals r (in magnitudes), as determined from the extinction solution, for stellar observations either before or after a given planetary observation ($r > 0$ indicates that the extinction has been underestimated, and vice versa).

Note that observations of Saturn include the effect of the rings. Because of problems with sky brightness, it proved impossible to obtain observations of Venus and Mercury at

small phase angles.

The accuracy of the results may be estimated by examining the rms residual (R) for each band for each monthly extinction solution and the standard error per star (S) for each band obtained in transforming the monthly periods to standard conditions. These quantities are indicated in Table IX. When there was substantial reason to believe that either error might be a serious underestimate, we included a note in Tables IV-VIII, or increased the error to what is believed to be a more realistic estimate (for example, if the color of a planet was outside the range of colors observed for standard stars during this particular period, the transformation to the standard period may be uncertain).

ACKNOWLEDGMENTS

Satisfactory completion of this project would have been impossible without the help of a large number of people. We would like to particularly acknowledge the assistance during the data reduction of Mrs. Constance Valette, Mrs. Marietta Huguenin, Mrs. Kathryn Dix, and Mr. Neil Hopkins.

REFERENCES

- Young, A. T. and Irvine, W. M. 1967, Astron. J. 72, 945 (Paper I).
 Irvine, W. M., Simon, T., Menzel, D. H., Charon, J., Lecomte, G., Griboval, P., and Young, A. T. 1968, Astron. J., in press (Paper II).
 Johnson, H. L., Mitchell, R. I., Iriarte, B., and Wisniewski, W. Z. 1966, Comm. Lunar Planet. Lab. 4, No. 63.

Table I
Effective Wavelengths of Pass Bands*

Band	v	u	s	p	m	l	k	h	g	e	d	c	b
λ_{eff}	3147	3590	3926	4155	4573	5012	6264	7297	8595	10,635	U	B	V
half-width	145	120	45	90	85	90	160	200	90	770	580	1020	800

*For details, see Papers I and II.

TABLE II

MAGNITUDES OF STANDARD STARS AT BOYDEN

STAR	v	u	s	p	m	l	k	h	g	e	U	B	V	n
α Aql *	.279	.449	-.256	.202	.457	.610	.929	1.100	1.244	1.378	1.046	0.976	0.755	135
α Ma			(-2.010)(-2.851)(-2.204)(-1.815)(-1.581)								(-1.453)(-1.404)(-1.366)			20
α Psa	.555	.770	-.088	.438	.758	.964	1.392	1.647	1.850	1.996	1.340	1.248	1.152	171
α Ser *	4.629	4.270	3.896	3.678	2.936	2.768	2.404	2.301	2.142	1.993	5.028	3.811	2.627	58
α Vir	-1.472	-.979	-.841	-.055	.433	.723	1.354	1.716	2.049	2.385	-0.196	0.725	0.961	170
β Cnc *		5.955	5.744	5.019	4.083	3.819					6.779	5.015	3.553	24
β Hy1	2.756	2.755	2.728	2.758	2.786	2.781	2.827	2.830	2.884	2.870	3.534	3.402	2.790	15
β Lib *	1.214	1.569	.925	1.695	2.125	2.377	2.926	3.224	3.468	3.702	2.128	2.479	2.592	34
β Ph *	4.760	4.404	4.028	3.806	3.083	2.916	2.564	2.438	2.322	2.141	5.163	3.938	2.757	25
β Ori *	-1.552	-1.233	-1.377	-.641	-.236	-.013	.460	.719	.890	1.149	-0.529	0.135	0.183	60
β Vir	3.468	3.475	3.388	3.462	3.531	3.562	3.640	3.683	3.710	3.752	4.250	4.153	3.604	128
γ Cet		3.039	2.194	2.717	3.063	3.272	3.745	3.977	4.141	4.275	3.580	3.532	3.449	52
δ Pav	(3.993)	3.906	3.741	3.710	3.575	3.572	3.498	3.491	3.500	3.495	4.730	4.292	3.531	63
κ Cet *		4.941	4.928	4.901	4.845	4.849	4.835	4.834	4.851	4.818	5.718	5.512	4.847	40
λ Ser	4.314	4.323	4.310	4.340	4.372	4.381	4.464	4.476	4.460	4.470	5.121	5.010	4.406	55
ξ^2 Cet	(3.227)	(3.645)	(2.733)	(3.457)	(3.856)	(4.094)					4.145	4.264	4.304	9
CHya	3.024	3.328	2.407	3.086	3.459	3.690					3.860	3.906	3.913	15
55Peg		7.270	6.945	6.201	5.143	4.921	4.289	3.666	3.372	3.022	8.014	6.102	4.518	51
85Peg *				5.808	5.808	5.795	5.744	5.656	5.608	5.619	6.548	6.444	5.762	15

App.
H
I

Table III
Magnitude Transformation from Boyden
Standard to Final System*

Band	α	β	ϵ^\dagger
v	0.022 \pm .045	3.220 \pm .013	0.025
u	-0.021 \pm .056	1.428 \pm .012	0.032
s	-0.107 \pm .043	1.099 \pm .009	0.025
p	-0.027 \pm .021	1.062 \pm .012	0.031
m	-0.136 \pm .039	0.923 \pm .008	0.020
l	-0.141 \pm .032	1.030 \pm .007	0.016
k	0.028 \pm .060	-0.774 \pm .012	0.027
h	0.063 \pm .063	-0.605 \pm .009	0.022
g	0.004 \pm .081	-0.496 \pm .012	0.029
e	0.074 \pm .049	-0.370 \pm .009	0.023
U	-0.021 \pm .008	0.001 \pm .007	0.025
B	0.018 \pm .009	-0.008 \pm .007	0.020
V	-0.001 \pm .009	-0.001 \pm .007	0.020

* Equation (1) was used, with starred quantities representing stellar magnitudes on the standard Boyden system. Colors were the same as in the extinction determination (see Paper I).

$^\dagger \epsilon$ = standard error per star

TABLE IV. MONOCHROMATIC MAGNITUDES OF MERCURY AT BOYDEN.

NO	DATE	TIME	PHASE	3147	3590	3926	4155	4573	5012	6264	7297	4595	10635	U	B	V
1	JUN 15 63	11 08.00			2.99	2.69	2.19	2.57	2.67	2.22	2.13	1.98	1.78		3.25	2.36
2	AUG 14 63	16 20 72.00			2.13	2.05	2.06	1.91	1.73	1.25	1.26	1.24	0.97			
3	AUG 15 63	15 43 73.00			2.03	1.94	1.96	1.75	1.66	1.42	1.73	1.19	1.06		2.32	1.57
4	AUG 15 63	16 24 73.00			2.07	2.03	1.96	1.79	1.67	1.41	1.34	1.33	1.11	2.44		
5	AUG 18 63	16 34 78.00			2.18	2.09	2.07	1.86	1.78	1.56	1.43	1.37	1.23	2.80	2.55	1.71
6	AUG 19 63	16 39 80.00			2.37	2.27	2.25	2.04	2.02	1.57	1.50	1.38		3.01	2.71	1.95
7	AUG 19 63	16 11 80.00								1.56	1.50	1.44	1.26			
8	AUG 22 63	17 00 84.00			2.39	2.33	2.32	2.10	2.03	1.75	1.61	1.53	1.38	3.10	2.71	1.94
9	AUG 25 63	17 06 90.00			2.69	2.61	2.59	2.37	2.29	1.96	1.82	1.78	1.61	3.42	3.06	2.15
10	AUG 26 63	16 52 92.00			2.85	2.77	2.73	2.53	2.43	2.09	2.00	1.91	1.73	3.73	3.33	2.46
11	JAN 27 64	13 46 75.00			2.00	1.93	1.89	1.82	1.73						2.56	1.53
12	MAY 18 64	21 53 115.00		4.08	3.84	3.55	3.55	3.41	3.34	2.88	2.68	2.58	2.41	4.63	4.15	3.25
13	MAY 18 64	22 13 115.00					3.56	3.44	3.34							
14	MAY 19 64	21 59 113.00		3.86	3.63	3.42	3.40	3.26	3.19	2.85	2.69	2.58	2.41	4.44	4.01	3.10
15	MAY 19 64	22 13 113.00												4.44		
16	MAY 19 64	22 17 113.00													4.05	3.14
17	MAY 21 64	21 57 108.00		3.54	3.37	3.33	3.28	3.08	2.91	2.57	2.43	2.32	2.14	4.14	3.70	2.82
18	MAY 21 64	22 25 108.00		3.56	3.39	3.31	3.20	3.06	2.93	2.64	2.46	2.34	2.22	4.31	3.78	2.94
19	MAY 27 64	22 35 96.00		3.10	2.81	2.72	2.65	2.50	2.35					3.67	3.23	2.30
20	MAY 27 64	22 51 96.00		3.17	2.92	2.77	2.69	2.58	2.40					3.89	3.32	2.35
21	MAY 27 64	22 55 96.00					2.81	2.63	2.48							
22	MAY 30 64	22 48 90.00		2.95	2.64	2.38	2.40	2.26	2.21					3.43	3.02	2.13
23	MAY 30 64	23 05 90.00		2.78	2.61	2.44	2.43	2.30	2.22					3.53	2.99	2.15
24	MAY 30 64	23 11 90.00						2.34	2.21							
25	MAY 31 64	22 54 87.00		2.91	2.68	2.49	2.47	2.34	2.25					3.55	3.08	2.15
26	MAY 31 64	22 59 87.00					2.50	2.35	2.24							
27	MAY 31 64	23 07 87.00			2.76	2.52	2.58	2.41	2.24						3.11	2.13
28	JUN 01 64	23 00 85.00		2.75	2.54	2.24	2.24	2.13	2.09					3.32	2.93	2.01
29	JUN 01 64	23 16 85.00		2.72	2.46	2.28	2.28	2.15	2.09					3.34	2.87	1.98
30	MAY 06 65	4 14 98.00		3.24	3.06	2.89	2.81	2.73	2.63	2.31	2.21	2.00	1.86	3.90	3.42	2.53
31	MAY 06 65	3 56 98.00								2.32	2.19	1.99	1.78			
32	MAY 06 65	4 47 98.00								2.27	2.19	2.03	1.91			
33	MAY 12 65	4 08 87.00		2.66	2.54	2.43	2.35	2.21	2.10					3.39	2.90	2.05
34	MAY 12 65	4 35 87.00					2.37	2.20	2.09						2.93	2.04
35	MAY 14 65	4 16 83.00		2.51	2.35	2.24	2.14	2.03	1.93	1.66	1.48	1.74	1.31	3.19	2.76	1.89
36	MAY 17 65	4 22 77.00		2.65	2.44	2.37	2.25	2.09	1.92	1.58	1.46	1.30	1.16		2.53	1.79
37	MAY 17 65	4 40 77.00												3.11	2.65	1.77
38	NOV 05 65	16 20 58.00								0.84	0.59	0.72	0.59			

Notes to Table IV

- (1) Jun 15 63: $3.2 \lesssim M \lesssim 4.1$ (khge), $r \approx -0.04$
- (2) Aug 14 63: $3.3 \lesssim M \lesssim 4.5$ (vus)
- (4) Aug 15 63: $4.0 \lesssim M \lesssim 5.8$ (bcd)
- (5) Aug 18 63: $3.0 \lesssim M \lesssim 4.8$ (bcd)
- (6) Aug 19 63: $2.8 \lesssim M \lesssim 4.9$ (bcd), dust
- (8) Aug 22 63: $3.1 \lesssim M \lesssim 5.6$ (bcd)
- (9) Aug 25 63: $3.0 \lesssim M \lesssim 5.0$ (bcd)
- (10) Aug 26 63: extinction uncertain (vuspmlbcd)
- (11) Jan 27 64: $M = 3.1$ clouds
- (12) May 18 64: $M = 4.0$
- (14)(15) May 19 64: $M = 4.0, 3.4$
- (17) May 21 64: $M = 4.5$ (khge: $M = 5.11$, extinction poorly determined)
- (18) May 21 64: $M = 3.2$, extinction poorly determined (khge)
- (19)(20)(21) May 27 64: $M = 3.9, 3.2, 2.8$, clouds?
- (22) May 30 64: $M = 3.9$
- (25) May 31 64: $M = 4.0$
- (26) May 31 64: $M = 3.4$, fading (?)
- (27) May 31 64: $M = 2.9$, fading (?)
- (28) Jun 01 64: $M = 4.3$, fading
- (29) Jun 01 64: $M = 3.4$, fading
- (30) May 06 65: $r \approx -.02$, $M = 3.5$
- (33) May 12 65: $M = 3.5$
- (35) May 14 65: $M = 3.4$
- (36) May 17 65: $M = 3.5$, fading
- (37) May 17 65: $M = 3.0$, fading

Notes to Table V

- (3) May 05 63: $M = 2.6$, $r \approx -0.03$
- (4) May 27 63: $M = 3.0$
- (5) Jun 09 63: $M = 3.2$
- (6) Dec 10 63: $M = 3.3$
- (7) Dec 15 63: $M = 3.0$
- (8) Dec 16 63: $M = 3.0$
- (9)(10)(11) Dec 17 63: extinction poorly determined
- (13) Dec 21 63: $M = 3.7$
- (15) Jan 03 64: extinction poorly determined (khge)
- (17)(18) Jan 09 64: clouds
- (19)(20) Jan 12 64: clouds
- (21)(22)(23) Jan 14 64: clouds
- (24)(25)(26) Jan 16 64: clouds
- (27) Jan 26 64: clouds, extinction poorly determined
- (31) Feb 02 64: $M = 2.6$
- (34) Feb 13 64: $M = 2.7$
- (43)(44) Feb 23 64: clouds
- (46) Mar 10 64: $M = 2.7$
- (47) May 08 64: extinction poorly determined
- (54) May 14 64: $M = 2.6$
- (55) May 18 64: $r \approx 0.04$
- (56) May 18 64: $M = 3.0$, $r \approx 0.04$
- (58) May 30 64: $M = 3.8$
- (59) May 30 64: $M \approx 5$
- (60) May 31 64: $M = 3.5$
- (61) May 31 64: $M = 4.5$
- (64) Jun 01 64: $M = 3.7$

Notes to Table V

- (66) Jun 02 64: $M = 3.5$
- (67) Jun 02 64: $M = 4.5$
- (70) Jun 08 64: $M = 4.0$
- (74) Sep 08 65: clouds
- (75) Sep 10 65: clouds
- (78) Sep 16 65: cirrus
- (79) Sep 21 65: extinction poorly determined
- (95) Dec 03 65: $r \approx -0.03$ (vuspmlbcd)
- (98) Dec 08 65: $r \approx +0.025$
- (99) Dec 10 65: clouds

NO	DATE	TIME	PHASE	3147	3590	3926	4155	4573	5012	6264	7297	8595	10635	U	B	V
56	AUG 14 63	17 06	28.98											0.90	0.32	-0.96
57	AUG 15 63	16 59	28.54		0.02	0.00	-0.02	-0.40	-0.63	-1.55	-1.77	-1.72	-1.76	0.89	0.39	-0.93
58	AUG 18 63	17 24	28.12		-0.05	0.10	-0.02	-0.35	-0.59	-1.39	-1.70	-1.67	-1.66	0.70	0.26	-0.99
59	AUG 19 63	17 31	28.98		0.06	-0.01	-0.01	-0.40	-0.61	-1.39	-1.72	-1.68	-1.65	0.87	0.38	-0.84
60	AUG 22 63	17 39	28.56		-0.04	-0.07	-0.12	-0.48	-0.70	-1.39	-1.68	-1.65	-1.60	0.81	0.28	-0.94
61	AUG 25 63	17 55	28.12		-0.08	-0.10	-0.13	-0.51	-0.71	-1.49	-1.75	-1.71	-1.69	0.71	0.26	-1.00
62	AUG 26 63	17 28	27.98		-0.01	-0.04	-0.10	-0.47	-0.69	-1.48	-1.75	-1.71	-1.74	0.41	0.31	-0.97
63	FEB 18 65	20 54	14.73							-1.84	-2.04	-2.04	-2.00			
64	FEB 18 65	23 07	14.73							-1.92	-2.15	-2.15	-2.12			
65	FEB 18 65	16 14	14.73							-1.92	-2.15	-2.15	-2.14			
66	FEB 18 65	13 32	14.73							-1.89	-2.10	-2.10	-2.11			
67	FEB 18 65	3 12	14.73							-1.86	-2.04	-2.09	-2.11			
68	FEB 21 65	21 44	12.60							-1.84	-2.01	-2.03	-2.00			
69	FEB 21 65	1 12.60								-1.91	-2.10	-2.13	-2.14			
70	FEB 21 65	2 27	12.60							-1.93	-2.12	-2.18	-2.19			
71	FEB 23 65	21 11	11.14							-1.83	-2.00	-1.98	-1.95			
72	FEB 23 65	22 30	11.14							-1.84	-2.01	-2.03	-2.02			
73	FEB 24 65	21 43	10.40	-0.37	-0.36	-0.44	-0.63	-0.92	-1.11	-1.86	-2.03	-2.01	-1.98	0.45	-0.08	-1.35
74	FEB 24 65	23 50	10.40	-0.39	-0.38	-0.46	-0.66	-0.94	-1.13	-1.93	-2.10	-2.09	-2.09	0.43	-0.10	-1.36
75	FEB 24 65	2 28	10.40	-0.23	-0.26	-0.37	-0.59	-0.91	-1.11	-1.96	-2.15	-2.16	-2.18	0.55	-0.05	-1.40
76	FEB 25 65	22 01	9.65	-0.38	-0.39	-0.48	-0.66	-0.95	-1.16	-1.91	-2.07	-2.08	-2.03	0.41	-0.10	-1.35
77	FEB 25 65	24 15	9.65	-0.34	-0.36	-0.46	-0.65	-0.95	-1.14	-1.90	-2.06	-2.06	-2.04	0.40	-0.12	-1.37
78	FEB 25 65	2 17	9.65	-0.26	-0.29	-0.38	-0.60	-0.93	-1.15	-1.94	-2.12	-2.14	-2.13	0.46	-0.09	-1.43
79	FEB 25 65	20 18	8.90	-0.31	-0.32	-0.39	-0.58	-0.91	-1.12	-1.89	-2.05	-2.07	-2.04	0.50	-0.06	-1.34
80	FEB 26 65	22 13	8.90	-0.40	-0.40	-0.47	-0.68	-0.98	-1.19	-1.90	-2.06	-2.06	-2.01	0.38	-0.13	-1.39
81	FEB 26 65	2 28	8.90	-0.42	-0.45	-0.53	-0.71	-1.00	-1.19	-1.90	-2.07	-2.07	-2.05	0.35	-0.16	-1.40
82	FEB 28 65	20 32	7.39	-0.38	-0.36	-0.45	-0.65	-0.96	-1.17	-1.92	-2.09	-2.08	-2.04	0.48	-0.11	-1.40
83	FEB 28 65	22 15	7.39	-0.43	-0.42	-0.51	-0.71	-1.02	-1.22	-1.95	-2.11	-2.10	-2.04	0.39	-0.16	-1.42
84	FEB 28 65	25 7.39		-0.43	-0.45	-0.54	-0.73	-1.01	-1.19	-1.91	-2.06	-2.07	-2.04	0.36	-0.17	-1.41
85	FEB 28 65	2 33	7.39	-0.45	-0.46	-0.56	-0.74	-1.03	-1.21	-1.95	-2.12	-2.12	-2.11	0.33	-0.19	-1.44
86	MAR 03 65	19 52	5.28	-0.43	-0.44	-0.53	-0.72	-1.02	-1.21	-1.94	-2.08	-2.06	-1.97	0.41	-0.18	-1.43
87	MAR 03 65	21 57	5.22	-0.43	-0.44	-0.54	-0.73	-1.05	-1.26	-1.97	-2.11	-2.10	-2.03	0.38	-0.20	-1.47
88	MAR 03 65	19 5.15		-0.42	-0.43	-0.54	-0.72	-1.03	-1.23	-1.96	-2.10	-2.11	-2.08	0.38	-0.19	-1.44
89	MAR 03 65	2 23	5.09	-0.53	-0.53	-0.63	-0.79	-1.09	-1.27	-1.98	-2.14	-2.13	-2.11	0.29	-0.23	-1.47
90	MAR 05 65	21 49	3.84	-0.46	-0.47	-0.57	-0.77	-1.08	-1.29	-1.96	-2.10	-2.11	-2.02	0.33	-0.23	-1.49
91	MAR 05 65	24 24	3.77	-0.46	-0.47	-0.57	-0.77	-1.08	-1.29	-2.00	-2.15	-2.16	-2.13	0.35	-0.23	-1.52
92	MAR 07 65	23 55	2.71	-0.43	-0.47	-0.57	-0.77	-1.08	-1.29	-2.00	-2.15	-2.09	-2.02	0.31	-0.26	-1.53
93	MAR 07 65	23 47	2.71							-2.00	-2.16	-2.13	-2.12			
94	MAR 09 65	21 31	2.41				-0.86	-1.16	-1.34	-2.00	-2.16	-2.13	-2.12	0.23	-0.31	-1.55
95	MAR 09 65	6 2.42					-0.77	-1.08	-1.28	-2.00	-2.16	-2.13	-2.09	0.36	-0.21	-1.51
96	MAR 12 65	18 26	3.59							-2.00	-2.16	-2.13	-2.09	0.23	-0.28	-1.53
97	MAR 12 65	19 38	3.62				-0.84	-1.13	-1.32	-2.04	-2.23	-2.19	-2.18	0.52	-0.00	-1.32
98	MAR 12 65	21 40	3.67				-0.81	-1.12	-1.31	-2.05	-2.20	-2.18	-2.13	0.50	-0.01	-1.36
99	MAR 22 65	17 59	11.20				-0.71	-0.98	-1.12	-1.96	-2.16	-2.17	-2.13	0.50	-0.01	-1.36
100	MAR 22 65	18 07	11.20							-2.00	-2.16	-2.13	-2.12	0.52	-0.00	-1.32
101	MAR 22 65	20 21	11.20							-2.00	-2.16	-2.13	-2.12	0.50	-0.01	-1.36
102	MAR 24 65	19 01	12.71							-2.00	-2.16	-2.13	-2.12	0.50	-0.01	-1.36
103	MAR 24 65	21 47	12.71							-2.00	-2.16	-2.13	-2.12	0.50	-0.01	-1.36
104	MAR 24 65	31 12.71								-2.00	-2.16	-2.13	-2.12	0.50	-0.01	-1.36
105	APR 12 65	17 07	25.00	-0.10	-0.09	-0.11	-0.23	-0.49	-0.71	-1.60	-1.80	-1.77	-1.72	0.16	0.20	-1.05
106	APR 12 65	19 19	25.00	-0.23	-0.21	-0.22	-0.38	-0.62	-0.82	-1.61	-1.79	-1.77	-1.72	0.50	0.18	-1.06
107	APR 12 65	22 02	25.00		-0.05	-0.09	-0.24	-0.51	-0.76	-1.63	-1.83	-1.82	-1.83	0.77	0.29	-1.07
108	APR 27 65	16 58	31.64		0.03	0.01	-0.16	-0.48	-0.76	-1.65	-1.83	-1.82	-1.83	0.83	0.31	-1.07
109	APR 27 65	19 13	31.64		0.12	0.06	-0.11	-0.45	-0.75	-1.66	-1.89	-1.92	-1.93	0.89	0.33	-1.08
110	APR 27 65	21 53	31.64							-1.57	-1.80	-1.83	-1.83			
111	APR 29 65	17 09	32.34							-1.63	-1.85	-1.86	-1.82			
112	APR 29 65	18 41	32.34							-1.69	-1.92	-1.94	-1.93			

NO	DATE	TIME	PHASE	3147	3590	3926	4155	4573	5012	6244	7297	8595	10635	U	B	V
113	APR 29 65	20 04	32.34							-1.64	-1.87	-1.91	-1.93	0.89	0.40	-0.92
114	APR 29 65	22 00	32.34	0.03	0.05	-0.00	-0.09	-0.40	-0.64	-1.63	-1.86	-1.90	-1.92	0.89	0.40	-0.92
115	MAY 06 65	17 00	34.45	-0.06	-0.03	-0.09	-0.18	-0.46	-0.69	-1.57	-1.68	-1.70	-1.62	0.80	0.33	-0.98
116	MAY 06 65	19 41	34.45	0.00	0.05	-0.02	-0.11	-0.35	-0.66	-1.52	-1.72	-1.75	-1.72	0.80	0.39	-0.93
117	MAY 07 65	17 52	34.71	0.13	0.16	0.08	-0.05	-0.35	-0.61	-1.48	-1.66	-1.69	-1.60	1.02	0.47	-0.90
118	MAY 10 65	16 46	35.45	0.07	0.11	0.04	-0.05	-0.35	-0.58	-1.40	-1.62	-1.65	-1.64	0.97	0.47	-0.88
119	MAY 10 65	19 14	35.45	-0.04	0.02	-0.03	-0.11	-0.41	-0.65	-1.46	-1.66	-1.67	-1.67	0.86	0.37	-0.92
120	MAY 10 65	21 12	35.45	0.13	0.17	0.09	-0.03	-0.36	-0.60	-1.45	-1.66	-1.66	-1.58	0.99	0.47	-0.89
121	MAY 12 65	16 32	35.90	0.21	0.21	0.13	0.03	-0.30	-0.54	-1.40	-1.62	-1.64	-1.67	1.07	0.54	-0.84
122	MAY 12 65	19 06	35.90	0.13	0.14	0.07	-0.04	-0.37	-0.61	-1.42	-1.63	-1.64	-1.54	0.98	0.45	-0.88
123	MAY 13 65	16 35	36.12	0.25	0.25	0.16	0.04	-0.28	-0.54	-1.40	-1.62	-1.67	-1.68	1.07	0.54	-0.84
124	MAY 13 65	18 58	36.12	0.07	0.09	0.02	-0.09	-0.40	-0.64	-1.42	-1.61	-1.62	-1.50	0.90	0.41	-0.90
125	MAY 14 65	16 30	36.32	0.22	0.25	0.17	0.04	-0.29	-0.55	-1.38	-1.61	-1.63	-1.64	1.08	0.54	-0.85
126	MAY 14 65	19 05	36.32	0.22	0.25	0.17	0.04	-0.29	-0.55	-1.38	-1.61	-1.63	-1.64	1.04	0.51	-0.84
127	MAY 14 65	21 02	36.32	0.14	0.17	0.11	0.00	-0.32	-0.56	-1.39	-1.60	-1.64	-1.63	1.04	0.51	-0.84
128	MAY 17 65	16 26	36.90	0.01	0.03	-0.04	-0.14	-0.41	-0.62	-1.37	-1.57	-1.56	-1.44	0.86	0.39	-0.87
129	MAY 17 65	18 58	36.90	0.13	0.15	0.07	-0.03	-0.34	-0.58	-1.35	-1.56	-1.59	-1.59	0.98	0.48	-0.84
130	MAY 21 65	16 36	35.57	0.12	0.15	0.08	-0.02	-0.34	-0.57	-1.38	-1.57	-1.59	-1.50	1.00	0.48	-0.85
131	MAY 21 65	19 28	35.57	0.12	0.14	0.09	-0.02	-0.29	-0.51	-1.25	-1.44	-1.47	-1.45	0.99	0.51	-0.78
132	MAY 21 65	21 12	35.57	0.11	0.21	0.18	0.04	-0.25	-0.50	-1.34	-1.54	-1.56	-1.59	1.02	0.50	-0.79
133	JUN 01 65	16 26	38.90	0.20	0.18	0.09	-0.03	-0.39	-0.66	-1.60	-1.82	-1.86	-1.77	1.07	0.44	-0.94
134	JUN 01 65	18 28	38.90	0.29	0.25	0.17	0.02	-0.33	-0.60	-1.53	-1.75	-1.81	-1.82	1.12	0.51	-0.90
135	JUN 01 65	20 30	38.90	0.27	0.28	0.20	0.07	-0.28	-0.56	-1.47	-1.69	-1.73	-1.73	1.15	0.56	-0.83
136	JUN 02 65	16 31	39.00	0.23	0.22	0.13	-0.02	-0.37	-0.64	-1.59	-1.81	-1.84	-1.76	1.08	0.47	-0.93
137	JUN 02 65	18 32	39.00	0.28	0.27	0.20	0.05	-0.31	-0.58	-1.52	-1.74	-1.80	-1.81	1.15	0.53	-0.89
138	JUN 02 65	20 38	39.00	0.38	0.34	0.24	0.12	-0.23	-0.50	-1.44	-1.66	-1.71	-1.72	1.23	0.61	-0.83
139	JUN 03 65	16 18	39.08	0.18	0.16	0.08	-0.06	-0.40	-0.64	-1.58	-1.79	-1.83	-1.75	1.02	0.43	-0.92
140	JUN 03 65	18 17	39.08	0.24	0.24	0.16	0.01	-0.36	-0.64	-1.56	-1.79	-1.85	-1.86	1.12	0.49	-0.92
141	JUN 03 65	20 18	39.08	0.30	0.30	0.20	0.04	-0.30	-0.58	-1.52	-1.75	-1.80	-1.83	1.17	0.55	-0.87
142	JUN 04 65	16 14	39.17	0.11	0.08	0.01	-0.11	-0.23	-0.67	-1.52	-1.73	-1.75	-1.67	0.96	0.40	-0.93
143	JUN 04 65	18 12	39.17	0.25	0.23	0.14	-0.01	-0.26	-0.63	-1.53	-1.76	-1.80	-1.82	1.09	0.47	-0.92
144	JUN 04 65	20 13	39.17	0.33	0.29	0.22	0.06	-0.29	-0.58	-1.53	-1.74	-1.80	-1.81	1.18	0.56	-0.87
145	JUL 08 65	17 08	39.65	0.37	0.36	0.33	0.13	-0.24	-0.55	-1.47	-1.74	-1.83	-1.86	1.21	0.55	-0.90
146	JUL 08 65	19 18	39.65	0.34	0.34	0.29	0.11	-0.26	-0.55	-1.42	-1.69	-1.76	-1.81	1.16	0.56	-0.87
147	JUL 09 65	16 56	39.61	0.29	0.29	0.22	0.04	-0.24	-0.63	-1.50	-1.76	-1.85	-1.88	1.10	0.49	-0.94
148	JUL 09 65	19 12	39.61	0.39	0.43	0.36	0.19	-0.21	-0.50	-1.40	-1.66	-1.76	-1.81	1.25	0.62	-0.82
149	JUL 14 65	16 52	39.40	0.12	0.09	0.01	-0.13	-0.45	-0.70	-1.46	-1.70	-1.73	-1.76	0.88	0.35	-0.96
150	JUL 14 65	18 12	39.40							-1.43	-1.68	-1.74	-1.79	1.05	0.47	-0.93
151	JUL 14 65	19 29	39.40							-1.50	-1.76	-1.82	-1.84			
152	JUL 14 65	20 07	39.40	0.18	0.27	0.16	0.06	-0.34	-0.70	-1.55	-1.82	-1.86	-1.91	1.12	0.50	-0.98
153	JUL 15 65	17 00	39.35	0.18	0.16	0.07	-0.09	-0.40	-0.65	-1.39	-1.63	-1.69		0.93	0.40	-0.94

Notes to Table VI

- (7) May 03 63: $r \approx +0.05$ (vus-pml)
- (10) May 04 63: $M = 2.0$
- (12) May 05 63: $M = 2.5$
- (13)(14) May 13 63: large extinction, clouds
- (16) May 27 63: $r \approx -0.03$ (pmlkhge)
- (24) Jun 03 63: $M = 2.8$
- (28) Jun 14 63: $M = 3.0$
- (29) Jun 15 63: $r \approx +0.03$ (pml)
- (30) Jun 23 63: $M = 2.7$
- (31) Jun 23 63: $M = 3.0$
- (34) Jun 24 63: $M = 3.0$
- (35) Jun 25 63: poor night
- (36)(37) Jul 01 63: poor night
- (38) Jul 05 63: $r > 0$ (pml)
- (40) Jul 11 63: $M = 3.4$
- (42) Jul 12 63: $M = 2.6$
- (43) Jul 13 63: $r \approx -0.03$ (pmlkhge)
- (46) Jul 17 63: $r \approx -0.03$ (pml)
- (48) Jul 23 63: $M = 3.3$
- (50) Jul 24 63: $M = 3.0$
- (52) Jul 25 63: $M = 2.5$
- (53) Aug 04 63: extinction not well determined
- (55) Aug 05 63: $M = 3.0$
- (59) Aug 19 63: $M = 2.5$
- (62) Aug 26 63: extinction not well determined
- (67) Feb 18 65: fading (kh)
- (72) Feb 23 65: clouds
- (91) Mar 05 65: clouds?

Notes to Table VI

- (94)(95) Mar 09 65: clouds
- (96) Mar 12 65: $M = 2.6$
- (98) Mar 12 65: clouds (pml)
- (99)(100) Mar 22 65: clouds
- (123) May 13 65: $r \approx -0.03$ (vuspmlbcd)
- (128) May 17 65: $r \approx -0.02$ (vuspmlbcd)
- (131) May 21 65: smoke
- (132) May 21 65: $M = 2.6$
- (139) Jun 03 65: twilight (khge)
- (145) Jul 08 65: $r \approx 0.02$ (pmlbcd)
- (148) Jul 09 65: smoke (khge)
- (149)(150) Jul 14 65: extinction overestimated?
- (152) Jul 14 65: extinction overestimated?, $M = 3.7$
- (153) Jul 15 65: clouds

TABLE VII. MONOCHROMATIC MAGNITUDES OF JUPITER AT BOYDEN.

NO	DATE	TIME	PHASE	3147	3590	3926	4155	4573	5012	6264	7297	8595	10435	U	B	V
1	JUN 03 63	23 13	10.18													
2	JUN 09 63	23 40	10.65	-8.81	-8.99	-9.02	-9.02	-9.24	-9.31	-9.45	-9.25	-8.80	-8.84	-7.99	-9.47	-9.36
3	JUN 15 63	23 36	11.05	-8.76	-8.95	-9.01	-9.02	-9.24	-9.29	-9.43	-9.23	-8.81	-8.80	-8.01	-8.50	-9.36
4	JUL 05 63	23 40	11.91	-8.81	-9.00	-9.02	-9.02	-9.24	-9.33	-9.46	-9.28	-8.84	-8.85	-7.95	-8.52	-9.35
5	JUL 11 63	50 11.91		-8.79	-8.93	-8.95	-8.95	-9.17	-9.24	-9.40	-9.20	-8.72	-8.77	-7.95	-8.62	-9.27
6	JUL 12 63	1 11 11.04		-8.74	-8.94	-8.97	-8.97	-9.21	-9.28	-9.43	-9.21	-8.75	-8.76	-7.97	-8.45	-9.32
7	JUL 12 63	2 12 11.84		-8.71	-8.89	-8.95	-8.95	-9.21	-9.28	-9.41	-9.21	-8.76	-8.78	-7.94	-8.43	-9.29
8	JUL 13 63	1 29 11.83		-8.71	-8.89	-8.94	-8.94	-9.18	-9.24	-9.40	-9.22	-8.75	-8.77	-7.94	-8.43	-9.29
9	JUL 14 63	1 22 11.82		-8.77	-8.99	-9.02	-9.02	-9.23	-9.32	-9.44	-9.23	-8.76	-8.77	-8.00	-8.47	-9.34
10	JUL 14 63	1 07 11.78		-8.78	-8.97	-9.02	-9.02	-9.25	-9.32	-9.44	-9.23	-8.76	-8.77	-8.02	-8.51	-9.15
11	JUL 23 63	1 22 11.60		-8.76	-8.95	-9.00	-9.00	-9.22	-9.30	-9.40	-9.20	-8.74	-8.74	-8.01	-8.49	-9.34
12	JUL 25 63	1 26 11.52		-8.78	-8.96	-9.00	-9.00	-9.24	-9.30	-9.43	-9.24	-8.76	-8.78	-8.00	-8.48	-9.33
13	AUG 01 63	23 17 11.12		-8.75	-8.97	-9.01	-9.01	-9.23	-9.30	-9.44	-9.22	-8.75	-8.77	-8.00	-8.49	-9.35
14	AUG 03 63	47 10.98		-8.74	-8.96	-9.00	-9.00	-9.22	-9.30	-9.41	-9.21	-8.74	-8.77	-7.98	-8.47	-9.34
15	AUG 03 63	1 59 10.98		-8.75	-8.96	-9.00	-9.00	-9.23	-9.31	-9.43	-9.22	-8.76	-8.76	-8.00	-8.49	-9.36
16	AUG 05 63	24 51 10.84		-8.71	-8.91	-8.97	-8.97	-9.20	-9.29	-9.40	-9.20	-8.72	-8.73	-7.95	-8.45	-9.32
17	AUG 06 63	2 00 10.76		-8.77	-8.95	-8.98	-8.98	-9.22	-9.31	-9.43	-9.25	-8.85	-8.79	-7.99	-8.50	-9.36
18	AUG 12 63	2 01 10.20		-8.77	-8.95	-8.98	-8.98	-9.22	-9.31	-9.43	-9.25	-8.85	-8.79	-7.99	-8.50	-9.36
19	AUG 14 63	1 02 9.99		-8.77	-8.95	-8.98	-8.98	-9.22	-9.31	-9.43	-9.25	-8.85	-8.79	-7.99	-8.50	-9.36
20	AUG 14 63	1 02 9.99		-8.77	-8.95	-8.98	-8.98	-9.22	-9.31	-9.43	-9.25	-8.85	-8.79	-7.99	-8.50	-9.36
21	AUG 14 63	1 16 9.99		-8.77	-8.95	-8.98	-8.98	-9.22	-9.31	-9.43	-9.25	-8.85	-8.79	-7.99	-8.50	-9.36
22	AUG 14 63	3 21 9.99		-8.77	-8.95	-8.98	-8.98	-9.22	-9.31	-9.43	-9.25	-8.85	-8.79	-7.99	-8.50	-9.36
23	AUG 15 63	2 33 9.87		-8.74	-8.90	-8.94	-8.94	-9.18	-9.26	-9.43	-9.24	-8.80	-8.76	-7.94	-8.44	-9.30
24	AUG 15 63	3 44 9.87		-8.76	-8.92	-8.96	-8.96	-9.21	-9.28	-9.43	-9.26	-8.80	-8.76	-7.99	-8.47	-9.33
25	AUG 18 63	2 49 9.52		-8.77	-8.95	-8.99	-8.99	-9.22	-9.32	-9.45	-9.25	-8.80	-8.75	-7.99	-8.48	-9.34
26	AUG 19 63	2 06 9.39		-8.75	-8.92	-8.97	-8.97	-9.20	-9.29	-9.48	-9.29	-8.84	-8.82	-7.96	-8.45	-9.32
27	AUG 22 63	2 49 9.01		-8.77	-8.94	-8.98	-8.98	-9.20	-9.28	-9.46	-9.29	-8.81	-8.81	-7.97	-8.44	-9.32
28	SEP 04 63	24 55 8.98		-8.74	-8.93	-8.97	-8.97	-9.22	-9.30	-9.46	-9.29	-8.81	-8.81	-7.97	-8.44	-9.32
29	SEP 10 63	1 55 8.89		-8.74	-8.93	-8.97	-8.97	-9.22	-9.30	-9.46	-9.29	-8.81	-8.81	-7.97	-8.44	-9.32
30	SEP 10 63	2 26 8.89		-8.74	-8.93	-8.97	-8.97	-9.22	-9.30	-9.46	-9.29	-8.81	-8.81	-7.97	-8.44	-9.32
31	SEP 21 63	2 04 3.66		-8.74	-8.93	-8.97	-8.97	-9.22	-9.30	-9.46	-9.29	-8.81	-8.81	-7.97	-8.44	-9.32
32	SEP 24 63	2 10 3.02		-8.77	-8.95	-8.99	-8.99	-9.25	-9.33	-9.46	-9.24	-8.82	-8.80	-8.52	-8.48	-9.33
33	SEP 26 63	2 48 2.59		-8.77	-8.95	-8.99	-8.99	-9.25	-9.33	-9.46	-9.24	-8.82	-8.80	-8.52	-8.48	-9.33
34	SEP 26 63	3 13 2.59		-8.77	-8.95	-8.99	-8.99	-9.25	-9.33	-9.46	-9.24	-8.82	-8.80	-8.52	-8.48	-9.33
35	OCT 01 63	3 06 1.49		-8.77	-8.95	-8.99	-8.99	-9.25	-9.33	-9.46	-9.24	-8.82	-8.80	-8.52	-8.48	-9.33
36	OCT 06 63	1 32 0.37		-8.77	-8.95	-8.99	-8.99	-9.25	-9.33	-9.46	-9.24	-8.82	-8.80	-8.52	-8.48	-9.33
37	OCT 06 63	2 58 0.37		-8.77	-8.95	-8.99	-8.99	-9.25	-9.33	-9.46	-9.24	-8.82	-8.80	-8.52	-8.48	-9.33
38	OCT 07 63	1 5 0.09		-8.73	-8.91	-8.95	-8.95	-9.21	-9.29	-9.41	-9.19	-8.79	-8.78	-8.50	-8.46	-9.36
39	OCT 07 63	1 42 0.09		-8.73	-8.91	-8.95	-8.95	-9.21	-9.29	-9.41	-9.19	-8.79	-8.78	-8.50	-8.46	-9.36
40	OCT 07 63	3 30 0.09		-8.73	-8.91	-8.95	-8.95	-9.21	-9.29	-9.41	-9.19	-8.79	-8.78	-8.50	-8.46	-9.36
41	OCT 11 63	1 51 0.88		-8.78	-8.96	-9.00	-9.00	-9.26	-9.33	-9.48	-9.26	-8.80	-8.80	-8.52	-8.48	-9.35
42	OCT 11 63	2 27 0.88		-8.80	-8.98	-9.02	-9.02	-9.28	-9.35	-9.50	-9.28	-8.82	-8.82	-8.54	-8.50	-9.39
43	OCT 12 63	1 47 1.09		-8.81	-8.99	-9.03	-9.03	-9.29	-9.37	-9.52	-9.30	-8.84	-8.84	-8.56	-8.52	-9.42
44	OCT 12 63	2 12 1.09		-8.76	-8.94	-8.98	-8.98	-9.23	-9.31	-9.46	-9.24	-8.81	-8.81	-8.53	-8.49	-9.36
45	OCT 13 63	1 48 1.29		-8.78	-8.96	-9.00	-9.00	-9.24	-9.32	-9.47	-9.24	-8.81	-8.81	-8.53	-8.49	-9.36
46	OCT 15 63	2 57 1.73		-8.73	-8.91	-8.95	-8.95	-9.22	-9.31	-9.46	-9.24	-8.81	-8.81	-8.53	-8.49	-9.36
47	NOV 15 63	2 36 7.78		-8.78	-8.97	-9.01	-9.01	-9.28	-9.35	-9.50	-9.28	-8.81	-8.81	-8.53	-8.49	-9.36
48	NOV 15 63	3 09 7.78		-8.78	-8.97	-9.01	-9.01	-9.28	-9.35	-9.50	-9.28	-8.81	-8.81	-8.53	-8.49	-9.36
49	DEC 10 63	3 00 10.67		-8.77	-8.95	-8.99	-8.99	-9.25	-9.33	-9.46	-9.24	-8.82	-8.80	-8.52	-8.48	-9.33
50	DEC 10 63	3 00 10.67		-8.77	-8.95	-8.99	-8.99	-9.25	-9.33	-9.46	-9.24	-8.82	-8.80	-8.52	-8.48	-9.33
51	DEC 14 63	3 22 10.93		-8.73	-8.91	-8.95	-8.95	-9.21	-9.29	-9.41	-9.19	-8.79	-8.78	-8.50	-8.46	-9.36
52	DEC 14 63	3 45 10.93		-8.73	-8.91	-8.95	-8.95	-9.21	-9.29	-9.41	-9.19	-8.79	-8.78	-8.50	-8.46	-9.36
53	DEC 15 63	2 55 10.98		-8.73	-8.91	-8.95	-8.95	-9.21	-9.29	-9.41	-9.19	-8.79	-8.78	-8.50	-8.46	-9.36
54	DEC 16 63	3 04 11.04		-8.73	-8.91	-8.95	-8.95	-9.21	-9.29	-9.41	-9.19	-8.79	-8.78	-8.50	-8.46	-9.36
55	JAN 05 64	3 15 11.43		-8.67	-8.81	-8.94	-8.94	-9.16	-9.25	-9.37	-9.21	-8.75	-8.70	-7.89	-8.42	-9.28
55	JAN 13 64	2 45 11.25		-8.67	-8.81	-8.94	-8.94	-9.16	-9.25	-9.37	-9.21	-8.75	-8.70	-7.89	-8.42	-9.28

NO	DATE	TIME	PHASE	3167	3590	3926	4155	4573	5012	6264	7297	8595	10635	U	R	V
56	JAN 13 64	3 32	11.25	-8.46	-8.64	-8.78	-8.89	-9.07	-9.17					-7.84	-8.39	-9.23
57	JAN 14 64	2 56	11.21	-8.58	-8.77	-8.93	-9.01	-9.14	-9.21					-7.99	-8.51	-9.33
58	FEB 02 64	4 37	10.11	-8.61	-8.78	-8.97	-9.05	-9.18	-9.23					-7.97	-8.51	-9.32
59	FEB 13 64	5 32	9.13	-8.60	-8.76	-8.91	-9.12	-9.22	-9.26					-7.94	-8.43	-9.22
60	FEB 16 64	4 45	8.82	-8.66	-8.81	-8.88	-9.01	-9.16	-9.29					-7.94	-8.51	-9.31
61	FEB 16 64	5 12	8.82	-8.77	-8.89	-8.90	-9.00	-9.16	-9.26					-8.02	-8.57	-9.36
62	FEB 23 64	5 18	8.07	-8.62	-8.73	-8.75	-8.88	-9.11	-9.29					-7.90	-8.51	-9.32
63	JUN 15 64	23 28	7.54	-8.58	-8.68	-8.79	-8.88	-9.09	-9.24					-7.94	-8.46	-9.36
64	FEB 18 65	17 37	11.11							-9.34	-9.04	-8.69	-8.73			
65	FEB 18 65	17 58	11.11							-9.36	-9.08	-8.70	-8.74			
66	FEB 18 65	18 16	11.11							-9.35	-9.07	-8.69	-8.70			
67	FEB 23 65	17 47	10.92							-9.30	-8.98	-8.66	-8.70			
68	FEB 23 65	18 28	10.92							-9.31	-9.00	-8.67	-8.73			
69	FEB 25 65	17 55	10.82	-8.60	-8.77	-8.94	-9.07	-9.24	-9.32	-9.34	-9.00	-8.68	-8.68	-7.99	-8.48	-9.31
70	FEB 26 65	17 40	10.77	-8.61	-8.76	-8.92	-9.05	-9.23	-9.31	-9.32	-8.99	-8.69	-8.71	-7.97	-8.47	-9.29
71	FEB 28 65	17 37	10.66	-8.66	-8.81	-8.98	-9.12	-9.28	-9.36	-9.36	-9.05	-8.71	-8.74	-8.00	-8.52	-9.35
72	MAR 03 65	17 52	10.48	-8.64	-8.76	-8.95	-9.06	-9.22	-9.29	-9.34	-9.01	-8.68	-8.69	-7.94	-8.44	-9.27
73	MAR 05 65	17 25	10.35	-8.66	-8.80	-8.98	-9.10	-9.27	-9.36	-9.35	-9.06	-8.70	-8.73	-8.01	-8.51	-9.35
74	MAR 07 65	17 27	10.21							-9.34	-8.99	-8.68	-8.68	-7.99	-8.48	-9.32
75	MAR 12 65	16 57	9.83							-9.36	-9.03	-8.71	-8.73			
76	MAR 12 65	17 16	9.83							-9.36	-9.04	-8.69	-8.73			
77	MAR 24 65	17 04	8.73						-9.34					-8.01	-8.46	-9.33
78	MAR 29 65	16 56	8.20						-9.31					-8.01	-8.42	-9.27
79	DEC 03 65	13	3.14	-8.72	-8.89	-9.07	-9.16	-9.34	-9.40	-9.44	-9.05	-8.76	-8.75	-8.09	-8.59	-9.42
80	DEC 07 65	3	2.28	-8.64	-8.89	-9.09	-9.18	-9.35	-9.40	-9.45	-9.07	-8.75	-8.75	-8.13	-8.61	-9.45
81	DEC 08 65	51	2.07	-8.56	-8.90	-9.07	-9.21	-9.39	-9.48					-8.15	-8.68	-9.51
82	DEC 10 65	23 57	1.63	-8.64	-8.91	-9.08	-9.19	-9.36	-9.42	-9.45	-9.08	-8.77	-8.74	-8.14	-8.63	-9.47

Notes to Table VII

- (3) Jun 15 63: $r \approx -0.03$ (pml,vus,bcd)
- (8) Jul 13 63: Fading? (pml)
- (9) Jul 14 63: clouds
- (19) Aug 12 63: $r \approx -0.03$ (khge)
- (22) Aug 14 63: Fading
- (27) Aug 22 63: Fading
- (29)(30) Sep 10 63: very large extinction
- (33)(34) Sep 26 63: large extinction
- (35) Oct 01 63: large extinction, poor night
- (57) Jan 14 64: clouds
- (59) Feb 13 64: $M \approx 2.8$
- (62) Feb 23 64: light clouds
- (64)(65) Feb 18 65: $R \approx -0.04$
(66)
- (72) Mar 03 65: clouds
- (77) Mar 24 65: poor night
- (78) Mar 29 65: poor night
- (79) Dec 03 65: fading
- (80) Dec 07 65: cirrus

TABLE VIII. MONOCHROMATIC MAGNITUDES OF SATURN AT BOYDEN.

NO	DATE	TIME	PHASE	3147	3590	3926	4155	4573	5012	6264	7207	8595	10634	U	B	V
1	MAY 02 63	18 09	5.75											-7.66	-8.23	-9.24
2	MAY 05 63	19 28	5.79	-8.44	-8.51	-8.65	-8.98	-9.13	-9.13					-7.49	-8.07	-9.13
3	MAY 06 63	19 40	5.81	-8.27	-8.40	-8.52	-8.88	-9.02	-9.13					-7.54	-8.09	-9.14
4	MAY 13 63	20 12	5.79	-8.33	-8.43	-8.53	-8.88	-9.02	-9.13					-7.61	-8.15	-9.18
5	MAY 20 63	22 11	5.68	-8.39	-8.45	-8.56	-8.93	-9.07	-9.13					-7.60	-8.14	-9.18
6	JUN 03 63	19 59	5.74	-8.40	-8.48	-8.57	-8.93	-9.08	-9.13					-7.66	-8.22	-9.25
7	JUN 03 63	22 51	5.36	-8.34	-8.42	-8.54	-8.90	-9.05	-9.14					-7.61	-8.16	-9.22
8	JUN 09 63	22 25	5.32	-8.38	-8.46	-8.54	-8.90	-9.08	-9.14					-7.61	-8.16	-9.20
9	JUN 14 63	23 07	5.09	-8.34	-8.42	-8.50	-8.86	-9.01	-9.14					-7.60	-8.16	-9.20
10	JUN 15 63	22 14	5.34	-8.39	-8.49	-8.57	-8.95	-9.09	-9.14					-7.60	-8.16	-9.20
11	JUN 23 63	22 18	4.58	-8.40	-8.49	-8.62	-8.97	-9.14	-9.14					-7.60	-8.17	-9.26
12	JUN 24 63	21 03	4.51											-7.64	-8.22	-9.25
13	JUL 05 63	19 53	3.72	-8.40	-8.50	-8.62	-8.97	-9.14	-9.14					-7.60	-8.16	-9.20
14	JUL 05 63	21 16	3.72	-8.34	-8.43	-8.57	-8.95	-9.08	-9.14					-7.64	-8.22	-9.24
15	JUL 05 63	22 33	3.72	-8.40	-8.48	-8.61	-8.90	-9.14	-9.14					-7.64	-8.22	-9.24
16	JUL 11 63	22 03	3.21	-8.39	-8.49	-8.65	-9.00	-9.14	-9.14					-7.66	-8.20	-9.24
17	JUL 12 63	20 42	3.12	-8.40	-8.53	-8.67	-9.01	-9.14	-9.14					-7.65	-8.21	-9.26
18	JUL 12 63	22 59	3.12	-8.39	-8.51	-8.65	-9.02	-9.14	-9.14					-7.63	-8.19	-9.24
19	JUL 13 63	22 14	3.04	-8.42	-8.53	-8.66	-9.02	-9.14	-9.14					-7.66	-8.22	-9.27
20	JUL 14 63	22 00	2.95	-8.38	-8.54	-8.64	-9.02	-9.14	-9.14					-7.67	-8.23	-9.27
21	JUL 14 63	22 13	2.95											-7.67	-8.23	-9.27
22	JUL 17 63	20 59	2.67	-8.44	-8.56	-8.71	-9.03	-9.14	-9.14					-7.67	-8.22	-9.28
23	JUL 17 63	22 46	2.67	-8.42	-8.56	-8.64	-9.03	-9.14	-9.14					-7.65	-8.21	-9.29
24	JUL 23 63	20 13	4.09	-8.40	-8.53	-8.67	-9.00	-9.14	-9.14					-7.66	-8.21	-9.25
25	JUL 24 63	23 55	2.09	-8.41	-8.52	-8.67	-9.00	-9.14	-9.14					-7.69	-8.23	-9.29
26	JUL 24 63	19 31	2.00	-8.46	-8.53	-8.68	-9.03	-9.14	-9.14					-7.65	-8.22	-9.30
27	JUL 25 63	19 54	1.90	-8.44	-8.50	-8.75	-9.08	-9.23	-9.23					-7.71	-8.28	-9.32
28	JUL 25 63	22 25	1.90											-7.75	-8.33	-9.35
29	JUL 25 63	24 49	1.90	-8.52	-8.65	-8.78	-9.12	-9.26	-9.26					-7.78	-8.33	-9.35
30	AUG 01 63	18 29	1.19	-8.54	-8.64	-8.78	-9.12	-9.26	-9.26					-7.78	-8.33	-9.35
31	AUG 01 63	22 05	1.19	-8.52	-8.63	-8.76	-9.10	-9.23	-9.23					-7.77	-8.32	-9.34
32	AUG 01 63	42	1.19	-8.43	-8.56	-8.72	-9.07	-9.22	-9.22					-7.63	-8.25	-9.33
33	AUG 03 63	22 02	0.99	-8.49	-8.62	-8.75	-9.09	-9.23	-9.23					-7.63	-8.25	-9.33
34	AUG 03 63	23 26	0.99	-8.52	-8.64	-8.78	-9.11	-9.25	-9.25					-7.77	-8.32	-9.35
35	AUG 05 63	20 20	0.77	-8.51	-8.63	-8.77	-9.09	-9.23	-9.23					-7.72	-8.25	-9.24
36	AUG 05 63	22 40	0.77	-8.56	-8.69	-8.82	-9.14	-9.28	-9.28					-7.81	-8.35	-9.38
37	AUG 05 63	1 36	0.77	-8.43	-8.59	-8.71	-9.07	-9.21	-9.21					-7.67	-8.27	-9.31
38	AUG 06 63	18 53	0.67	-8.59	-8.70	-8.83	-9.16	-9.29	-9.29					-7.84	-8.37	-9.38
39	AUG 06 63	22 11	0.67											-7.84	-8.37	-9.38
40	AUG 06 63	22 32	0.67	-8.57	-8.73	-8.84	-9.15	-9.29	-9.29					-7.84	-8.37	-9.38
41	AUG 06 63	24 47	0.67	-8.57	-8.69	-8.82	-9.15	-9.29	-9.29					-7.81	-8.37	-9.38
42	AUG 10 63	21 48	0.27	-8.64	-8.73	-8.86	-9.17	-9.32	-9.32					-7.88	-8.41	-9.42
43	AUG 10 63	22 40	0.27	-8.65	-8.74	-8.86	-9.18	-9.32	-9.32					-7.87	-8.39	-9.42
44	AUG 10 63	23 53	0.27	-8.64	-8.73	-8.85	-9.17	-9.32	-9.32					-7.85	-8.38	-9.39
45	AUG 12 63	17 36	0.13	-8.63	-8.72	-8.85	-9.15	-9.29	-9.29					-7.87	-8.40	-9.40
46	AUG 12 63	18 42	0.13	-8.66	-8.75	-8.88	-9.17	-9.30	-9.30					-7.87	-8.40	-9.40
47	AUG 12 63	19 35	0.13	-8.62	-8.72	-8.82	-9.13	-9.27	-9.27					-7.84	-8.37	-9.38
48	AUG 12 63	20 36	0.13	-8.64	-8.72	-8.84	-9.15	-9.28	-9.28					-7.86	-8.38	-9.38
49	AUG 12 63	21 48	0.13	-8.66	-8.77	-8.86	-9.18	-9.32	-9.32					-7.89	-8.42	-9.41
50	AUG 12 63	22 46	0.13	-8.67	-8.77	-8.87	-9.20	-9.34	-9.34					-7.91	-8.43	-9.44
51	AUG 12 63	23 51	0.13	-8.66	-8.73	-8.86	-9.17	-9.31	-9.31					-7.89	-8.41	-9.41
52	AUG 12 63	50	0.13	-8.70	-8.80	-8.90	-9.22	-9.36	-9.36					-7.92	-8.46	-9.46
53	AUG 14 63	21 48	0.23	-8.65	-8.73	-8.85	-9.18	-9.32	-9.32					-7.87	-8.40	-9.41
54	AUG 14 63	23 47	0.23	-8.63	-8.71	-8.83	-9.16	-9.31	-9.31					-7.87	-8.37	-9.39
55	AUG 15 63	22 37	0.33	-8.62	-8.69	-8.82	-9.13	-9.28	-9.28					-7.82	-8.35	-9.38

Notes to Table VIII

- (1) May 02 63: $r \approx -0.05$
- (2) May 05 63: $r \approx -0.04$
- (12) Jun 24 63: $r \approx +0.03$
- (21) Jul 14 63: fading, $r \approx 0.03$
- (32) Aug 01 63: inadequate cooling?
- (63) Sep 04 63: clouds
- (64)(65) Sep 10 63: very large extinction
- (68) Sep 26 63: large extinction
- (69) Oct 01 63: large extinction
- (70) Oct 05 63: extinction poorly determined
- (82) May 25 64: fading
- (83)(84) May 27 64: clouds
- (90) May 06 65: fading (vuspmlbcd)
- (95) Aug 31 65: extinction poorly determined
- (96) Sep 02 65: poor night

TABLE IX

ESTIMATED ERRORS FOR EACH OBSERVING PERIOD

Period	*	v	u	s	p	m	l	k	h	g	e	d	c	b
2/9/63-	R		.037	.019	.042	.040	.068					.021	.014	.015
2/10/63	S		.049	.028	.059	.019	.023					.058	.050	.020
5/1/63-	R		.031	.030	.027	.023	.023	.018	.019	.019	.020	.029	.022	.025
5/27/63	S		.041	.036	.054	.022	.020	.050	.025	.039	.031	.054	.026	.027
5/23/63-	R		.022	.022	.025	.019	.020	.018	.017	.020	.024	.022	.020	.021
6/25/63	S		.055	.032	.054	.021	.024	.026	.011	.021	.018	.048	.023	.027
7/5/63-	R		.020	.020	.020	.020	.019	.014	.013	.014	.018	.020	.019	.017
8/6/63	S		.058	.030	.046	.012	.020	.025	.016	.016	.025	.054	.018	.016
8/10/63-	R		.023	.020	.019	.018	.018	.011	.014	.013	.014	.020	.019	.019
9/4/63	S		.056	.016	.037	.017	.019	.007 ¹	.010	.020	.032	.062	.027	.025
8/12/63-	R							.015	.016	.015	.020			
8/14/63	S							.012 ¹	.020	.023 ²	.020			
9/10/63-	R		.023	.025	.022	.021	.021	.019	.014	.016	.016	.021	.023	.019
10/15/63	S		.050 ⁴	.025 ⁴	.027	.025	.019	.031	.020 ²	.021 ²	.030	.071	.050	.016
11/15/63-	R		.013	.016	.010	.010	.010	.009	.008	.009	.011	.019	.017	.013
12/16/63	S		.019	.050	.020	.025	.032	.040	.020	.016 ²	.010 ³	.102	.045	.036
12/21/63-	R		.015	.015	.013	.014	.012	.007	.008	.009	.039	.014	.012	.014
1/12/64	S		.015	.018	.040	.012	.030	.050	.020	.037	.058	.056	.020	.015
1/13/64-	R	.025	.027	.025	.031	.017	.022	.014	.017	.013	.010	.014	.016	.010
2/2/64	S	.030	.010	.036	.023	.019	.021	.028	.011	.033	.030	.070	.025	.049
2/13/64-	R	.023	.022	.025	.030	.025	.019					.020	.020	.014
3/12/64	S	.030	.009	.004	.020	.010	.013					.020	.016	.011

5/12/64-	R	.025	.021	.025	.024	.020	.018	.013	.014	.013	.013	.023	.021	.017
6/15/64	S	.022	.009	.010	.020	.009	.008	.015	.015	.020	.020	.025	.015	.020
2/18/65-	R							.011	.015	.011	.016			
2/28/65	S							.030	.010	.010	.010			
2/24/65-	R	.021	.018	.016	.016	.011	.011	.010	.011	.010	.016	.016	.012	.010
3/29/65	S	.010	.010	.010	.050	.033	.022	.018	.014	.009	.009	.032 ¹	.027 ¹	.025
4/12/65-	R	.014	.017	.013	.013	.010	.012	.012	.013	.017	.012	.018	.019	.017
5/7/65	S	.015	.009	.007	.030	.015	.030	.030	.020	.030	.010	.030	.030	.020
5/6/65-	R	.018	.013	.013	.014	.011	.013	.013	.013	.013	.021	.015	.013	.013
5/21/65	S	.021	.007	.007	.020	.010	.011	.008	.009	.007	.015	.020	.020 ¹	.010 ¹
6/1/65-	R	.014	.012	.014	.012	.012	.012	.011	.011	.012	.025	.013	.013	.012
6/4/65	S	.049	.010	.018	.039 ¹	.037	.039 ¹	.030	.019	.009	.014	.050	.039 ¹	.035 ¹
7/8/65-	R	.013	.017	.010	.015	.014	.015	.008	.010	.009	.009	.021	.015	.012
7/15/65	S	.026	.002	.016	.029	.024	.019	.030	.020	.040	.070	.035 ¹	.033 ¹	.027 ¹
9/7/65-	R	.017	.013	.014	.013	.012	.011	.009	.007	.007	.012	.014	.012	.011
9/21/65	S	.100	.012	.020	.020	.020	.016	.010	.010	.010	.010	.017	.016	.011
10/13/65-	R	.022	.013	.015	.015	.014	.015	.007	.007	.011	.012	.013	.014	.014
11/12/65	S	.017	.020	.029	.029	.027	.025	.021	.010	.012	.013	.029	.023	.019
11/12/65-	R	.019	.025	.017	.016	.015	.014	.012	.012	.009	.012	.015	.017	.017
12/10/65	S	.100	.020	.010	.044	.031	.030	.024	.012	.040	.011	.040	.027	.028

*R = rms residual from extinction solution; S = standard error per star in transformation to standard conditions

¹transformation extrapolated to color of Mars; for Mars, est. error $\lambda \pm 0.05$

²transformation extrapolated to color of Jupiter; for Jupiter, est. error $\lambda \pm 0.05$

³transformation extrapolated to color of Saturn; for Saturn, est. error $\lambda \pm 0.04$

⁴transformation extrapolated to color of Jupiter; for Jupiter, est. error $\lambda \pm 0.100$

APPENDIX III

UNIVERSITY OF MASSACHUSETTS

FINAL REPORT

on Harvard Sub-Contract #A24658
under NASA Grant NsG 89-60, Supplement 2

UNIVERSITY OF MASSACHUSETTS
FINAL REPORT ON
Harvard Sub-Contract #A24658
Under NASA Grant NsG 89-60, Supplement 2
MULTICOLOR PHOTOELECTRIC PHOTOMETRY OF THE MOON,
VENUS, MARS, AND OTHER PLANETS.

January 1, 1967 - January 31, 1968

Principal Investigator on Sub-Contract: William M. Irvine

Research Conducted

The research carried out under this sub-contract may be divided into 3 categories. Papers referred to in this report are listed in the bibliography at the end of the report. Abstracts to these papers are given in the final report for NASA grant NsG 89-60.

A. Theoretical Research on Radiative Transfer. Dr. Irvine obtained solutions to the equation of radiative transfer applicable to the continuum and line spectra of planets in the visible and near infrared. In order to increase the speed and flexibility of radiative transfer computations for use in the study of absorption line strengths and shapes a comparison of the exact solutions with approximate procedures was made (Irvine, 1968a and 1968b). The results indicate that the small angle approximation due to Romanova is quite rapid and accurate, but that the traditional two-stream and Eddington-type approximations may give misleading results when applied to the computation of line shapes. This research was supported in part by NASA Grant NGR 22-010-023.

B. Reduction and Interpretation of Observational Data Obtained Under NsG 89-60. During the first part of this sub-contract Dr. Irvine made regular visits to Cambridge to supervise the continued reduction of the observational data at the Harvard College Observatory. The reduction procedures are described by Young and Irvine (1967). Final reduction of the data was carried out at the University of Massachusetts. The results are presented in tabular form in papers by Irvine, Simon, Menzel, Charon, Lecomte, Griboval and Young (1968) and Irvine, Simon, Menzel, Pikocs, and Young (1968). These papers will be included as appendices in the final report on the principal grant.

C. Experiments on Planetary Atmospheres. Initial progress has been made on a laboratory study of a simulated Venus atmosphere. It is known that multiple scattering in a cloud layer will change the relative strength and shape of absorption lines formed by any gaseous constituents present in a planetary atmosphere. This effect is surely present for the near infrared lines observed on Venus. Interpretation of observed Venus spectra is further complicated because the features attributed to the different substances (CO_2 , H_2O) overlap, and the relative strengths depend both on particle composition and size in the clouds and on temperature and pressure. Any attempt to sort out these effects experimentally must use a long-path absorption cell in order to study the weak lines and create an environment in which clouds

can be formed. Such research is being carried out at the University of Massachusetts in the long-path absorption cell at the Astrophysics Laboratory under the direction of Dr. William T. Plummer. This cell is 100 ft. long and 3 ft. in diameter and has a capability for increasing the path length through multiple reflections. Studies of the spectra obtained when the absorption cell contains CO_2 , CO_2 and water vapor, and CO_2 , water vapor and water clouds are being made. Support for the continuation of this research is being sought elsewhere.

BIBLIOGRAPHY

Publications Supported by this Sub-Contract:

Irvine, W.M. 1968a, "Multiple Scattering by Large Particles.

II. Optically Thick Layers", Astrophys. J., June (in press).

_____ 1968b, "An Evaluation of Romanova's Method in the Theory of Radiative Transfer", in Atmospheres of Venus and Mars, edited by Brandt and McElroy, Gordon and Breach Science Publishers Inc., New York, in press.

Irvine, W.M., T. Simon, D.H. Menzel, J. Charon, G. Lecomte, P. Griboval and A.T. Young, "Multicolor Photoelectric Photometry of the Brighter Planets. II. Observations from Le Houga Observatory", to be published.

Irvine, W.M., T. Simon, D.H. Menzel, C. Pikoos, A. Young, "Multicolor Photoelectric Photometry of the Brighter Planets. III. Observations from the Boyden Observatory", to be published.